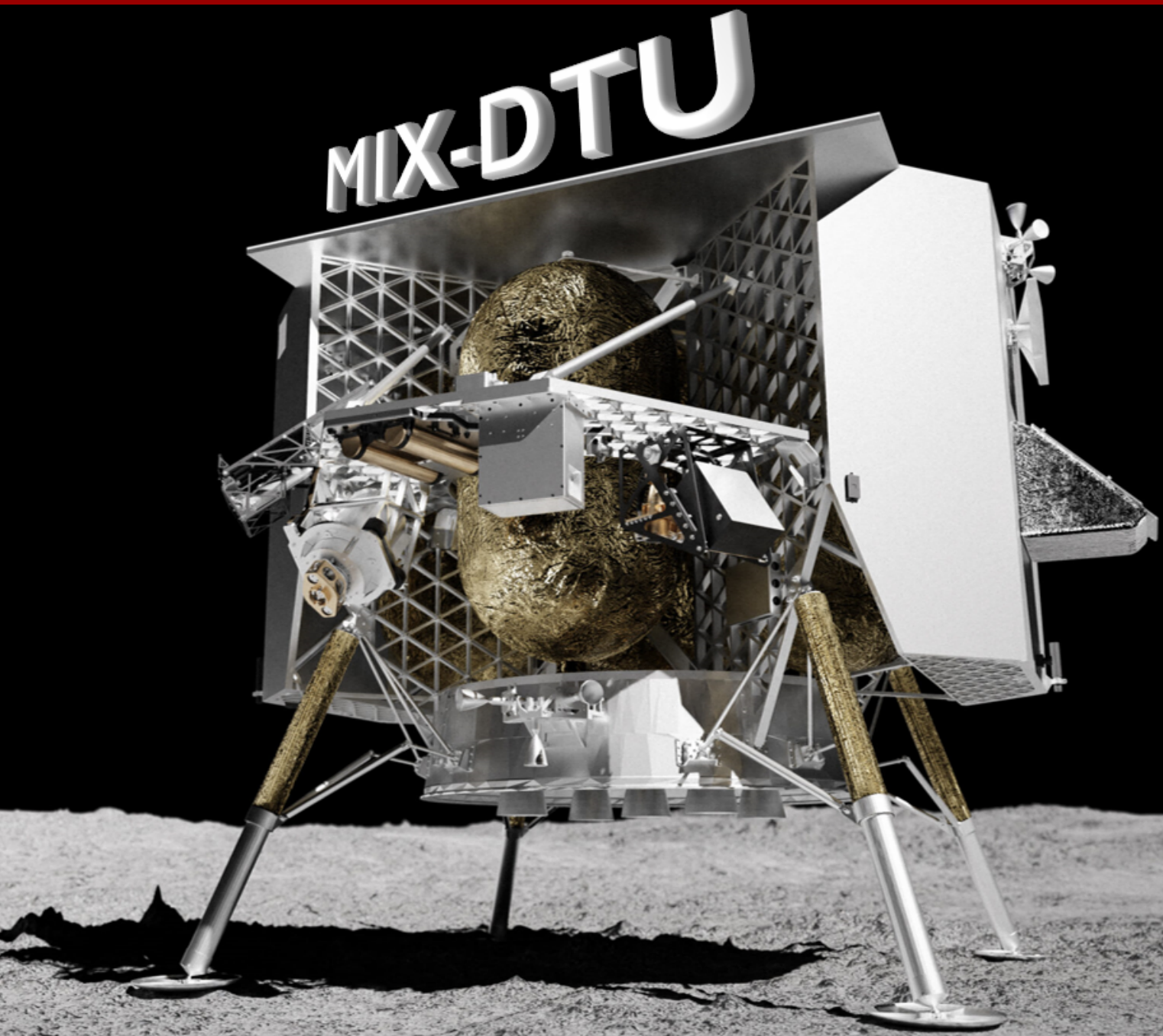


# MINIATURE XRF FOR DELICATE TERRAIN UNDERSTANDING

---

## MIX-DTU

Space Systems Engineering Project



Course responsible:

David Arge Klevang Pedersen, *Associate Professor*  
dak@dtu.dk

Katcha Koch Winther, *PhD Student*

katwi@dtu.dk

## Miniature XRF Tech Demo

Space Systems Engineering Project

May, 2023

By	Student no.	Primary group	
Lasse Leth S Berthelsen	s213457	ConOps	Starts at page 3
Lasse Schrøder-Sevald	s111582	ConOps	
Maria Niemann Madsen	s194130	ConOps	
Mechid Paiman	s194730	ConOps	
Gustav Vindeløv	s183822	LOL	Starts at page 16
Mathias Robert Jeppesen	s174039	LOL	
Rasmus Møller Blangsbøll	s183805	LOL	
Thomas Benfer	s215931	LOL	
Ben Holdstock	s221818	Payload	Starts at page 36
Gergely Pap-Takács	s222677	Payload	
Nicklas Rasmussen	s183810	Payload	
Thomas Le Cozannet	s182485	Payload	
Albert Hende	s183509	Mech	Starts at page 54
Anna Boese	s226428	Mech	
David Listl	s226808	Mech	
Elisabet Hallström	s174494	Mech	
Bjørn Thuesen	s194152	EPS	Starts at page 73
Kian Vatan	s174854	EPS	
Magnus Kvamme	s213199	EPS	
Benjamin Elsholm	s180641	Comms	Starts at page 87
Christian Broberg Christensen	s172539	Comms	
Christian Solgaard	s183821	Comms	

Copyright: Reproduction of this publication in whole or in part must include the customary bibliographic citation, including author attribution, report title, etc.

Cover photo: Ben Holdstock, 2023

Published by: DTU, Elektrovej, Building 328, 2800 Kgs. Lyngby Denmark  
[www.space.dtu.dk](http://www.space.dtu.dk)

## **Abstract**

This report investigates the feasibility of using X-ray fluorescence (XRF) technology to analyze the composition of celestial bodies and proposes the miniaturization of the technology for cost-effective deployment on planets, moons, and asteroids. The report introduces the mission concept of a Miniature XRF for Delicate Terrain Understanding (MIX-DTU), which aims to demonstrate a smaller and improved XRF technology on the Moon's South Pole. The project, which includes a mini XRF, a telescopic rod and rotator, power, and communications, has a total mass of 3 kg, with the mini XRF weighing around 1 kg and occupying 1134 cm<sup>3</sup>, smaller than the XRF used in Perseverance's PIXL. The report details the communications, power, mechanical structure, concept of operations, management requirements of the project, a distance image sensor and evaluations of thermal and radiation environments. The Miniature XRF Tech Demo, currently in its pre-phase A, aims to operate the mini XRF for about two weeks on the lunar south pole to advance our understanding of the lunar environment and other celestial bodies while promoting technological advancement. Overall, the completion of the pre-phase A brings the project closer to its ambitious mission.

# Contents

Abstract . . . . .	ii
<b>1 Introduction</b>	<b>1</b>
<b>2 ConOps</b>	<b>3</b>
2.1 Project description . . . . .	3
2.2 Overview of the Envisioned System . . . . .	5
2.3 Mission phases . . . . .	9
2.4 Risk Assessment . . . . .	13
2.5 Cost analysis . . . . .	14
2.6 Long-term considerations . . . . .	14
<b>3 Launch, Orbit and Landing</b>	<b>16</b>
3.1 Spacecraft Environment Overview . . . . .	16
3.2 Orbit Description and Stages . . . . .	17
3.3 Stages . . . . .	18
3.4 Environmental Constraints from CLPS . . . . .	25
3.5 Environment Management . . . . .	27
3.6 Distance and imaging sensor . . . . .	30
3.7 Conclusion . . . . .	34
<b>4 Payload</b>	<b>36</b>
4.1 XRF Theory . . . . .	36
4.2 Payload Requirements . . . . .	37
4.3 X-ray Sources . . . . .	39
4.4 X-Ray Detectors . . . . .	41
4.5 XRF Optics . . . . .	43
4.6 XRF Design Selection . . . . .	44
4.7 Verification, Validation and Future Work . . . . .	53
4.8 Payload Conclusions . . . . .	53
<b>5 Mechanical Structure</b>	<b>54</b>
5.1 Early thoughts . . . . .	54
5.2 Astrobotic . . . . .	54
5.3 XRF chassis . . . . .	56
5.4 Telescopic Rod Design Journey . . . . .	65
5.5 Telescopic and Rotating Mechanism Design . . . . .	67
5.6 Complete and Final Design . . . . .	71
<b>6 Electrical Power System</b>	<b>73</b>
6.1 Power source . . . . .	73
6.2 Power budget . . . . .	78
6.3 Power Management . . . . .	81
6.4 The On Board Computer . . . . .	83
6.5 Conclusion . . . . .	85

<b>7 Communications and ground segment</b>	<b>87</b>
7.1 Requirements and limitations . . . . .	87
7.2 Internal payload communication . . . . .	88
7.3 Lander to ground station . . . . .	93
7.4 Ground Segment . . . . .	98
7.5 Conclusion . . . . .	99
<b>8 Conclusion</b>	<b>100</b>
<b>9 Action items from PDR</b>	<b>101</b>
<b>A Appendix</b>	<b>111</b>
A.1 USA Frequency Allocation overview . . . . .	111
A.2 X-123 FAST SDD Specifications . . . . .	112
A.3 X-123 FAST SDD CdTe Specifications . . . . .	112

# 1 Introduction

Space exploration has been a topic of fascination and intrigue for centuries. From the first human-crewed mission to space in 1961 to the current Mars rover missions, space exploration has come a long way in terms of technology and scientific advancement. As we continue to explore the vast expanse of space, the importance of advanced technology cannot be overstated. It is through technology that we are able to push our limits, reach further out, and gain a better understanding of other celestial bodies.

One particular technology that has revolutionized space exploration in recent years is X-ray fluorescence (XRF). XRF instruments, such as the Planetary Instrument for X-ray Lithochemistry (PIXL) on board the Mars rover [1], have allowed us to analyze the composition of soil samples from distant planets and moons. This technology has provided invaluable information about the chemical makeup of these celestial bodies, helping us to better understand their origins and evolution.

Due to its ability to analyze unique astromaterials effectively, XRF spectroscopy has been utilized in planetary exploration for decades. In fact, it is an essential tool for answering key scientific questions in planetary science exploration through *in situ* geochemical analysis [2]. XRF is a fascinating technique where high-energy X-rays are directed at a sample, causing the atoms to become excited and release fluorescent X-rays with characteristic energies specific to each element. By analyzing the energy and intensity of these X-rays, scientists can determine the composition of the sample, providing insights into the geological and chemical processes that have shaped the celestial body under investigation [3].

But the use of XRF is just one example of the advanced technologies that make space exploration possible. From propulsion systems to communication networks, every aspect of a space mission relies on cutting-edge technology. And the planning that goes into each mission is just as important as the technology itself. Every space mission requires careful consideration of objectives, priorities, and risks. The planning stage is where scientists and engineers determine where to go, what to do, and what scientific objectives are most important.

This report will investigate the process of miniaturizing XRF technology to make it more cost-effective and viable for deployment on various planetary bodies, such as asteroids, moons, and other celestial objects. Furthermore, this report will examine the comprehensive planning process that goes into space missions, from conception to execution. We will showcase the intricacies and multi-faceted nature of space missions.

As part of our mission concept studies, we will present MIX-DTU, a mission concept aimed at landing on the south pole of the Moon. The primary objective of this mission is to conduct a technical demonstration of a smaller and improved XRF technology, surpassing the current available ones. The Moon's lack of atmosphere creates challenges, including extreme temperatures, radiation, and dust, which make it an excellent location to test the XRF technology. Successful testing on the Moon can lead to the deployment of this technology on many other planetary bodies in the future. The mission, planned and led by DTU Space in collaboration with Astrobotic and ESA, could be scheduled for launch in the early 2030s.

This report is structured into six main chapters that cover key areas of preliminary mission design and conceptualization. These chapters are listed below:

- The Concept of Operations (ConOps) chapter provides a road map for the entire space mission, outlining the mission's objectives, scope, and timeline.
- The Launch, Orbit and Landing (LOL) chapter discusses the key mission stages in detail, including orbital and landing maneuvers.
- Payload delves into the XRF technology, examining the desired materials analyses, optics, detection, and design.
- Mechanical Structure (Mech) covers the XRF chassis set to lower the payload to the surface, including rotating mechanisms, thermal and vibration control.
- Electrical Power System (EPS) focuses on the power budget, power source, and the onboard computer.
- The Communications and Ground Segment (Comms) chapter investigates the communication network and the team's ground operations.

## 2 ConOps

Developing Concept of Operations as early as possible is essential for a successful project or mission. ConOps is important for capturing stakeholder expectations, and it is also an important driver in the system requirements. ConOps is used in defining requirements and it should describe the system from an operational perspective and thereby help facilitate an understanding of the system goals. Fundamentally, ConOps serves as the basis on which the technical teams can build their parts of the overall system [4, p. 52]

### 2.1 Project description

#### 2.1.1 Project proposal

This project was proposed by David Flannery of the Queensland University of Technology. David contributed to the design of PIXL, and he is currently spearheading the development of a miniature XRF, to be used for *in situ* planetary exploration. The project was aimed at investigating the possibilities of future technologies that are identified and recognized by world leading engineers and researchers. At kick-off the project was presented as: “Minature lander instrument measuring elemental composition using XRF”. More specifically the goal was to bring the technology to TRL9 (Technology Readiness Level 9). Technology Readiness Level is a description of the performance history of a given system, subsystem, or component relative to a set of levels. At TRL 9 the actual system is “flight proven” through successful mission operations [4, Fig. G.4-1, p. 211]. This goal is therefore the level 1 requirement of this project (A001 in Table 2.1). Our definiton of miniature XRF, is an XRF one order of magnitude smaller in volume than PIXL.

#### 2.1.2 Project constraints

Based on the given information, described in section 2.1.1, the mission was classified as a Type D mission as described in Figure 2.1.

Classifying the mission type thereby gave a set of constraints that could be used for the project going forward. In the initial stages of the project, the stakeholders were also defined. They were classified as the scientific community (for example ESA and NASA), the public, the CLPS and relevant government agencies (for example USGS). The scientific community, government agencies and the public are stakeholders, because a possible advancement in technology along with new or improved XRF results are very relevant to them. Our CLPS (Astrobotic) is a natural stakeholder given the close collaboration with this mission.

Criteria	Type A	Type B	Type C	Type D	Type E	Type F
Description of the Types of Mission	Human Space Flight or Very Large Science/ Robotic Missions	Non-Human Space Flight or Science/Robotic Missions	Small Science or Robotic Missions	Smaller Science or Technology Missions (ISS payload)	Suborbital or Aircraft or Large Ground based Missions	Aircraft or Ground based technology demonstrations
Priority (Criticality to Agency Strategic Plan) and Acceptable Risk Level	High priority, very low (minimized) risk	High priority, low risk	Medium priority, medium risk	Low priority, high risk	Low priority, high risk	Low to very low priority, high risk
National Significance	Very high	High	Medium	Medium to Low	Low	Very Low
Complexity	Very high to high	High to Medium	Medium to Low	Medium to Low	Low	Low to Very Low
Mission Lifetime (Primary Baseline Mission)	Long. >5 years	Medium. 2–5 years	Short. <2 years	Short. <2 years	N/A	N/A
Cost Guidance (estimate LCC)	High (greater than ~\$1B)	High to Medium (~\$500M–\$1B)	Medium to Low (~\$100M–\$500M)	Low (~\$50M–\$100M)	(~\$10–50M)	(less than \$10–15M)
Launch Constraints	Critical	Medium	Few	Few to none	Few to none	N/A
Alternative Research Opportunities or Re-flight Opportunities	No alternative or re-flight opportunities	Few or no alternative or re-flight opportunities	Some or few alternative or re-flight opportunities	Significant alternative or re-flight opportunities	Significant alternative or re-flight opportunities	Significant alternative or re-flight opportunities
Achievement of Mission Success Criteria	All practical measures are taken to achieve minimum risk to mission success. The highest assurance standards are used.	Stringent assurance standards with only minor compromises in application to maintain a low risk to mission success.	Medium risk of not achieving mission success may be acceptable. Reduced assurance standards are permitted.	Medium or significant risk of not achieving mission success is permitted. Minimal assurance standards are permitted.	Significant risk of not achieving mission success is permitted. Minimal assurance standards are permitted.	Significant risk of not achieving mission success is permitted. Minimal assurance standards are permitted.
Examples	HST, Cassini, JIMO, JWST, MPCV, SLS, ISS	MER, MRO, Discovery payloads, ISS Facility Class payloads, Attached ISS payloads	ESSP, Explorer payloads, MIDES, ISS complex subrack payloads, PA-1, ARES 1-X, MEDLI, CLARREO, SAGE III, Calipso	SPARTAN, GAS Can, technology demonstrators, simple ISS, express middeck and subrack payloads, SMEX, MISSE-X, EV-2	IRVE-2, IRVE-3, HiFIRE, HyBoLT, ALHAT, STORM, Earth Venture I	DAWN Air, InFlame, Research, technology demonstrations

Figure 2.1: Example of Program/Project Types [4, Fig. 3.11-1, p. 38]

One of the first big decisions to be made was the target location of the mission. The Moon was ultimately chosen for several reasons; it is accessible, for example with commercial lunar payload services (CLPS), it is well-known territory and it is a cheap space destination. More specifically the preferred location would be the South Pole of the Moon, as it has been explored less than other regions. From this, combined with our level 1 requirement, we can state the level 2 requirement of this mission: "The mission shall test the mini-XRF on the lunar surface" (A002 in Table 2.1). This requirement then led to the scientific level 1 requirement: "The mission shall be able to detect rare-earth elements in lunar soil." (P001 in Table 2.1). More specifically Sc, Co, La, Ce, Nd, Zr, Y with a secondary objective of finding bulk compositions: Si, Fe, Al, Ti, O. The reason behind looking for these materials were both to test the XRF, but also for possible future industrial applications.

The other big decision made early on was whether to develop an entire mission from scratch, or to piggyback on another mission. Here, piggyback was chosen in order to focus on the primary goal of the project. Many different CLPS were considered for the piggyback, but ultimately the Peregrine Lander from Astrobotic was chosen. Astrobotic is an official commercial lunar payload partner of NASA and NASA currently has a mission

planned with them. Astrobotic was also the company with the most available information about their provided services, which made them the ideal choice. The alternative choice is Nova-C from Intuitive Machines, but due to lack of available information and a higher price, Astrobotic was chosen instead.

With the choice of the Peregrine Lander from Astrobotic the specifications of the mission were narrowed down further. Astrobotic charges 1.2 million dollars per kilogram of payload, and they offer 1 W of power and 10 kbps per kilogram of payload [5].

## 2.2 Overview of the Envisioned System

In this section, an overview of the system is given. The overall architecture is described, along with expectations and objectives of the system. The requirements of the system is also presented, as well as the external interfaces of the system.

### 2.2.1 System description

The proposed system is aimed at bringing a miniaturized XRF instrument to TRL 9 by showcasing functionality in a lunar environment. The instrument shall be used to measure Rare Earth minerals and elements in the soil, as well as measure bulk composition, while also being smaller than other flight-proven XRF's, such as PIXL on the *Curiosity* rover. Given the mission profile, the system shall be flown on a CLPS, bringing it to the lunar south pole, where measurements shall be conducted. Power, thermal stability and communications is provided by the CLPS.

The mini-XRF instrument weighs 1.3 kg and measures 18 cm x 9 cm x 7 cm in dimensions. Compared to the PIXL instrument on board the Perseverance rover, the mini-XRF is more than 11 times smaller in size and over 3 times lighter in mass [6]. Further information and a detailed comparison can be found in Section 5.3.4.2 and Table 5.7.

### 2.2.2 High-level overview

The system is designed in two main parts: The scientific payload, and the movable structure. The payload is mounted onto the movable structure, which is then in turn installed on the mount deck of a CLPS lander, such as the Peregrine lander from Astrobotic Technology Inc, as discussed in Section 2.1.2. A schematic view of the system can be seen in the block diagram below (Fig. 7.1). The payload is comprised of an X-ray source, and a detector setup, along with a LiDAR, for distance measurements, and the necessary electrical circuitry – all contained within a chassis as seen on Figure 2.3. The chassis includes a dust cover to protect the detectors from lunar dust during the powered descent. This chassis is mounted on a telescopic rod, that is also capable of rotating.

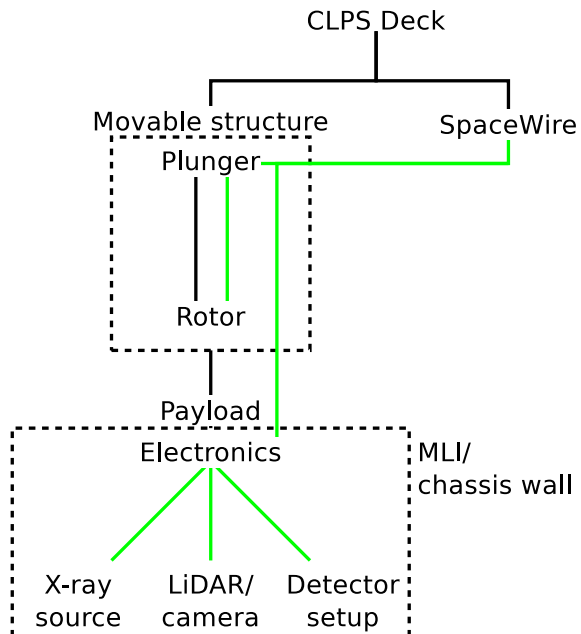


Figure 2.2: Block diagram

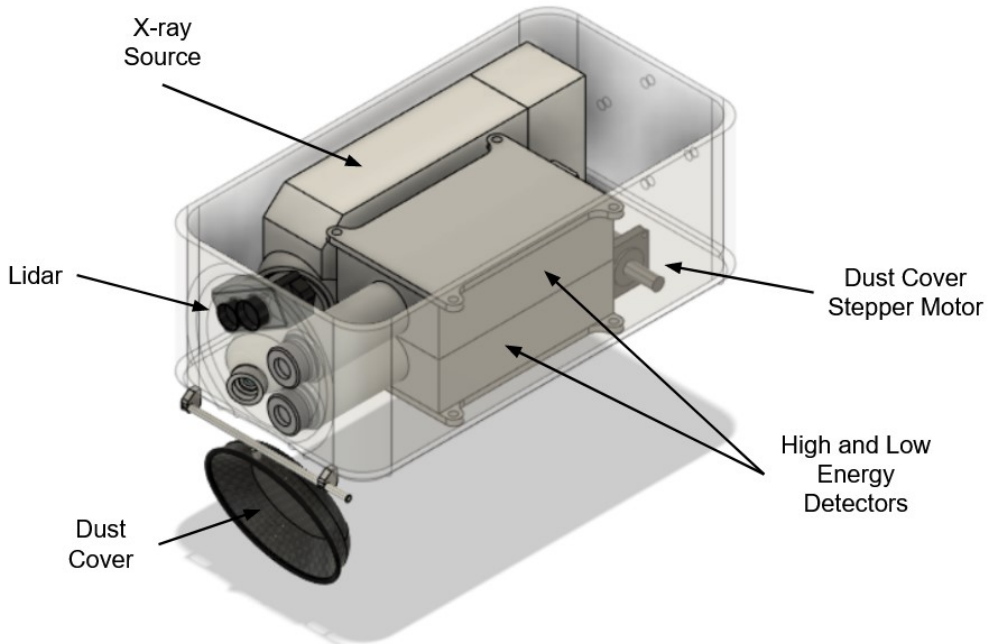


Figure 2.3: Payload chassis, with annotated components.

Under nominal conditions, the telescopic arm will deploy, bringing the chassis close to the surface in order to do measurements. The ranging lidar ensures that the chassis does not strike the surface. To do a measurement, the X-ray tube is switched on and the fluorescent photons from the sample area is measured with the detectors for the duration of an integration.

### **2.2.3 System complexity**

The chassis containing the payload – the X-ray tube, detectors, lidar and electronics is approximately 18x9x7 cm. The entire setup is to be mounted on the side deck of a Peregrine lander, in the polar configuration. The payload and telescopic arm is powered by the CLPS, that delivers up to 2.5 W (at peak) per kg of mission mass ([5]) nominally, and 30 W for deployables. Communication with the ground segment is likewise handled by the CLPS. Given the purpose of the mission, it is beyond the scope of this project to develop a lander/rover with all the corresponding benefits (and limitations).

### **2.2.4 System expectations**

The system requirements all flow from the Level 1 requirement for the mission, as stated in section 2.1. All of the subsequent requirements are stated in the RTM below (Fig. 2.1), and will be referenced throughout the report. The requirements for the individual sub-groups is listed as well. The RTM is useful to trace which requirements depends on each other, and how the different requirements are upheld: there are references to where in this document the requirement is met, if applicable.

The overall system requirements are stated and briefly described below.

Requirement A001 is the mission's level 1 requirement as stated in Section 2.1. In the same section it was argued that the instrument shall be tested in a lunar environment, req. A002. Along those lines, it was deemed suitable to fly the mission on a CLPS (req. A003). It is expected that a lander on the lunar south pole can receive several hundred days of sunlight [7], while on the mid-latitudes a sun-lit day lasts for approximately 14 (Earth) days. Given these limitations, the mission lifetime shall be no less than 14 days - req. A004, and subsequently the system shall survive radiation, thermal environment, bit-flips, vibrations etc., resulting in requirement A005. It flows from A003 that the communication with the ground segment is handled by the CLPS, which is req. A006.

### **2.2.5 External interfaces**

In order to facilitate data transfer from the instrument to the CLPS and further to the ground segment – and the mission control center – the mission shall use a routing switch to transfer data packets to and from the instrument. This element is the gate between the CLPS and the payload/movable structure, as it ensures that commands from the ground segment are passed to the correct elements in the system. This will be further expanded upon in Section 7.2. As a requirement from the CLPS, a VPN connection shall be set up to the command center of the CLPS (as stated in requirement C004). This is to facilitate faster communication between the two teams, and to quickly deal with potential anomalies during launch, cruise or operation.

Req. ID	Shall Statement	Verification	Parent of	Child of
A001	The mission shall bring a miniature XRF to TRL 9	Mission success	A002	
A002	The mission shall test the mini-XRF on the lunar surface	Sec. 2.1.2	A003, P001	A001
A003	The payload shall be mounted on an CLPS lander	Sec. 2.1.2	A004, A006, A007, E002	A002
A004	The mission lifetime shall be minimum 14 days from landing	Sec. 2.3.1	A005, E001, M005	A003
A005	Total risk of system must equal to or less than high risk fig. 2.1	Sec. 2.4	M003, M007	A004
A006	Science data from payload shall be transmitted by the CLPS to ground station on Earth	Sec. 7.1	C001, C002	A003
A007	CLPS will land on South Pole of Moon	Sec. 2.1.2		A003
A008	The payload shall be able to withstand a cumulative ionizing dose of 1 krad	Sec. 3.3.3		A004
P001	The mission shall be able to detect rare-earth elements in lunar soil.	Sec. 2.1.2	P002, P003	A002
P002	The scientific measurements shall be done at a maximum distance of 15 cm	Sec. 4.2	M001	P001
P003	The mission should be able to measure bulk compositions.	Sec. 4.6.5		P001
P004	Science payload must use a maximum of X W for measurements	Tab. 6.5		E002
M001	The scientific payload shall be mounted on a movable structure	Sec. 5.5	M002	P002

Table 2.1: Requirement Traceability Matrix (RTM). Continued on the next page.

M002	The movable structure shall be mounted on the CLPS Lander	Sec. 5.2		M001
M003	The payload shall be rigid until deployment	Sec. 5.3.4.1	M006	A005
M004	Movable structure must use a maximum of 15 W for deployment and repositioning	Tab. 6.5		E002
M005	The payload shall be thermally stable within -30 to 80 deg C, during the mission lifetime	Sec. 5.3.4		A004
M006	Payload shall be able to withstand loads in regards of vibrations, acoustic load and shock	Sec. 5.3.4.1		M003
M007	The payload shall be protected against lunar dust during powered landing	Sec. 5.3.3.3		A005
E001	The EPS shall store and redistribute power to the other subsystems	Sec. 6.3		A004
E002	The EPS shall receive the necessary power from the CLPS	Sec. 6.1.3	P004, M004	A003
C001	Scientific data shall be transmitted by CLPS within 24 hours, under nominal operation conditions	Tab. 7.1	C003, C004	A006
C002	Comms system shall encode data with error correction	Sec. 7.2.4		A006
C003	Scientific data should be transmitted once per day	Tab. 7.1		C001
C004	There shall be setup ground station communication through a VPN to the CLPS command center	Sec. 7.4.1		C001

Requirement Traceability Matrix (RTM). Continued from previous page.

## 2.3 Mission phases

This mission follows the NASA handbook's standard phases, which include Pre-Phase A, Phase A, Phase B, Phase C, Phase D, Phase E, and Phase F.

Figure 2.4 depicts the various stages of a standard mission, which are divided into the "formulation program" (consisting of pre-phase A, phase A, and phase B) and the "imple-

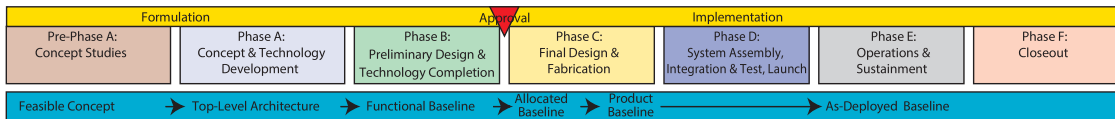


Figure 2.4: NASA systems engineering handbook's project life cycle phases [4, Figure 2.2-1]

mentation program" (comprising the remaining phases). This figure offers a succinct yet valuable summary of the mission's evolution, from its early development to its ultimate fulfillment.

Starting in March 2023, the mission is currently in its pre-phase A with preliminary designing and building the skeleton of the mission as a whole. Figure 2.5 below illustrates the mission phases and their estimated durations with some key points on the content of each phase. We are aiming at launching in the early 2030s with an operational lifetime of between one to two months.



Figure 2.5: Operational phase, in detail

Pre-Phase A involves concept studies, identifying mission objectives, stakeholders, initial requirements, and developing the mission concept. Additionally, piggyback agreements are evaluated, initial technical risks are identified, and the concept of operations is developed and base-lined. The roles and responsibilities required for performing mission objectives are identified. The initial design for the payload, as well as the holder and mover of the payload at the lunar ground, are determined. The preliminary communications and electronics design, as well as the atmospheric conditions on the Moon and other celestial bodies, are also described.

Phase A is focused on concept and technology development, including identifying requirements and constraints, management, safety, risk, performance, mission assurance, and mission architecture. This phase involves base-lining top-level requirements and constraints, system requirements, and developing the preliminary verification and validation plan. Additionally, different environment evaluations are conducted.

Phase B is the preliminary design and technology completion phase. It includes detailed preliminary design, technology development, cost budget, mass budget, and risk evaluation. During this phase, a plan for technology completion is developed.

Phase C is the final design and fabrication phase, including hard- and software designs, refinement, launch site preparation, orbital debris assessment, and piggyback preparation and clarification.

Phase D involves the final stages of the mission, where the spacecraft's design is finalized, fabricated, and assembled. This includes integrating and verifying the various components and performing validation tests on the spacecraft. Operator's manuals, maintenance manuals, and operations handbooks are also developed during this phase, along with detailed hardware and software designs. The project's progress is closely monitored, and risks are identified and updated as necessary. Additionally, launch, operations, and ground support sites are prepared, and relevant systems engineers receive training to ensure a successful mission.

Phase E focuses on operations and sustainment, including system assembly, integration and test, launch and checkout, operation and sustainment, launch, orbit, landing, initial check, test measurements, science measurements, data retrieval and verification, and launch covered by EPSP (External Payload Service Provider). During this phase, the payload is launched, initial checks are performed, test measurements are taken, and science measurements are performed. Data is retrieved from the payload, and launch vehicle lift-off, separation from the launch vehicle, insertion into lunar orbit, touchdown on the lunar surface, replacement of payload, start-up of payload, measurements collection, and data reception from payload are performed.

Phase F is the closeout phase, which includes the checkup of data, turn-off, storage possibilities, decommissioning, and close-out. During this phase, remaining data is checked and sent, mechanical structures are set to storage mode, XRF, detector, and onboard computer are turned off, and storage and decommissioning are planned.

Overall, following these mission phases ensures that the mission is conducted efficiently and safely and that all team members are on the same page.

Diving into the specifics of Phase E, the timeline below outlines the subphases and durations during the active operational lifetime of the spacecraft. Further details on this will be provided later in the report.

### 2.3.1 Nominal operation

During Phase E, the scenario for nominal operation starting from launch, orbit and landing on the Moon shall function as described in Section 3.2. The current information from Astrobotic limits precision on an exact date for launch and duration during flight. Therefore, nominal operation is an interval of time from launch to landing, where actual duration is not as important as the timing of the lunar day when landing. Given a minimum of 14 Earth days, all science goals should be achievable.

A specific landing spot, other than somewhere on the South Pole of the Moon, is also not important to achieve mission success, other than that it needs enough sunlight to acquire enough operation time on the surface. This system is also not dependent on actually landing on the South Pole of the Moon, other than given the chosen configuration of the Astrobotic lander, it is designed to generate power on the poles of the Moon. The lander need only land stably on a relatively flat surface, thus ensuring the height from the position of the system to the surface is within expected.

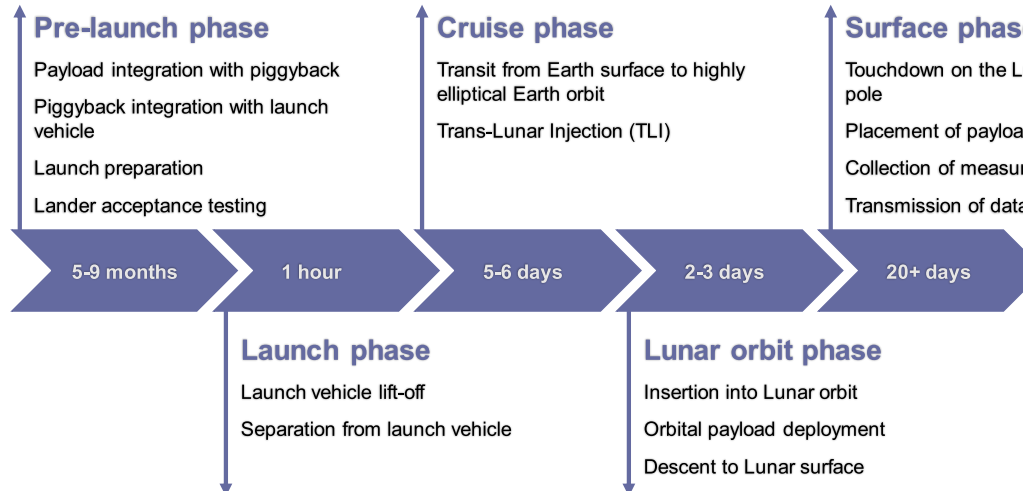


Figure 2.6: Operational phase, in detail

After landing, a communications and general functions test will be performed. This check, along with information from the Astrobotic team, will provide information on the actual communication bandwidth and power available. Given nominal power and communication bandwidth, the system can proceed to slowly deploy the telescopic rod, performing several distance checks during the deployment. Given nominal performance of the LiDAR and the camera, the XRF source and detector will be placed close enough to the surface to function to specifications. The LiDAR will perform the first distance checks, before the payload is closer than 10 cm to the surface where the camera will take over. The camera will then send pictures to Ground Control, where the surface can be inspected, and decisions can be made to go closer or not to the surface.

When the desired distance is achieved, the first X-ray measurements can be performed with integration time chosen in accordance with distance and power available. The data will then be sent to Ground Control, where it will be evaluated for how well the instrument has performed (is the data significant, is the signal to noise ratio good enough). If the bulk composition of the surface soil can be determined, the overall scientific objective has been achieved. If not, integration time or distance may need to be altered, or the system need to be error checked in other ways. In any case, the system is designed to perform multiple measurements at different surface locations, to ensure maximum scientific output and that the payload has been tested more than once. The rotor will rotate the payload around the telescopic rod, and a new measurement will be performed. The measurements will not be performed quickly after one another, but with hours in between, ensuring enough time for analysis of data, and sending commands to control the position of the payload. Ground control will continuously monitor the measurements, and will continue operation while possible. Data of measurements can then be compared to see if the soil is similar around the telescopic rod, or if the bulk compositions changes. Pictures from the camera will be used to compare the bulk composition results to visible differences on the surface. Overall evaluation of the instrument's performance will determine mission success.

### 2.3.2 Off-Nominal operation

There are many scenarios for off-nominal operation, some of the most plausible scenarios are reviewed here.

**The timing of the landing in the lunar day gives less than 14 days of operation.** Unless operation time is less than a few days, it will still be possible to perform at least one – or a few measurements, and therefore completing the overall mission goal. Though this results in fewer measurements, TRL-9 is still achievable.

**The communication bandwidth is lower than stated by Astrobotic.** The overhead on communication bandwidth is so large, that communication should not have any effect on operations after landing.

**Power available is less than nominal.** Depending on how much less power is supplied, this can result in longer integration times for measurements, or making it impossible to operate the XRF source.

**One or multiple telescopic rod motor(s) fail.** The telescopic rod is made with springs (see Section 5.5.1) to ensure operation even if a motor has trouble. Since there are multiple shells in the lowering mechanism, even if one fails it should not effect scientific performance if integration time and/or power used is adjusted. Similarly for the dust cap, springs should ensure deployment in case of motor failure.

**The rotor does not function.** The measurements can in this scenario only be taken from the same spot. This reduced the scientific output, but mission success can still be achieved if one or multiple measurements are taken, and the bulk composition can be determined.

## 2.4 Risk Assessment

Since this mission is classified as a Type D mission, a high risk level is acceptable [4, p. 38]. In this section the highest risks are reviewed. Note that some risks have already been mitigated or redundancy has implemented in the design, while others would be further investigated and mitigated in future works.

The timing of landing during the lunar day is a risk, since it can reduce the operational time. It is not a high risk, though it is difficult to classify, since actual launch and flight time is not known at this point in time. Since it would affect all customers onboard the Astrobotic lander, one would assume Astrobotic would do what is possible to ensure the promised operation time on the surface.

The actual provided bandwidth could be lower than stated, this is entirely possible depending on the actual landing position, but the big overhead in communication bandwidth makes this a very low risk.

A higher risk is if the lander cannot provide enough power to our payload. While a higher integration time can be implemented to help with this, there exists a lower limit while integration times are still deemed acceptable (see section 6.2.1). Since it is needed to buy additional power from the CLPS, the risk factor cannot be classified, since no details can be found on what the possibilities are for this, and/or how the CLPS will manage their power budget.

The telescopic rod motors is designed to minimize malfunctions, and even if one section malfunctions deployment is still partially possible, because of the multiple shells in the rod.

The dust cover is currently powered by a single stepper motor. This poses a high risk for the mission, since if the dust cover cannot be removed, measurements cannot be performed. Thus a secondary opening mechanism, would likely be included in the design, if the project is taken to the next stage.

The XRF source and detector can fail in multiple ways, as is the case with most sensitive electronics. The components are however chosen to either already tested in flight or be simple and therefor have a high probability to survive flight. If the source cannot be operated it is mission over, but one detector can function without the other, though it would limit the scientific output.

If the LiDAR cannot provide distance measurements, the distance cannot be determined during deployment of the telescopic rod. This will slow the deployment process, but since the telescopic rod is lowered with gearing, the deployment cannot be done incrementally until the camera can perform distance measurements.

If the camera fails to perform close to specifications, and therefore cannot provide reference pictures and/or distance measurements, the LiDAR must take over distance measurements close to the ground, and a bigger safety margin must be adopted. The integration time must be increased, but scientific output should still be possible. The pictures for reference will decrease the scientific value, but if the bulk composition can still be determined, it can still be deemed a mission success.

The system is not designed to withstand a large solar storm or other large cosmic radiation events. During a 14 Earth day expected minimum lifetime, this is however a small risk (section 3.5.2). Cosmic rays which incur bit flips or similar, will be taken into account if the project is taken to the next stage.

In conclusion, there exists multiple instances of higher risk, and while most risks have been reduced, the inherent risk of components untested in space will always be a risk, and this is acceptable under the mission Type D requirements.

## 2.5 Cost analysis

The total mass budget of the mission, including the mini-XRF, mechanical components, and other necessary equipment, is 3.53 kg. A detailed breakdown of this budget can be found in Section 5.6 and Table 5.10.

In terms of the cost budget, the main expenses include purchasing space in Astrobotic's lander Peregrine to transport the payload to the Moon, which is currently priced at 1.2 million USD per kg of payload, and the payment of systems engineers and other team members working on the mission throughout. Many of the components used in the mission are off-the-shelf, but a detailed cost analysis is yet to be conducted regarding these and other costs.

Based on the NASA Type D project guidelines, the expected total cost for the mission is estimated to be between USD 50-100 million (Fig. 2.1). While this is a rough estimate at this point, we cannot provide more accurate information on the cost budget until a detailed analysis is conducted.

## 2.6 Long-term considerations

Our instrument's development takes into account the requirements of different celestial bodies, with a focus on withstanding environments similar to the Moon's. General and specific requirements have been considered, as detailed in Section 3.4, ensuring the instrument is well-suited for the Moon's atmosphere-less environment.

While the primary mission goal is to miniaturize and improve performance, the long-term objective is to develop an instrument adaptable to various celestial bodies. It is important to clarify that this goal is beyond the current mission scope. To prepare for future exploration, the instrument will e.g. be equipped with additional thermal protection to withstand different environments.

# 3 Launch, Orbit and Landing

This chapter covers an introduction to the environment that both the S/C and payload will be exposed to throughout the duration of the mission, i.e. the pre-operational payload environment will be presented. To ensure that the overarching mission objectives are achieved, one must ensure to consider the general environment of the mission. If not, it could result in catastrophic consequences, and may even lead to mission failure. In general, the requirements for the payload are a result of the mission environment, which will be presented. There are a plethora of environmental factors to consider, but only the very crucial ones will be presented; these include the mechanical, thermal, pressure, and radiation environment. Furthermore, both thermal and radiation management will also be touched upon.

## 3.1 Spacecraft Environment Overview

### 3.1.1 Pre-launch Spacecraft Environment

The design, manufacture, assembly, integration, and verification is a lengthy process lasting years. Components and subsystems may be stored for long periods before the eventual launch. Careful environmental control during storage is essential in order to avoid any degradation of the spacecraft system as a whole.

The engineering discipline AIV (*Assembly, Integration, and Verification*) is performed during the last stages before launch, to verify to a very high level of confidence and probability that the hardware will perform the desired mission. Assembly is the process of mechanically bringing together all hardware components large and small from all suppliers to build up the spacecraft. This ranges from spacecraft structures to subsystem electronics and payload sensors and further down to cables, thermal blankets, bolts, and washers. Integration is the process of physically and functionally combining equipment in a controlled and measured sequence. Each interface between two components needs to be shown to be correct.

Finally, verification is the total process by which all applicable performance requirements are demonstrated. This is the sum of two stages, qualification, and acceptance, which can be applied by different methods such as tests, analysis, inspection, and review of the design. As this needs to be a very thorough process, a verification plan is normally worked out, and standards for Verification Engineering can also be found in official instances such as the *European Cooperation for Space Standardization* (ECSS) [8]. Verification is not included as a product of project Phase A in the NASA Systems Engineering Handbook [4]. However, this phase produces a baseline for functionality that can be used in to prepare the project's downstream processes such as verification. We will thus conclude that AIV will be a major part of the time spent "pre-launch" and that verification plans should be produced in later project phases.

### 3.1.2 Electromagnetic Environment

In the NASA Systems Engineering Handbook [4] under the Concept and Technology Development, which is defined as the Space Flight Projects Phase A, a typical activity and product is the baseline plan of Electromagnetic Compatibility(EMC) and Interference(EMI) control plan. Electromagnetic Interference is the phenomenon in which one component or subsystem interferes with the proper operation of another subsystem due to the propagation of electromagnetic energy, whereas Electromagnetic Compatibility is the discipline

of ensuring that electronic components function together in the resulting electromagnetic environment. Thus we wish to control the EMI to obtain EMC. The Electromagnetic Compatibility requirements are defined in [9] as

- The payload and its elements shall not generate electromagnetic interference that could adversely affect its subsystems and components, other payloads, or the safety and operation of the launch vehicle and launch site.
- The payload and its subsystems and components shall not be susceptible to emissions that could adversely affect their safety and performance. This applies whether the emissions are self-generated or emanate from other sources or whether they are intentional or unintentional.

All EMC problems have several aspects in common, namely a source or transmitter that produces emissions, a receiver that receives emissions, and a transfer or coupling path between transmitter and receiver.

#### **3.1.2.1 A systems approach to EMC**

To obtain the requirements set by the EMC it must be considered as an integral part of the specification, design, manufacturing, and testing phases of any spacecraft. System margins and budgets are attached to the EMC performance in the same sense as e.g. power budgets are applied to Power Systems [8]. As this mission applies an external space-craft provider, our payload has to be designed in compliance with radiated and conducted electromagnetic emissions standards based on the payload type. From Astrobotic's point of view, the miniature-XRF payload is categorized as a "Static Active" payload [5], as it remains attached to the lander and performs mission tasks. The set of EMC requirements that have to be fulfilled are shown in Tab. 3.2. These requirements are from the US Department of Defenses Interface Standard [10]. The requirements document divides the EMC into four categories

- Conducted Emissions
- Conducted Susceptibility
- Radiated Emissions
- Radiated Susceptibility.

For all requirements, a testing procedure is outlined with specific requests for the data presentation. From this document, the Electromagnetic compatibility tests can be performed before integration with the spacecraft as well as after to determine whether the payload's electromagnetic performance can affect the spacecraft.

## **3.2 Orbit Description and Stages**

Astrobotic and their respective launch vehicle was selected for the mission, from which general information was provided. Astrobotic provided a mission profile that included five phases, each with its own specific time schedule. These time schedules lack precision, as time ranges from a few days to more than a month. This occurrence is likely due to the nature of Astrobotics as a company, as time schedules are most often based on demands set by the customer [5].

Taken this into account, and for ease of understanding the environment that the S/C will encounter, the mission is categorized into multiple stages. These stages will indicate the specific ranges of the environmental factors and duration. It can be noted upon that these factors will be describing the pre-operational payload environmental. Furthermore it can be noted that the actual placement of the payload structure, is defined in section 5.

In general, it is assumed that the S/C launches into a low Earth orbit, and from there performs a Hohmann transfer to reach lunar orbit. Specifically, this time-line can be categorized into the following stages: (1) Launching from Earth, (2) orbit around Earth, (3) Earth-lunar transfer orbit, (4) lunar injection, (5) lunar orbit (6) and landing onto the surface located at the southern pole of the lunar surface. From the mission objectives, these are the stages before payload operational usage. This can be written into a table, comparing stage, with designated time-allocation and number of orbits, as seen in Table 3.1.

Pre-Operational Payload Time Schedule		
Stage	Time [hours]	Nr. of Orbits
(1) Launch	1	-
(2) Earth Orbit	2.15	2
(3) Earth-lunar Transfer	120	0.5
(4) lunar Injection	-	-
(5) lunar orbit	2.15	2
(6) lunar South Pole Landing	1	-

Table 3.1: Pre-operational payload time schedule of each stage, based on information derived from Astrobotic and general mission objective. The values are derived from trivial orbital mechanics and yield an accurate estimate of the pre-operations timeline.

Furthermore, in the upcoming sub-chapters, the software Space Environment Information System (SPENVIS) by the European Space Agency (ESA) is used to conduct an in-depth analysis of the environment that both the S/C and payload will be subjected to. This in tandem with observed data from NASA will serve as a basis for what can be expected throughout the mission, such that appropriate precautionary measures can be set in place.

### 3.3 Stages

The upcoming paragraphs will delve into the specific environmental factors that are relevant to this stage of the mission. These factors will form a basis for the payload requirements moving forward.

#### 3.3.1 Launch

The launch stage marks the beginning of the mission and presents the first major shift in environmental conditions. Especially, the mechanical environment will undergo significant changes during the phases of the launch. A SPENVIS simulation has been carried out to show a launch trajectory for a spacecraft reaching an altitude of 2000km.

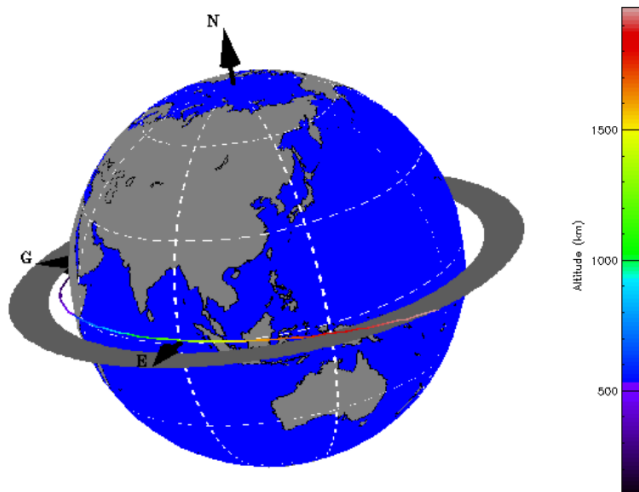


Figure 3.1: SPENVIS orbit generator simulation with planet Earth, Launch trajectory for an S/C reaching an altitude of 2000 km. The magnitude of altitude in units km is described by the rainbow bar.

In order to set the specific environmental constraints for the mission a launch vehicle should be selected. The selection of a launch vehicle will fall to the chosen spacecraft provider Astrobotics. The different Commercial Lunar Payload Services applies multiple launch vehicle providers and Astrobotics themselves have for their two planned mission two different launch providers

- The Peregrine Mission 1 scheduled for 2023 launch will fly on a United Launch Alliance Vulcan Centaur rocket [11].
- The Griffin Mission 1 scheduled for 2024 launch will fly with a SpaceX Falcon Heavy rocket [12].

One could assume either SpaceX or United Launch Alliance as a launch partner. Going forward environmental considerations for the spacecraft i.e. the Astrobotics lander holding the system will be considered without further consideration of the launch vehicle or launch partner.

### **Thermal Environment**

The temperature ranges from 0-30 Celsius. The integrated lander is encapsulated throughout the launch phase in an environmentally controlled launch vehicle payload fairing [5].

### **Mechanical Environment**

The most demanding environment for the structure of the spacecraft is probably during launch. During the launch phase, the spacecraft and launch vehicle will be exposed to high levels of vibration, associated with both noise fields and structural vibrations, high levels of acceleration, mechanical shocks, and rapidly declining ambient pressure. The effect of these are examined separately below.

### **Acoustic Vibrations**

Payloads are subjected to sound pressure loads, which peak during lift-off and transonic flight.

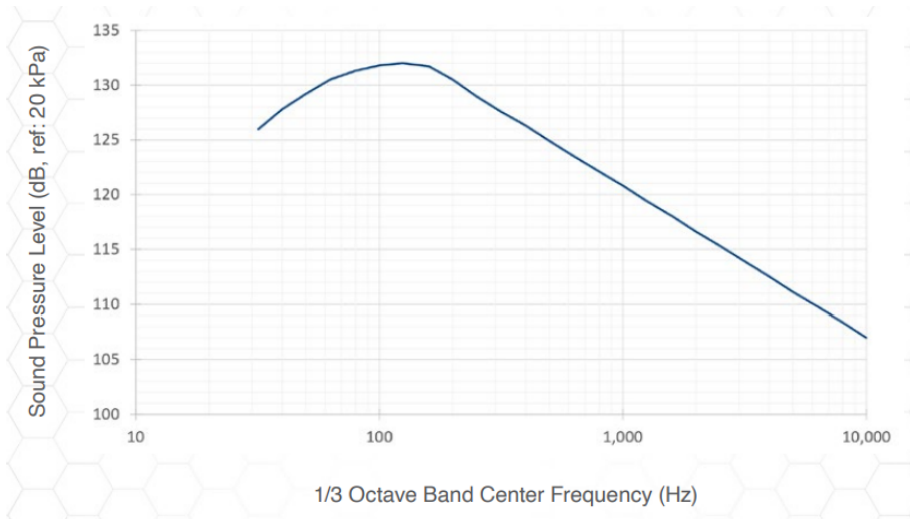


Figure 3.2: Plot of limiting acoustic qualification loads. The expected duration of these loads is less than two minutes [5].

## Random Vibration

Random vibration loads can arise from unsteady engine combustion, exhaust noise, and turbulent flows along the launch vehicle.

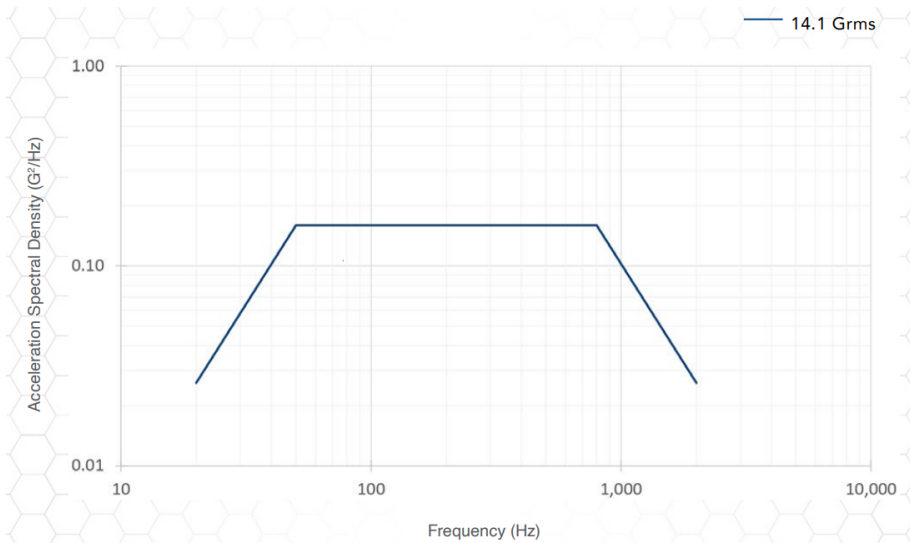


Figure 3.3: Plot of limiting loads for random vibration along all axes. A duration of two minutes per axis may be assumed [5].

## Mechanical Shocks

Payloads will encounter multiple shock events during launch and injection, namely at launch vehicle fairing release, lander separation, and landing itself. These instantaneous events can provide high-acceleration levels lasting only a few milliseconds locally or globally through the system.

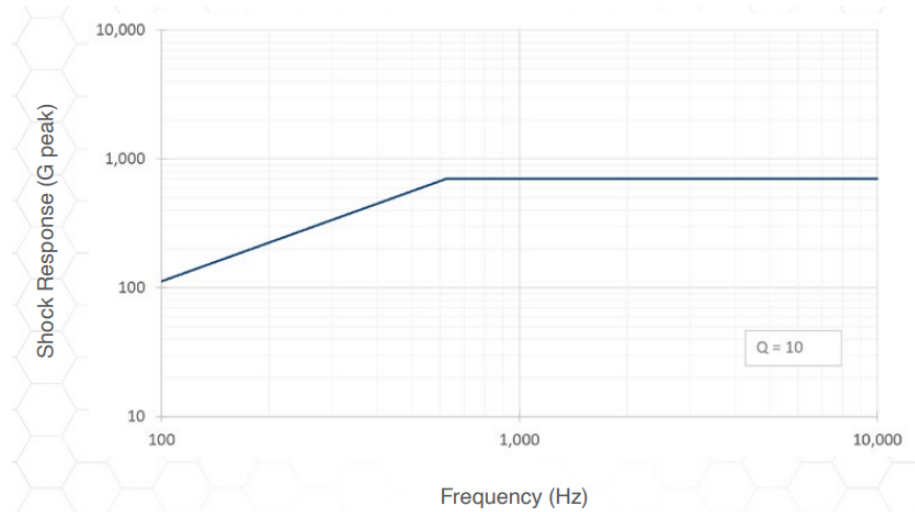


Figure 3.4: Plot of the limiting shock loads. Payloads should be prepared to endure a few shock events with these limiting loads [5].

### Pressure Environment

The ambient atmospheric pressure declines during launch. The rate at which depressurization occurs depends on the venting of the shroud volume, which can be fixed by the inclusion of venting ports. Astrobotics provides a typical pressure drop curve for launch, which envelopes the pressure drop for all mission phases.

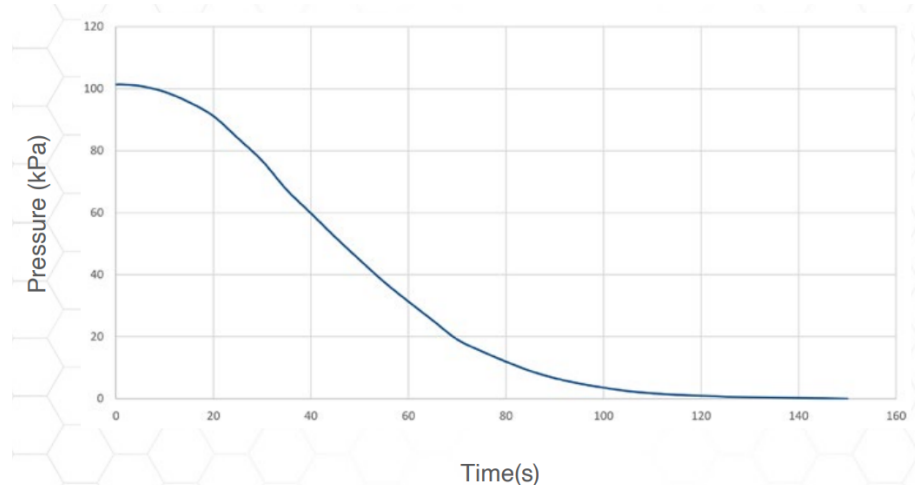


Figure 3.5: The expected pressure drop during launch. The drop is expected to surpass  $-2.5 \text{ kPa/s}$  only briefly during transonic flight [5].

For the rest of the mission stages, the lander is exposed to a pressure of  $3.2 \times 10^{-5} \text{ kPa}$ , due to the vacuum of space.

### Radiation Environment

The radiation environment is negligible for the Earth's environment. This is due to the Earth having an atmosphere that protects against solar radiation which is the biggest producer of radiation in a space mission to the Moon.

### EMC Environment

As described earlier great care is required during integration to ensure that EMC is obtained and thus does not present a hazard to the mission. Assuming that verification

of EMC is obtained, the electromagnetic environment will not change during the pre-operational part.

### 3.3.2 Earth Orbit

At this stage of the mission design, the launch vehicle has reached a stable circular orbit at an altitude corresponding to that of an LEO. The S/C altitude is situated at 2000 km above the surface of Earth, with an inclination of  $5.145^\circ$  to match that of the lunar orbital inclination. These values are set with the aim of ensuring that geometries concerning the transfer orbit are as simple as possible. This is to ensure preparations for stage (3), the Earth-lunar transfer. As previously mentioned in Table 3.1, the number of orbits at this altitude is, as of now two, however, this number can be adjusted based on external factors concerning either Astrobotic or general mission adjustments. But as of this analysis, it is assumed that the number of orbits will remain at two.

In the software, SPENVIS, a simulation of this orbit was conducted, where it is possible to see the inclination of the orbit, compared to that of the Earth's axis of rotation, which is seen in Figure 3.6. The main environmental shift at this stage is due to the Earth's magnetic environment.

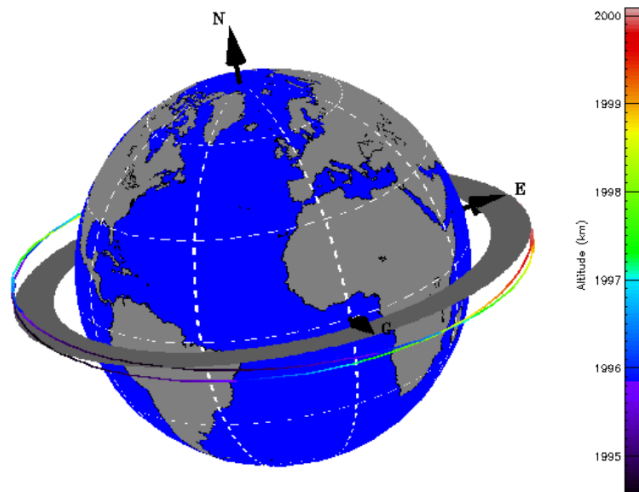


Figure 3.6: SPENVIS orbit generator simulation with planet Earth, for a circular orbit at an altitude 2000 km at an inclination of  $5.145^\circ$ . The magnitude of altitude in units km is described by the rainbow bar.

### Thermal Environment

Same as Earth-lunar transfer phase.

### Radiation Environment

In the radiation environment near the Earth's orbit, the radiation is defined by the trapped radiation from the Earth's magnetic field. Radiation can reach as high as 20 rads/day when the spacecraft is directly passing through the Van Allen belts. This ionizing dosage is based on the expected electron as well as heavy ion and proton radiation per Earth day. In our case the spacecraft may spend anywhere from 1 to 15 days in this environment, depending on the specific mission trajectory [5]. Since Van Allen belts has the highest amount of radiation, spending as little time as possible here, is ideal.

### 3.3.3 Earth-Lunar Transfer

The next stage spans the longest, in both time and distance of the pre-payload operation period. This stage is the Earth-lunar transfer orbit. As this stage is not specifically denoted

by Astrobotic, it can be assumed that the orbital maneuver will be a Hohmann transfer. This is simply based on that a Hohmann transfer is the most fuel-efficient maneuver one can have, with the downside of a longer half-period of transfer. However, since the objective of the mission is located at the lunar surface, it is possible to derive that a lunar transfer, initially from LEO, will take approximately five Earth days derived from trivial elliptical geometries. This timescale are considered to be adequate when compared to the entire mission profile.

Calculation regarding the necessary  $\Delta v$ 's to perform a Hohmann transfer was conducted. It was determined that for the initial maneuver located at the LEO, requires a  $\Delta v$  of 2.752 km/s to go into a highly elliptical orbit. Once the S/C reaches the apogee of the elliptical orbit at a distance of  $3844 \cdot 10^5$  km, the S/C will perform a second, similar maneuver which will transfer the S/C into orbit around the Moon. This maneuver's a  $\Delta v$  of 0.807 km/s. The total  $\Delta v$  which is required for this stage is 3.56 km/s, which will also contribute to the bulk of changes in velocity throughout the mission. Furthermore, throughout the transfer, it is noted that small thrusts will be performed, to angle the S/C will inject with lunar orbit at a polar inclination angle.

In the following figures, the Hohman transfer was simulated and plotted using SPENVIS, similar to previous stages. This trajectory was plotted in two different coordinate systems, the Geocentric Equatorial Inertial system (GEI) and the Geographic coordinate system (GEO). The GEI is a non-rotating fixed frame of reference, which yields trajectories similar to ones that could be described on paper. On the other hand, the GEO is a rotating frame of reference, at the same rate to that of Earth. Figure 3.7 show the Hohmann trajectory in both frames of reference.

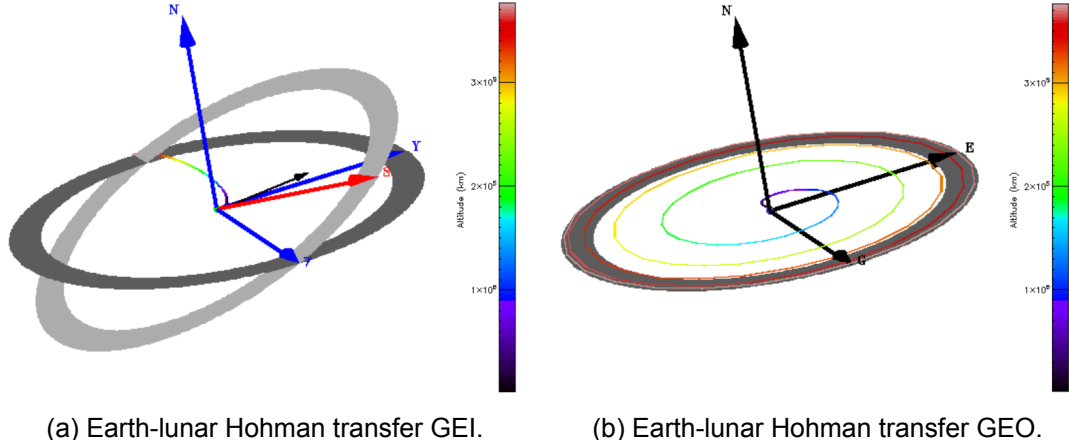


Figure 3.7: SPENVIS orbit generator simulation with planet Earth. Both sub-figures are the same Earth-Moon transfer orbit. Figure 3.7a is the Hohmann transfer plotted in the GEI reference frame, and 3.7b is the same Hohman transfer, plotted in the GEO reference frame.

The upcoming paragraphs will delve into the specific environmental factors that are relevant to this stage of the mission. These factors will form a basis for the payload requirements moving forward.

### Thermal Environment

The temperature ranges from -40 to 60° During the Earth-lunar transfer, the thermal environment is significantly colder for objects in shadow and much hotter for objects in direct

sunlight. Throughout the flight, the landers are nominally oriented with the top-mounted solar panel facing the Sun. As a result, the lander's top side receives the most incident solar radiation, and resulting heat, during the Earth and lunar Orbit phases.

#### **Radiation Environment**

For the rest of the space mission, the radiation environment occurs in the region outside of the shielding effects of Earth's magnetic field. An ionizing dosage of 1 rad/day is predicted there based on the expected electron radiation per Earth day.

#### **3.3.4 Lunar Injection**

As mentioned in the previous stage, the amount of  $\Delta v$  required to reach the Moon is 3.56 km/s. From this the S/C will reach the Moon's sphere of gravitational influence, injecting at an altitude of 200 km above the lunar surface. The calculated  $\Delta v$  to make a capture maneuver will be performed on the far side of the Moon. This is to ensure that the S/C makes an appropriate insertion into the lunar orbit.

#### **Thermal Environment**

Same as an Earth-lunar transfer.

#### **Radiation Environment**

The radiation environment is the same as for Earth-lunar transfer.

#### **3.3.5 Lunar orbit**

At this stage, the S/C is in a stable circular orbit with an altitude of 200 km above the Lunar surface. As stated in section 3.3.3, the S/C will inject the lunar orbit at a polar inclination. This will result in two orbits at the specified polar inclination angle. This is to ensure that the lander is aligned to the mission location of the Lunar south pole. Moving forward from this, it is possible to note that gravity anomalies are abundant on the Moon. This means that potential major perturbation of an orbit can happen at altitudes of less than 500 km. Taking this into account from the time schedule defined in Table 3.1, it can be deemed appropriate with two orbits with periods of about an hour. However, depending on Astrobotic's own time schedule, the altitude of the orbit should be increased to avoid unnecessary orbital maneuvering. At this stage the only major environmental shift is seen in the temperature due to the presence of the Moon.

#### **Thermal Environment**

The Temperature ranges from -20 to 100 Celsius. The thermal environment is significantly colder for objects in shadow, particularly during lunar eclipse, and much hotter for objects in direct sunlight, which can be compounded by light and infrared radiation from the lunar surface.

#### **Radiation Environment**

The radiation environment is the same as for Earth-Lunar transfer.

#### **3.3.6 Lunar South Pole Landing**

This stage is the lunar south pole landing. Firstly a little about the general descent. Due to the lack of an atmosphere, luckily no atmospheric drag will occur when decelerating towards the Lunar surface. However, this comes with a price, as there is nothing to slow the lander when nearing the surface, and parachutes can not be used for obvious reasons. As Astrobotic was the chosen company for the south pole mission, it is assumed that an attitude control to make sure that the angle of the S/C is pointed towards the surface, and a propulsion system adequate for such a decent is provided. The lunar surface environment is described in below paragraphs.

#### **Thermal Environment**

The temperature ranges from -30 to 80 Celsius. The thermal environment is significantly colder for objects in shadow and much hotter for objects in direct sunlight. This range

is relevant for the nominal lunar surface operations duration and does not include lunar nights or missions to equatorial latitudes. If the Sun is visible for 14 days with sustainable shadows and the opposite for when the pole is in the shadow.

### **Mechanical Environment**

Some mechanical shock is expected during the impact of the lander on the lunar surface. The mechanical shock expected during landing is enveloped in Fig. 3.4 and managing the mechanical shock due to the landing is included in the Lander design. If needed absorbing materials could be included in the system design. Astrobotics will without a doubt perform landing simulations with the conditions of lunar gravitational acceleration, soil stiffness, soil damping, frictions as well as various falling heights and surface angles.

### **Radiation Environment**

The radiation environment is the same as for Earth-Lunar transfer.

### **Electromagnetic Environment**

This stage differs from the previous stages in terms of the electromagnetic environment as all operational equipment is now turned on. The EMC testing and validation also cover this scenario, so all are able to function together.

## **3.4 Environmental Constraints from CLPS**

In the previous sections, the environmental conditions to which the spacecraft will be exposed have been described and evaluated. Defining environmental requirements is key to any space mission in order to ensure that the system and the environment are compatible during flight and operation. This section summarizes the environmental constraints set by spacecraft partners on their spacecraft landers and by those on our payload. This can also be viewed as a summary of the previous section. Both the primary spacecraft partner, Astrobotic [5] and alternative spacecraft partner, Intuitive Machines [[IM\\_2022lunarGuide](#)], are examined in the table.

Company	Astrobotic	Intuitive Machines	Comment
<b>Mechanical Environment</b>			
Random Vibration Loads	0.025 G <sup>2</sup> /Hz @ 20 Hz. 0.105 G <sup>2</sup> /Hz @ 50 - 800 Hz. 0.025 G <sup>2</sup> /Hz @ 2000 Hz.	0.015 G <sup>2</sup> /Hz @ 20 Hz. 0.08 G <sup>2</sup> /Hz @ 50 - 800 Hz. 0.015 G <sup>2</sup> /Hz @ 2000 Hz	Loads from unsteady engine combustion, exhaust noise, and turbulent flows. Better viewed in Fig. 3.3
Acoustic Loads	Peaks 132 dB @ 140 Hz	Peaks 132 @ 125 Hz.	Sound pressure loads which peaks during lift-off and transonic flight. Better viewed in Fig. 3.2
Shock Loads	110 G @ 100 Hz. 700 G @ 600 - 10.000 Hz	50 g @ 100 Hz. 1000 g @ 1000 - 10.000 Hz.	Shock events during launch and injection such as lander separation and landing.
<b>Thermal Environment</b>			
Pre-Launch Temperature (storing)	0 - 27 °C	5-30 °C	Pre-launch processing is climate controlled to a specified temperature range.

Launch (storing)	0 - 27 °C	20 ± 3 °C	Landers are encapsulated in environmentally controlled launch vehicle payload fairings.
Cruise (storing)	-40 - 60 °C	-100 - 100 °C	Temperature varies during the cruise depending on whether the lander is in shadow or Sun.
lunar Orbit (storing)	-120 - 100 °C	-100 - 100 °C	The lunar orbit is the most extreme thermal environment, as the lander will orbit through the Moon's shadow and transition between the Sun and shadow regularly.
lunar Surface	-30 - 80 °C (Operational)	-100 - 150 °C (Storing)	Astrobiotic temperature range applies for nominal lunar surface operations i.e. does not include nights. Intuitive Machines range applies night conditions.
<b>Pressure Environment</b>			
Pre-launch	101.25 kPa	91.19 - 101.33 kPa	The pressure slightly varies depending on the exact location of launch and integration facility.
Launch lower limit	-5.0 kPa/s.	-6.18 kPa/s	Pressure drops during launch. Examine Fig. 3.5 for more detail.
<b>Electromagnetic Environment</b>			
EMI Category	Requirement		Applicability
Conducted Emissions	CE102	X	Applicability for active payloads.
Conducted Susceptibility	CS101 CS114 CS115 CS116	X	Applicability for active payloads.
Radiated Emissions	RE102	X	Applicability for active payloads.
Radiated Susceptibility	RS103	X	Applicability for payloads with antennas.
<b>Radiation Environment</b>			

Near-Earth (max)	20 rad/day	X	Radiation peaks when lander passes through Van-Allen belts. Orbits are designed to have the least possible passes through the belts.
Interplanetary (max)	1 rad/day	0.5 rad/day	The ionizing dosage is predicted based on the expected electron radiation per Earth day.
Total (max)	1 krad	X	Astroscopic provides a top value for the expected dosage value. IM expects 0.5 rad/day during surface operations as well and then has a total dose expected mission lifetime.

Table 3.2: Table of environmental requirements as set by the primary and secondary spacecraft operations providers.

During the validation of the system, tests will be carried out which ensure that the system can survive the relevant environments and operate, meeting expectations, in the operational environment.

#### Note on Thermal Environment

It is noted that while most temperature ranges indicate storing temperatures, the nominal lunar surface operation temperature is indicated for Astroscopic. Operations are only expected during lunar days, reducing the temperature range significantly.

#### Note on Mechanical Environment

The mechanical environment is highly affected during launch. While the above figures apply to any payload mounting location, the mission-specific mounting should be analysed, and the location may impact the expected load. This process would be carried out in cooperation with Astroscopic during integration and verification.

## 3.5 Environment Management

In the coming section, an overview of management's concerning the thermal and radiation environment described previously will be presented. Other factors such as the mechanical management and structure thickness are addressed as a part of Section 5. It can be noted that these management techniques are defined only on the basis of external environmental factors, and do not account for parameters such as internal dissipated heat from the S/C.

### 3.5.1 Thermal Management

In general two methods of thermal management have been used throughout time. Specifically, passive and active thermal management. During the design phase, it was determined that passive thermal management was the preferred method. This will be elaborated on further in the following sub-chapter.

Considering passive thermal management, as the name suggests, this method passively maintains temperatures of the payload and S/C without using powered equipment. Passive systems are in general very attractive, as they are often associated with characteristics, such as reduced cost, volume, mass, and risk [13].

When looking into management techniques, simple is in general always better. These include but are not limited to: material selection, coatings, and S/C orientation. For most of S/C's mission life, it will be located at or close to the surface of Moon. Taking this into account it can be assumed half of the time, direct sunlight of solar radiation which is  $1371 \text{ W/m}^2$ , with a lunar albedo around 12%. Furthermore, the Moon itself has been measured to emit inferred radiation of approximately  $269 \text{ W/m}^2$  [14].

**Surface Coating** Taking all of these contributions into consideration it is possible to determine an estimate for the external equilibrium temperature of S/C based on the absorptance  $\alpha$  and emittance  $\varepsilon$  ratio, from the surface coating. In general, the determination of the equilibrium temperature, is a tricky task, as it takes all of these environmental factors in tandem with internally dissipated power. However, as stated in the introduction, this is not taken into account, and only the external environmental factors are concerned. Although, in comparison to the maximum amount of internal dissipated power, it would not change too much the equilibrium temperature.

External Heat Load of S/C on lunar Surface			
Surface Finish	Polished aluminium	Black Paint	White Paint
$\alpha/\varepsilon$	3.00	1.06	0.31
<b>Night Temp</b>	164.9 K	127.2 K	91.5 K
<b>Day Temp</b>	377.5 K	291.0 K	214.0 K

Table 3.3: Three surface finishes with respective absorptance  $\alpha$  and emittance  $\varepsilon$  ratios, and corresponding day and nighttime external equilibrium temperatures of an S/C located at the lunar surface. The model used to determine these values are seen in [15] on p. 363.

This is in itself a very attractive approach, as the mass of surface coating is negligible compared to many other techniques of thermal management.

**Multi-Layer Insulation** Next one can consider what is referred to as a super insulation, namely Multi-Layer Insulation (MLI). This is a state-of-the-art thermal insulation, which works by a composition of multiple thin sheets in the form of aluminum foil or aluminized material. These sheets possess in general also a highly reflective exterior layer. These layers are separated by a netting/spacer layer to reduce heat transfer through conduction. The number of layers in general provides a better insulation. However, in general, this effectiveness stagnates after a certain number of layers. Considering this, it is possible to determine how effective the MLI is from such models. However, without in-depth analysis, a rough estimate for the number of layers would be around 20-40 layers as seen in [16]. A general idea of this concept can be seen in Figure 3.8.



Figure 3.8: Close up of MLI with visible layer structure with alternating foil and spacer. Picture was taken by John Rossie from AerospaceEd.

It is possible to derive an estimate of the weight of the MLI needed for the bulk of the payload. Using values described from the manufacturer Frakoterm, an aluminized polyester with a fiberglass spacer was chosen. Where the weight of a single aluminized polyester is  $0.018 \text{ kg/m}^2$ , and the spacer is  $0.014 \text{ kg/m}^2$ . Next, derived from section 5 the main chassis structure will cover approximately  $0.07\text{m}^2$ . Thus, to achieve complete coverage of the structure,  $0.044 \text{ kg}$  and  $0.088 \text{ kg}$  of MLI material would be required, corresponding to 20 and 40 layers, respectively.

In conclusion, it was determined that MLI was the preferred method, as it is a non-intrusive method with much heritage from prior space missions, also from the lunar environment.

### 3.5.2 Radiation Management

When looking at ways to manage the limitation of radiation for a spacecraft you have to be aware of the stages your spacecraft is going to survive. In our solar system, the most significant producer of radiation is the Sun. To combat that amount of radiation that comes from the Sun the normal way is to use layered titanium or aluminium, according to a NASA radiation test facility [17].

The minimum optimal thickness is about a tenth of an inch according to Megan Casey from the radiation test facility. This is equivalent to 2.54 mm.

Through SPENVIS we have made our own simulation for the space trip to the Moon and the following image shows our findings:

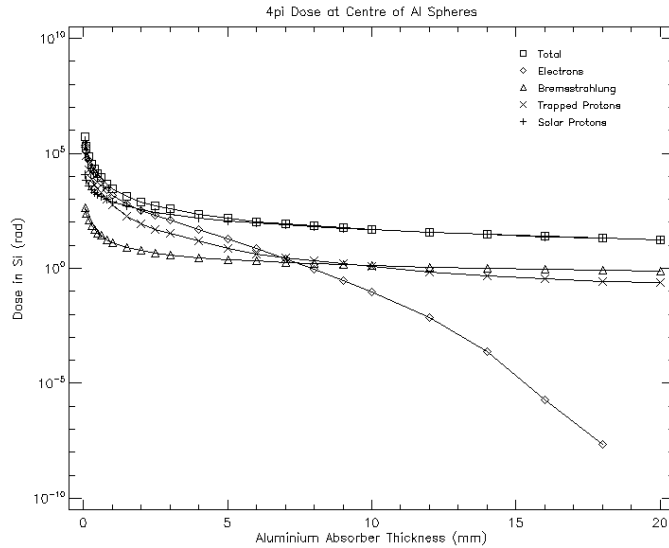


Figure 3.9: SPENVIS simulation over the thickness of layered aluminum versus the amount of radiation.

It can be seen from figure 3.9 that the minimum optimal thickness for the simulation is around 3mm which is close to what NASA's radiation test facility figured out.

When choosing between titanium and aluminum the obvious metal is aluminum since its density is lower thus providing less weight for the total spacecraft, and in the Astrobiotic launch vehicle case, the cost is a little bit lower since the price is determined by weight. This solution is not perfect since the most energetic particle is impossible to avoid even with heavy shielding, but the estimation for such a particle is estimated to hit once in 1000 days. Though such a particle could hit day 1 but is a necessary risk to run. A common strategy is to run multiple parts at the same time if one is temporarily disabled. But this is all up to the mission designers to look at how much risk they are willing to bear. This is the standard at NASA.

## 3.6 Distance and imaging sensor

In order to determine the distance to the ground, to ensure the safety of our instrument as well as making sure we get sensible measurements, we will need to chose a distance sensor for our mission. In this section, we discuss different types of distance sensors considered, the different possible setups for the sensor, and finally, a description of the camera and why it was chosen.

### 3.6.1 Types of distance sensors

Generally, there are three different types of depth measurement increasing in complexity: single point, multiple point, and full frame depth measurement. The depth measurement for this mission does not need to be especially complex. Since we have a mechanical arm that will only move up and down, as described in section 5, and because of the inclusion of a camera on our mission, we have chosen to focus on single point depth measurement. A trade study between different types of single point depth measurement distance sensors can be seen in table 3.4.

Type of distance sensor	Works on surface with no features?	Works on surface with complex features?	Works in darkness?	Works in sunlight?	High reading frequency?	Stable in a dusty environment?	Works in a vacuum?
Ultrasound	Yes	No	Yes	Yes	No	Yes	No
Infrared	Yes	Yes	Yes	Yes	No	No	Yes
Microwave	Yes	Yes	Yes	Yes	No	No	Yes
LiDAR	Yes	Yes	Yes	Yes	Yes	Yes	Yes

Table 3.4: Trade study between different types of single depth measurement distance sensors, inspired by [18].

The instrument must be able to work on a surface with no features and on a surface with complex features, as the complexity of the Moon's surface where we land is not reliably predictable. The instrument must work in darkness and in sunlight, since the Moon's orbit forces us to be either in a lit environment or in complete darkness. It is favourable that the instrument has a high reading frequency for increased accuracy of movement. The instrument must be stable in a dusty environment, as the landing site might be very dusty. Finally, the instrument must be able to work in a vacuum, because of the Moon's thin atmosphere.

Since the ultrasound distance sensor relies on sound, and sound needs a medium to travel through, it will not work in a vacuum. We therefore chose to discard the ultrasound distance sensor early on.

The infrared distance sensor works through triangulation. Infrared light is emitted, the beam hits an object and is reflected off at a certain angle, the reflected light reaches the detector in the sensor, the sensor will then determine the distance of the reflective object [19].

The microwave distance sensor can detect distance by transmitting and receiving radio waves. It then uses the time measured between transmitting and receiving together with the speed of the wave in order to determine the distance to the object [20].

The LiDAR (Light Detection And Ranging) distance sensor works by emitting laser light and uses the time taken for the light to return together with the speed of light in order to calculate the distance [19].

In order to determine which method to chose, we have found an example of a sensor based on each method and compared the most important specifications, as seen in table 3.5. A sensor that is already space-graded was considered, but we were not able to find any available for purchase, as most missions simply design their own.

Component name	Working voltage	Operating current	Dimensions	Volume	Measurement range	Cost
Grove - 80cm Infrared Proximity Sensor [21]	5V	33mA	3.7cm x 1.89cm x 1.55cm	10.839cm <sup>3</sup>	10cm - 80cm	15.30USD
24GHz Doppler Radar Motion Sensor [22]	5V	53mA	2cm x 2cm x 0.254cm	1.016cm <sup>3</sup>	50cm - 2000cm	15USD
TFmini S LiDAR module [23]	5V	140mA	4.2cm x 1.5cm x 1.6cm	10.08cm <sup>3</sup>	10cm - 1200cm	43.90USD

Table 3.5: Important specifications for examples of different types of distance sensors.

Since cost and power is so small compared to the rest of the mission, these will not have

a large influence on our choice. The two most important specifications to consider is the size and measurement range of the sensor. The microwave sensor is the smallest in size, however, since our payload is around 40cm - 80cm above the surface according to the payload user's guide, the high minimum measurement range will make it difficult to measure the distance. Furthermore, the higher reading frequency and stability in a dusty environment compared to the infrared distance sensor lead to the TFmini S LiDAR module being chosen as our distance sensor for this mission, which can be seen in figure 3.10.



Figure 3.10: The TFmini S LiDAR module [23].

### 3.6.2 Different setups for the distance sensor

Since our chosen distance sensor has a minimum measurement range of 10cm, and an uncertainty of  $\pm 6\text{cm}$  when we get closer to the surface than 6m, we will need to consider what do to when our instrument is within 10cm of the Moon's surface. There are two different setups for the distance sensor that have been discussed during the planning of this mission.

The first setup is to place the distance sensor 10cm above the XRF on the mechanical arm and account for this when measuring the distance. This is a simpler solution, but since the sensor needs to be shielded, it will cost extra, since we need to build a separate housing for the sensor that can withstand the Moon's environment.

The second setup is to simply place the distance sensor in the housing together with the XRF and a camera. Then when the instrument is within 10cm, the camera will provide reference. Ultimately, this setup was chosen, as the camera will provide additional benefits, as described in section 3.6.3.

### 3.6.3 Camera for scientific context

Because of our chosen setup for the distance sensor, described in section 3.6.2, a camera will be needed for reference when the instrument is within 10cm of the surface of the Moon. When within 10cm the camera can provide visual reference, as well as being used as its own distance sensor, based on the focusing of the camera. Both PIXL [24] and SHERLOC [25] had cameras for scientific context. On both missions the camera provided valuable context, especially with the XRF on PIXL, as images of what the instrument was measuring could be obtained. Furthermore, on the business side, it is useful to have images to show investors of our tech demo, as well as the public. For all these reasons, a camera for scientific context was chosen for our mission.

There are three main requirements for the imaging sensor and lens. (1) the imaging sensor should have a suitable resolution in order to capture usable images, (2) the imaging sensor should be as small as possible in order to fit inside the XRF housing, and (3) the minimum focusing distance of the lens should be 1cm as that is the minimum distance from which we would like to perform XRF measurements. A flash was considered for this mission, but since it is only a tech demo, and because of the constraints on communication, the periodic light from the Sun was deemed sufficient.

Requirements (1) and (2) can be satisfied by choosing an imaging sensor based on phone optics and one that already has heritage in space applications. The Ingenuity Mars helicopter [26] used two cameras; a larger high resolution camera from Sony and a small imaging sensor from Omnivision. We adopt the Omnivision OV7251 [27] imaging sensor used on Ingenuity. The imaging sensor is very small with a size of 3.91mm x 3.41mm and has a resolution of 640 x 480 with capabilities of capturing black and white images at 10 frames per second. Requirement (3) can be satisfied by choosing the correct focal length for the lens used for the camera. The minimum focusing distance,  $MFD$ , can be calculated using:

$$MFD = \frac{f^2}{SD \cdot M} \quad (3.1)$$

where  $f$  is the focal length,  $SD$  is the length of the sensor diagonal, and  $M$  is the magnification factor. In order to determine which focal length we need, we first need to define the sensor diagonal and the magnification factor. In order to find the sensor diagonal we first need to find the sensor size,  $SS$ , which is based on the pixel size of the imaging sensor at  $3\mu\text{m} \times 3\mu\text{m}$  and the resolution:

$$SS = 3\mu\text{m} \cdot 640 \cdot 3\mu\text{m} \cdot 480 = 2.765\text{mm}^2$$

The sensor diagonal can then be estimated as follows:

$$SD = \sqrt{SS} = 1.663\text{mm}$$

The magnification factor can be defined as:

$$M = \frac{SD}{f}$$

Setting the minimum focusing distance to 1cm according to requirement (3):

$$MFD = 1\text{cm}$$

We now only have the focal length as an unknown. Solving for the focal length,  $f$ , in equation (3.1) we get:

$$f = 3.024\text{mm}$$

So in order to obtain a minimum focusing distance of 1cm we need a lens with a focal length of 3mm. We adopt the Blue Series M12 Lens [28] for this mission, which has a physical length of only 17mm. The chosen imaging sensor and camera lens can be seen in figure 3.11.

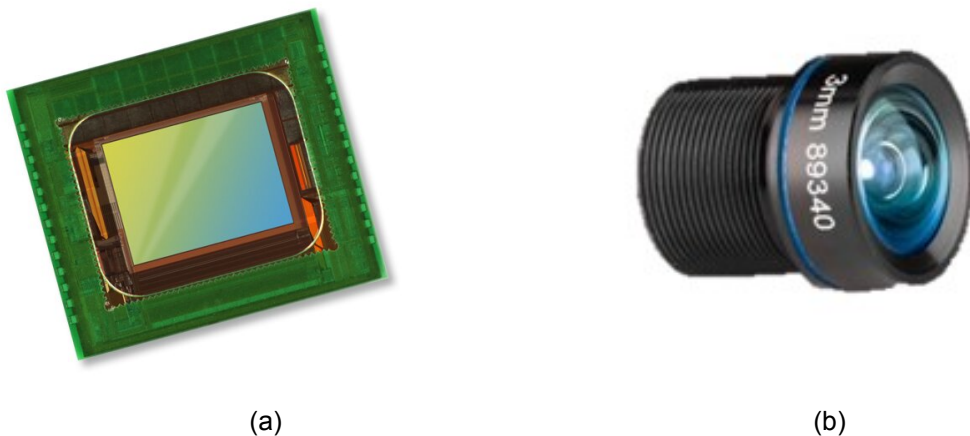


Figure 3.11: (a) the Omnivision OV7251 imaging sensor [27] and (b) the Blue Series M12 Lens [28].

### 3.6.4 Conclusion

We have defined the requirements for the distance and imaging sensor and chosen components available for purchase based on these requirements.

A trade study was conducted for different types of distance sensors based on the following: The instrument must be able to work on a surface with no features and on a surface with complex features, as the complexity of the Moon's surface where we land is not reliably predictable. The instrument must work in darkness and in sunlight, since the Moon's orbit forces us to be either in a lit environment or in complete darkness. It is favourable that the instrument has a high reading frequency for increased accuracy of movement. The instrument must be stable in a dusty environment, as the landing site might be very dusty. Finally, the instrument must be able to work in a vacuum, because of the Moon's thin atmosphere. We then found examples of each type of sensor and based mostly on the size and measurement range of the sensor, decided to adopt the TFmini S LiDAR module as the distance sensor for our mission.

Three main requirements for the imaging sensor and lens were defined: (1) the imaging sensor should have a suitable resolution in order to capture usable images, (2) the imaging sensor should be as small as possible in order to fit inside the XRF housing, and (3) the minimum focusing distance of the lens should be 1cm as that is the minimum distance from which we would like to perform XRF measurements. Requirement (1) and (2) were satisfied by adopting the Omnivision OV7251 imaging sensor that was used for the Mars helicopter Ingenuity. Requirement (3) was satisfied by estimating the needed focal length for a minimum focusing distance of 1cm. The resulting needed focal length was estimated to be 3mm, and thus the Blue Series M12 Lens was adopted.

Future work includes defining the specific electronics used to process the imaging sensor data, as well as image analysis methods in order to determine distance using the focus of the camera.

## 3.7 Conclusion

In conclusion, it can be noted that despite the limited information provided by the company Astrobotic, a preliminary assessment of pre-operational payload environmental overview

was constructed. Assumptions for both the S/C time-scheduling and maneuvering were set in place, and was deemed realistic, as they only used non-intrusive methods. These decisions were achieved in tandem with group discussions and estimations from Astrobotic.

Furthermore general management techniques concerning the thermal and radiation environment was set in place based specifically on the environment which was analysed. Here passive thermal management was chosen, as it is a non-intrusive method with much heritage from prior space missions, also from the lunar environment. The radiation solution is to cover the system in a layered aluminium of thickness 2.54 mm and that will protect against most significant radiation that our spacecraft will experience when going to the Moon.

# 4 Payload

## 4.1 XRF Theory

X-Ray Fluorescence (XRF) refers to the process where an atom in a sample is excited by bombardment with high-energy X-rays, which results in the emission of characteristic fluorescent X-rays: When incoming X-rays are absorbed by an atom in the sample, an inner-shell electron is ejected leaving a vacancy in the inner shell. An outer-shell electron will then fall into the vacancy and emit a photon corresponding to the energy difference between the two states. As each atom has a unique configuration of electrons and thus a unique set of atomic energy levels, the XRF emission spectrum is unique for each element. This can and has been used extensively within elemental analysis.

The atomic energy levels from the inner to the 4th shell are denoted K, L, M, and N, and the characteristic X-rays are denoted likewise depending on where the vacancy appears and where the outer-shell electron drops from, see fig.(4.1). For example, a vacancy in the K-shell that is filled by an electron in the L-shell is denoted  $K\alpha$ , and the energy of the emitted photon is equal to  $\Delta E = E_K - E_L$ .

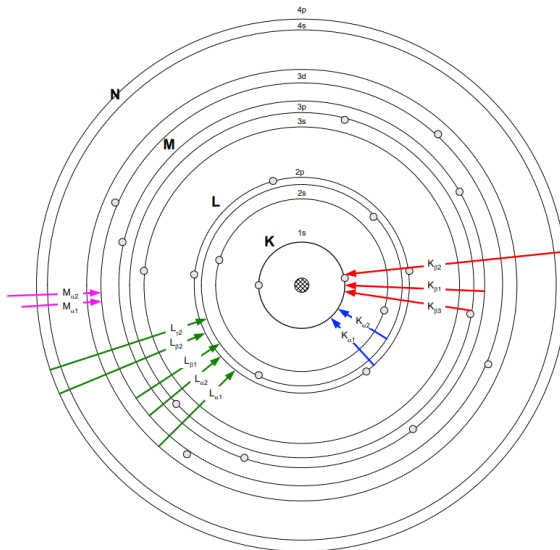


Figure 4.1: Siegbahn notation of electron transitions between atomic shells and their orbitals [29].

As inner-shell electrons for heavy atoms are more tightly bound to the nucleus compared to lighter atoms, the energy required to eject an electron from a given shell is higher for heavy atoms than for smaller ones, meaning that a more powerful source is required. As the size of an XRF source increases considerably with increasing power, the choice of elements to be detected and which energies to detect them at will thus affect the design of an XRF considerably.

A detector can be used to count the number of emissions as a function of energy, which makes up a spectrum. The resolution of the detector determines the extent to which it is possible to distinguish two photons emitted with different energies. This is visualized in fig.(4.2), where the XRF spectrum of pure lead, zinc, and copper are shown individually along with a spectrum representing a sample including all three elements.

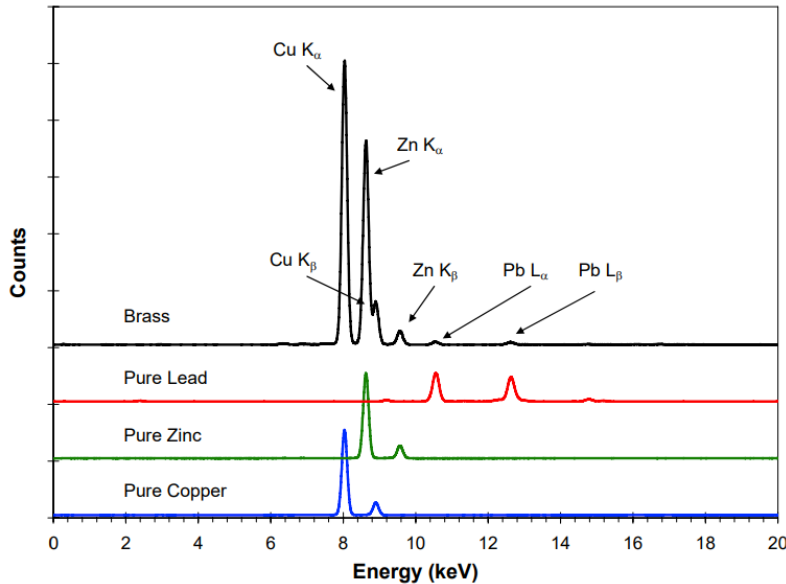


Figure 4.2: *Individual XRF spectrum of pure lead (red), zinc (green), and copper (blue), and spectrum of a sample including all three elements (black)* [29].

The detector used to generate the above spectrum is able to distinguish between the  $\text{Cu } K_{\beta}$  and  $\text{Zn } K_{\alpha}$  emissions. However, using a detector with a slightly lower resolution would result in the two peaks blending into one another, thus making it impossible to observe the  $\text{Cu } K_{\beta}$  peak. The resolution of an XRF detector is generally described as the full width at half maximum of a peak at a specified energy. For instance, the detector used in the above example has a resolution of at least 0.3 keV at 9 keV since it is able to distinguish the two peaks. Finally, it should be stressed that the reason why the spectrum is showing curves rather than lines is due to inherent noise and uncertainty in the measurements [29].

## 4.2 Payload Requirements

The key driving requirements of the payload cover the resolution of the detector and the peak energy of X-ray emissions from the source. The former is based on the energy of the characteristic X-rays for the elements described in the scientific mission statement. The strictest requirement on the resolution to the XRF is represented by the two lightest REMs as the peak energy difference increases with atomic number, and the electron transitions of REMs from  $L_{\alpha}$  emissions constitute a range of (relatively) low energies. Using the table provided by [30] shows a peak energy difference between the REMs 57-La and 58-Ce of  $\sim 0.2$  keV at 5keV for  $L_{\alpha}$ -lines. As the resolution of a detector is given in FWHM, the resolution of the detector shall be somewhat better than 0.2 keV. This requirement affects the secondary objective directly, as it defines a lower bound to the range of elements that can be detected in bulk compositions: The elements that have a peak energy difference of  $\sim 0.2$ keV at 1 keV for  $k_{\alpha}$ -lines are 11-Na and 12-Mg.

The key driving requirement of the source is determined using the same table, but now by inspection of the energy required to excite the heaviest REM (71-Lu), and it shows that an energy of 7.6keV is required for  $L_{\alpha}$  emissions. As the spectrum is generally affected by noise, the requirement of the peak energy of the source is increased slightly.

More general requirements include the integration time of the XRF and the minimum and maximum distance between the XRF and the sample under investigation. These are

highly correlated as the intensity of an X-ray decreases according to the inverse square law; increasing the distance to the sample by a factor of ten will increase the integration time by a factor of 100 and vice versa (assuming a linear relationship between the intensity of the X-rays and the integration time). To define some realistic requirements for this XRF, typical integration times and distances to samples for present space operating XRFs is provided in table (4.1).

Instrument	PIXL (Perseverance)	APXS (Curiosity)
Integration Time	~10 sec (10-16hrs for complete scan )[6]	order of minutes (13-30hrs for complete scan) [31]
Distance	1cm - 30cm	2 cm

Table 4.1: *Overview of the integration time of Martian XRFs*

Note that the XRFs onboard the Martian rovers are supposed to make a geological map of the sample rather than obtain a rough estimate of the bulk composition, meaning that a lot of measurements are required. This is not the objective for this mission, and therefore the requirement of the payload for the integration time is that it shall be below one hour. Although one could relax this requirement for missions using a stationary lander (like this), the XRF is supposed to be able to be operated by industrial rovers where a short integration time might be important. The requirement of the payload regarding distance is that it shall be able to conduct measurements of a sample at a minimum distance of 1cm and a maximum distance of 15cm. The lower limit is set to ensure that the XRF does not hit the surface during measurements. Finally, the payload should also be able to detect higher energy emissions. The resolution does, however, not need to be very good, as potential ambiguities (blending of two or more energy peaks into one peak due to low resolution) can be resolved using the high resolution of the detector from lower energy emissions. The requirement for the resolution of the high energy emissions is arbitrarily based on the peak energy difference between 79-Au and 80-Hg of  $\sim 2$  keV at 70keV for K $\alpha$ -lines. All payload requirements are summarized in table (4.2).

Device	Requirement	Comments
Detector	The detector shall be able to detect low-energy characteristic X-ray emissions (<8keV) with a resolution of at least $150\text{eV} \pm 30\text{ev}$ FWHM	Key Driving Requirement
Source	The source shall be able to emit X-rays with a peak at at least $8\text{ keV} \pm 0.2\text{ keV}$	Key Driving Requirement
XRF	The XRF shall use an integration time of less than an hour	
XRF	The XRF shall be able to detect characteristic X-rays at a minimum distance of 1cm and maximum distance of 15cm	
Detector	The detector should be able to detect high-energy characteristic X-ray emissions (>8keV) with a resolution of at least $2\text{ keV} \pm 0.2\text{ keV}$ FWHM	

Table 4.2: *Overview of payload requirements*

## 4.3 X-ray Sources

Most X-ray sources consist of an electron source, an electric field to accelerate the electrons, and an anode to slam the electrons into. This electron matter interaction will produce X-rays. Both the characteristic X-rays of the anode material, and bremsstrahlung X-rays. Many different variations of this have been made and we are looking into three of them. Of other X-ray sources things such as particle accelerators can be used, but they are obviously huge, and X-ray lasers, which are quite big and at last radioactive materials.

### 4.3.1 X-ray tubes

X-ray tubes consist of an anode and a cathode. The cathode will consist of a filament that acts as the electron source, the electrons are then accelerated and hit the anode. Hitting the anode will produce X-rays in a spectrum depending on the material of the anode. The intensity of the X-rays is defined by the material of the anode and by the intensity of the electron source. The energy of the X-rays is defined by the acceleration voltage. Two types of anode configurations are available, both a reflection type and a transmission type.

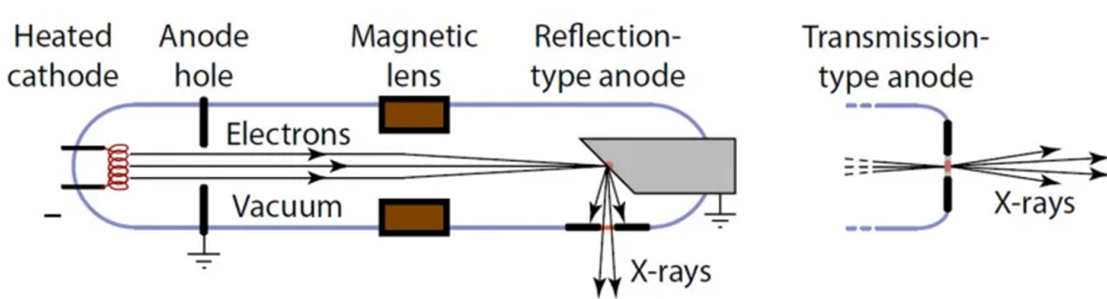


Figure 4.3: Illustration of X-ray tube concepts[32]

### 4.3.2 Radioactive materials

Radioactive materials emit some electromagnetic radiation when decaying. The wavelength is very isotope specific, so this has to be chosen carefully. Am-241 and Cm-244 are common isotopes. With an X-ray emission line at 60keV for Am-241 this isotope is very simple and plenty energetic for exciting our target elements. Cm-244 is a case of an isotope to be used as an alpha particle source. The alpha particles will excite the target in a similar way to an x-source. This type of source has quite some space heritage from the Alpha Particle X-ray Spectrometer (APXS)[31], which has flown many missions including Curiosity[33] and Philae[34] amongst others.

### 4.3.3 Exotic electron sources

Novel approaches to miniaturizing X-ray sources are generally based on the same principle of the X-ray tube, but in the transmission anode configuration. The issue is that the electron source up until now has been quite bulky. We investigated two new approaches to this design.

#### 4.3.3.1 Pyroelectric

The pyroelectric source consists of a pyroelectric crystal and a transmission anode. During a heat cycle, the source will emit electrons, which are accelerated toward the copper anode. By the same mechanism as in an X-ray tube, x-rays are emitted. This creates a very small and low-power consumption x-ray source.[35]

Seemingly a great option for the instrument, one drawback has to be noticed. The intensity of the X-rays is very low at 5 mSv/h at a distance of 10 cm. For some reason, the only available pyroelectric source has been discontinued in 2020. One could speculate that

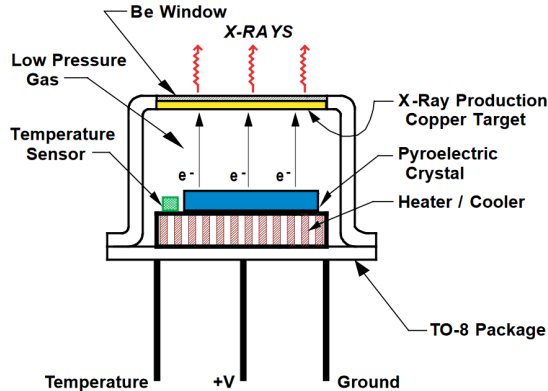


Figure 4.4: Illustration of pyroelectric source[36]

this is due to the low intensity of X-rays. That being said a lot of scientific papers have been written about this device all the way up until its discontinuation.

#### 4.3.3.2 Carbon nanotubes

Carbon nanotubes(CNT) are a promising new electron source. They are very bright, operate at low voltage, and are stable.[37] That being said it's about 30 years ago the first CNTs were made and still there are no commercially available products. This is mostly down to production complications. Apparently, it's more difficult than you would think to place pure, defect-free carbon nanotubes in an electrical device. A major concern would

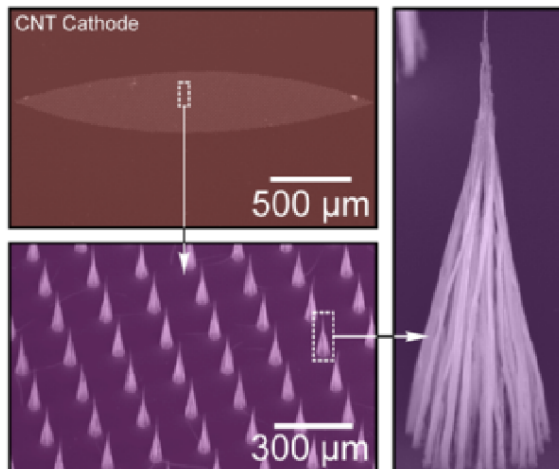


Figure 4.5: SEM-picture of vertically grown CNT's. In the bottom right, a small process flow of how they are grown on a Ni catalyst with Plasma Enhanced Chemical Vapour Deposition(PECVD).[37]

be the structural integrity after launch. If it was possible to develop such a source then it would surely be a great candidate. It has been shown to have a better brightness than the usual Schottky emitters.[38]

#### 4.3.4 Summary

At this point, one can already discard the pyroelectric and nanotube sources. This is due to the fact that further development is needed and the implied uncertainties. Both the regular X-ray tube and the radioactive source are viable, proven, and can be scaled to our needs.

Source	Peaks	Integration time (at 15cm)
Am-241	60 keV [39]	1 hour(3Ci source)
Mini X-2	9.7 keV, 11.5 keV, 13.4 keV [40]	1 hour(50kV source)

Table 4.3: Comparison of Am-241 and Mini X-2

The intensities are difficult to compare as they are given as Ci in radioactive sources and W in the X-ray tubes. Furthermore, the X-ray tubes with transmission anodes don't specify how much of the watts are electrons and photons.

## 4.4 X-Ray Detectors

### 4.4.1 Initial requirements



**Alloy Elements and Detection Limit Guidelines:**  
Elements Detected: Magnesium (Mg), Z=12) through Neon (Ne), Z=10)  
(Sc, Z=14) through Thorium (Th, Z=23) through Protactinium (Pa, Z=94); typically 0.1% - some elements as low as 0.01%

**Low-Density Sample Types**

(Solids, powders, liquids)

Symbol  $\frac{K_{\alpha}}{K_{\beta}}$  Principal lines off Principal lines on Atomic Number

Requires vacuum, LOD 0.2 – 3%      250 – 2,500 ppm      50 – 150 ppm  
LOD 1% – 5%      10 – 100 ppm      Not Measured

Figure 4.6: Periodic table showing which elements are detectable by a commercial, handheld XRF system (on Earth), the lightest distinguishable elements according to the requirements (yellow rectangle), the REMs (red rectangle), and the element with L<sub>α</sub> lines more energetic than 14 keV (black rectangle)[41].

Central to the XRF payload is the detector - together with the x-ray source, it is this which governs which elements can be detected (and thus whether the main mission requirements are met). Detector research began with an investigation into the capabilities of the technology as a whole, to try and find some feasible target elements.

In general, lighter elements are more challenging to detect - for an Earth-based, commercial XRF device (Figure 4.6), gold may still be detected at concentrations below 50ppm, whereas magnesium may only be detected at concentrations approaching 3%. Lithium would be completely out of reach. When setting the scientific requirements, therefore, it was important to pick a sensible threshold for the lightest element that could be detected. While pushing to detect as many elements as possible would be desirable, as this would

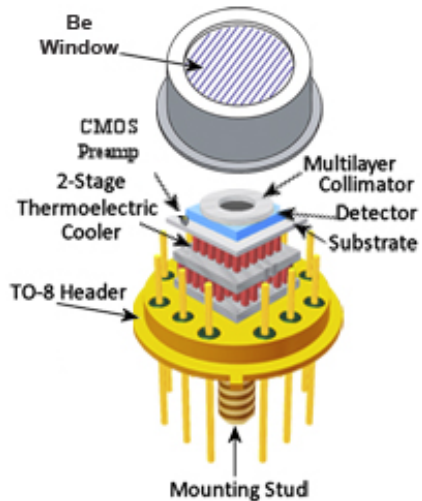


Figure 4.7: Internal structure of a FAST SDD, as manufactured by Amptek. The CdTe is similar, but with different elements involved [42].

increase the range of applications for the finished device, this would come at a financial cost - a more sensitive, and thus more expensive, detector would be required.

Another consideration made at this stage was whether particular detectable elements would be useful. After some research, it was concluded that a miniature XRF payload could see use in both scouting out planets for building materials (with the eventual goal of the colonisation of alien worlds) and potential mining locations. Both of these require the detection of rare-earth metals, so our detectors were selected on the basis of being able to detect these.

#### 4.4.2 Detector technologies

Many different detector types were analysed, but on the bases of size, cost, and performance (both integration time and resolution - see Appendix A.2 and Appendix A.3) the selection pool was quickly whittled down to two: silicon drift detectors (SDDs<sup>1</sup>), and cadmium telluride detectors (CdTe). Both of these technologies effectively offer a single pixel, as they provide one measurement value per exposure - to form an image of an area, and to find something out about the distribution of different elements across the field-of-view, a more advanced detector such as a charge-coupled device (CCD) camera would be required. Such a feature was determined surplus to requirements, as it did not help to meet the mission objectives, and would come at additional cost, so CCDs were not pursued.

Both the CdTe and the SDD work in a similar way, like a traditional X-ray tube (see Section 4.3.1) in reverse - here X-ray photons are absorbed, and the resulting ionisations cause charge fluctuations in the material (silicon or cadmium telluride here) which are measured via electronics. Both systems are fairly small and cheap and work well as long as they can be kept cool enough (lower-energy photons can impact the detector surface and lead to noise). The general structure is shown in Figure 4.7 - this shows an SDD, but a CdTe detector is very similar internally.

#### 4.4.3 Factors which may impact detector performance

As well as the specific models selected, there are many outside factors that may affect the performance of the detectors. Any optics present, for example, would increase the

---

<sup>1</sup>Not to be confused with solid-state drives (SSD)

intensity of x-rays received (and hence decrease the integration time needed to make a reliable measurement), at a cost in financial and mass terms. Given the relatively large detecting area and the presence of some inbuilt optics within the detector casings, it was determined that providing separate optics would be an unnecessary expense (so do not feature in the final design).

The choice of source plays a major role in performance as well - a more intensely radiating source will greatly reduce the integration time. The distance between the detector and the ground will also have an influence, as the intensity of x-rays received will decay with distance with an inverse-square relation. To compensate for the removal of the optics, and allow us to use a lower-energy source if needed, this distance was reduced to the lower end of the specified range (1cm). This will allow integration times of several minutes (rather than the hours required at 15cm for the same setup) to be obtained for the radioactive source and much lower times for the regular source.

Device	Specifications
X-123 FAST-SSD detector	Resolution of 130 eV FWHM at 5.9 keV
X-123 CdTe detector	Resolution better than 1.5 keV FWHM at 122 keV

Table 4.4: Specs of the two detectors

## 4.5 XRF Optics

Four different types of optics were investigated in order to reduce the integration time needed to obtain measurements of the sample of sufficient quality. The first possibility was to include Multilayer Laue Lenses (MLL), consisting of many layers of two alternating materials with different refractive indices. X-rays traveling through the MLL will undergo destructive and constructive interference to focus at a focal spot diameter down to sub-micron levels [43]. The second possibility was the use of Fresnel Zone Plates (FZPs) consisting of a series of concentric rings alternating between materials that are opaque and transparent to X-rays. Incoming X-rays are focused to a point of nanometer spot size when passing through the FZP due to diffraction [44]. The two options are, however, very challenging to fabricate, and their performance is highly dependent on the precision and surface roughness of the design dimensions (layer thickness in MLL and ring dimensions for FZPs). The third option was Kirkpatrick-Baez Mirrors (KBMs), which consist of at least two elliptically curved mirrors placed in series, where the first and second mirror is typically aligned horizontally and vertically respectively. These can provide focal spot diameters in the 50 nm range [**KMBs**], but are extremely sensitive to thermal and mechanical stress, as they need accurate alignment, and are to this day quite large and heavy. Finally, capillary optics were considered, which consists of a bundle of capillaries that guide incoming X-rays via reflection to a focal spot diameter on the order of microns. This type of optics is an integrated part of PIXL. Although these are not as sensitive to mechanical stress and alignment as the aforementioned solutions, they are impractical for miniature designs as they are elongated structures that would fill up a significant amount of volume.

To summarize, keeping the scientific mission statement in mind, the secondary objective is to determine the bulk composition of a sample, which does not require a sub-micron or nanometer focal spot diameter. Furthermore, integrating optics into the design of the XRF will not only increase the complexity but also the price of the XRF as optics are generally very expensive [45].

## 4.6 XRF Design Selection

### 4.6.1 Possible combinations

In the previous sections, numerous distinct approaches were investigated in great detail, in order to find the optimum selection of components for the XRF instrument. Several different solutions were analyzed and evaluated for their possible use as sources, detectors, and optics. Some of those were found to be impractical, immature, or too expensive to be seriously considered for selection. However, in each of the categories, two distinct solutions were deemed worthy of further consideration.

Both an ordinary X-ray tube and the use of radioactive isotopes were judged as viable X-ray sources. With the detectors, it quickly became apparent, that both an SDD and a CdTe detector are necessary for the accurate detection of all the elements outlined in the Level 1 scientific requirement. However, this still leaves open the question of whether a standalone off-the-shelf product should be chosen, or instead, by selecting each part individually, a custom-made one should be preferred. Finally, in the case of optics, the main question revolves not around the specific type of optics used, but whether optics should be used at all, given the extra cost and complication it would bring into the mix.

Admittedly, these choices are not of the same kind, since the one about optics concerns the very necessity of the part, whereas for the source there are two very disparate solutions - and the question regarding the detector seems rather trivial, compared to the previous two. Nonetheless, this results in three different and important design choices: whether to use an X-ray tube or a radioactive source, the inclusion or exclusion of optics and finally between going with a standalone solution or with a custom-made detector.

This gives 8 possible combinations:

1. Radioactive source + optics + complete, standalone detector
2. Radioactive source + optics + complete, custom-made detector
3. Radioactive source + no optics + complete, standalone detector
4. Radioactive source + no optics + custom-made detector
5. Ordinary source + optics + complete, standalone detector
6. Ordinary source + optics + custom-made detector
7. Ordinary source + no optics + complete, standalone detector
8. Ordinary source + no optics + custom-made detector

Obviously, the XRF instrument could only use one of these, and all of the above-listed combinations have their advantages and disadvantages. Moreover, their relatively large number makes it hard to easily compare them to each other, since listing the pros and cons for each case works best when direct comparisons can be made between only a handful of designs - this can evidently not be done here.

As a consequence, a method is needed to compare a large number of different designs relatively easily, quantifying their strengths and weaknesses in an objective way against a wide range of different design criteria of varying degrees of importance.

### 4.6.2 Design Decision Matrix

A suitable solution to the aforementioned problem is a grading process called Design Decision Matrix, also known as Design Scoring Function.

Countless different variations exist for this process, from the fairly rudimentary to the extremely complicated. However, in this case, a simpler implementation is preferred, especially since some of the design choices are rather high-level and the project at this stage is primarily aimed at passing PDR. As a result, the steps listed below were followed during the process:

1. Definition of the different designs in broad terms: This step was already fulfilled by selecting the above-listed 8 possible combinations.
2. Creation of a list of criteria used for grading: This step determines the different design criteria on which the different designs are judged. In general, these can be derived from the mission concept, the design specifications, and requirements, based on the possible sources of engineering challenges, trade-offs, and limitations set by real-world physics.
3. Specification of weights for each criterion: Based on the requirements and the mission concept, the design team has to decide the relative importance of the previously defined criteria, such that the chosen weights are faithful representations of the requirements set by the mission. The chosen range of numerical values for the weights is usually broader if the criteria have vastly different importance (e.g.: 1, 10), while if finer distinctions in importance are required, the weights might be closer to each other while having a high absolute value (e.g.: 9, 10, 11).
4. Finalization of the score range: Choosing a wider range is important if the differences are expected to be high or more subtle distinctions are possible based on *a priori* knowledge.
5. Evaluation of the different designs by each team member based on a previously agreed upon scoring philosophy: Everyone assigns a grade for every category for each of the designs, based on his objective assessment. It is also important to use the same grading philosophy, for example, whether the grades in each category should have an average value, whether each design should be evaluated on its own with regard to a criterion, or whether differences in performance should be inflated. In an optimal scenario, after averaging the results a clear leader emerges.
6. Reevaluation of the criteria, weights, and grades: It is possible that multiple designs end up with a very similar score or the design with the highest score does not intuitively fulfill the requirements very well compared to others. This could have several reasons each requiring the reevaluation of one or more parts of the process. The first possible reason is the incompleteness of the list of criteria. The second is if the weight does not properly reflect the requirements or the engineering constraints. It is also possible, that the selected score range is too narrow, and it is hard to express more subtle differences that are necessary to distinguish between the designs. Finally, the grading could be off, in which case, most commonly, not assuming personal bias, the reason is the incomplete or different *a priori* knowledge of some of the team members - if everyone were using the same *a priori* knowledge and grading philosophy, they would not give widely dissimilar grades. Usually, in this situation, it's a good idea to try to reconcile widely different assessments by exchanging information or reviewing each other's controversial grading decisions, so the underlying reasons can be discovered.
7. Selection of the best design: After the previous steps, hopefully, a clear favorite emerges, which can be selected for further development. It can happen, that despite all the steps taken earlier, two designs are still neck and neck. In this case, it is

advised to develop both designs further, because it is very likely that some new difference emerges.

#### 4.6.3 Implementation of the process

The selected criteria and their associated weights were as follows:

	Price	Space Heritage	Complexity	Power	Weight	Size	Temperature requirements	Thermal control	Energy resolution	Spatial coverage	Lifetime	Integration time
Final weights	3	2	4	3	5	5	2	5	4	2	3	4

Figure 4.8: Final weights

Price includes both the equipment, material, and launch costs. Space heritage measures the risks of a new design choice - more risk is attached to a design that has not been tested in space. The complexity of the design includes the ease of development, testing, licensing, integration, and possible troubleshooting, and impacts the chance of premature system failure. Power, weight, and size need no explanation. Temperature requirement quantifies how much the operating temperature is constrained by the different design choices, while thermal control considers the challenge of heat dissipation. The energy resolution is the smallest distinguishable energy range, which impacts the type and number of detectable elements. Spatial coverage is the resolution, but for physical distances, which are determined by the beam size. Lifetime is the amount of time, that is expected to be reached without malfunction with 95% probability. Finally, integration time determines the necessary time to complete a measurement.

The weights were chosen to fall into the 2-5 interval since it was deemed that the differences in importance didn't justify a larger range or a finer resolution. For similar reasons, the score range for grading fell into the 0-5 interval. 0 represents a fail grade, so any design with a 0 automatically gets disqualified. The grading philosophy tried to emphasize and amplify the differences even for small actual performance differences, while the mean for one criterion was required to fall between 2.5 and 3.5. As a result, the grades for one criterion should aggressively highlight small differences while simultaneously having a similar mean value.

The implementation itself took multiple iterations because two similarly high-scoring solutions emerged: both of these had custom-made detectors and lacked optics, but one of them used a conventional X-ray tube as a source, while the other used a radioactive source. These could be interpreted as solutions based on two different kinds of requirements. The radioactive source is more of a "poor man's solution", the cheapest possible solution with possibly lower accuracy, while the ordinary source is more of a higher-end solution that can obtain better results, however for a higher price in terms of mass, money, and energy budget.

Changes between different iterations included re-weighting, adjusting grades based on new information and a more complete understanding of the field, and the addition of a completely new criterion, the thermal control.

#### 4.6.4 Results

The 8 different design proposals were evaluated based on 12 criteria. It is important to emphasize, that each grade evaluates the solution as a whole. Individual parts might be advantageous on their own but combined with different solutions they may behave differently. For example, not using optics, but choosing a radioactive source will likely result in a long measurement time, but this is not necessarily the case if you change one part of the setup by either including optics or using an X-ray tube. The final results are presented in the table in Figure 4.9.

	Price	Space Heritage	Complexity	Power	Weight	Size	Temperature requirements	Thermal control	Energy resolution	Spatial coverage	Lifetime	Integration time	Final score
Radioactive source + optics + standalone detector	1	2	1	5	1	1	2	1	3	4	3	3	86
Radioactive source + optics + custom detector	1	5	1	5	1	1	3	1	3	4	3	3	94
Radioactive source + no optics + standalone detector	3	2	4	5	4	4	4	1	2	1	3	2	124
Radioactive source + no optics + custom detector	3	2	4	5	5	5	5	1	2	1	3	2	136
Ordinary source + optics + standalone detector	1	2	1	1	1	1	1	4	5	5	4	5	108
Ordinary source + optics + custom detector	1	5	1	1	1	1	2	5	5	5	4	5	121
Ordinary source + no optics + standalone detector	5	2	3	1	2	2	3	4	4	3	4	4	130
Ordinary source + no optics + custom detector	5	2	3	1	3	3	4	5	4	3	4	4	147

Figure 4.9: Final results

The reasoning can be summarized as follows:

1. It is obvious, that including optics substantially increases the price, thus earning the minimum score. The required amount of money necessary to purchase enough radioactive material to have the same intensity is a lot higher, resulting in a penalty, even after accounting for the weight difference. Using a custom-made detector also incurs a small penalty.
2. The most reliable combinations are the already tested ones (PIXL, APXS), while the rest of the field gets a low mark.
3. Optics introduces a lot of complexity, thus again scoring at the bottom. A radioactive source has the disadvantage of being radioactive, resulting in potential legal issues and requiring extra shielding, however, it doesn't need power, or control electronics like the ordinary source, which results in a slight score difference. Using a custom-made detector also incurs a small penalty.
4. Based on the most promising X-ray tube and detector specifications, a solution with a radioactive source will consume half as much power.
5. Using optics always results in extra mass compared to equivalent designs. A custom-made detector can be lighter and smaller, thus gaining a slight bonus. Finally, for similar intensity, the radioactive source is lighter, than the tube, even after accounting for shielding.
6. The exact same argument goes for the size.
7. Considering the temperature requirements, fine-tuned optics are always an additional liability, especially considering, that electronics can be somewhat shielded from extreme cold by powering them up. However, using a radioactive source is one less electronic device resulting in one less temperature requirement, giving it a slight boost. Finally, custom detectors can be made more temperature tolerant, thus also gaining an extra mark.
8. Thermal control of a radioactive source is a big problem, especially for vacuum or close-to-vacuum applications, since they can't be turned off, resulting in a constant heat build-up. Either the intensity has to be cut down radically or a complex cooling system has to be designed. In any case, they can't get better than the lowest passing grade. Custom detectors enjoy a slight advantage here as well.
9. When it comes to energy resolution, optics is a clear advantage. However, after careful consideration, it became apparent, that the inability to turn off the radioactive source (at least without greatly increasing the design complexity by building some openable container around it) is a much more impactful factor. This comes from the inability to establish a clear baseline by measuring the background radiation, inherently degrading the signal-to-noise ratio of the measurement and possibly introducing false measurement data in certain environments.
10. Spatial coverage greatly benefits from the inclusion of optics, however, based on calculations, the most promising detector types can handle bulk composition and element detection measurements without optics if a traditional X-ray source is used, and the ability to establish a baseline helps out as well, resulting in a slightly smaller score loss for the exclusion of optics compared to the case with a radioactive source, which greatly depends on the optics.
11. Lifetime is hard to decide without extensive testing and experimentation. On the one hand, a radioactive source requires one less electronic component, that can go bad.

On the other hand, it is radioactive and it can not be shielded from all directions and can't be turned off unless a complex openable container is designed, which negates its advantages since it requires electronics and prone-to-break mechanics. This results in a slight score difference in favor of the use of the X-ray tube. Half-life is calculated not to be a serious problem, although it can affect the intensity if the destination takes a lot of time to reach.

12. Finally, in the case of integration time, optics is an advantage again. However using a radioactive source is an even bigger disadvantage, due to the inability to establish a baseline and the lower signal-to-noise ratio, and most importantly the smaller intensity for comparably priced solutions.

It is evident, that the highest-scoring solution is the one, which uses an X-ray tube, with a custom-made detector and doesn't include optics.

#### **4.6.5 The selected design**

Based on the results, the solution, which uses an X-ray tube, with a custom-made detector and forgoes optics is selected for further development. Also, the solution doesn't contradict intuition, and each of the design decisions can be argued for:

1. The exclusion of optics mainly comes from the fact, that it is cheaper, lighter, smaller, and less complicated without it. At the same time, calculations showed, that it is not strictly necessary to use it for bulk composition and element detection measurements when it is used in concert with an X-ray tube, while the trade-offs of not including optics are much larger in the case of a radioactive source. It is a classical case when moderate scientific benefits are overshadowed by the massive increase in other areas.
2. The decision of going with the custom-made detector is a fairly straightforward one. It is slightly better with thermal management while being smaller and lighter. On the other hand, any potential cost and complexity increase is somewhat offset by the necessity to adapt to and plan around the limitations and requirements of a standalone, off-the-shelf design, which has its own cost and complexity issues. The gains are visible, while the trade-offs are minor.
3. The choice between the ordinary source and the radioactive one was the hardest. Radioactive source clearly provides substantial size, and weight benefits, coupled with reduced power consumption and overall complexity. At the same time, it has somewhat worse scientific parameters, due to the inability to establish a clear baseline by turning the source off. Notwithstanding the slightly higher price, the decisive factor against it was the very poor thermal management due to the constant heat build-up, supposing similar integration times and thus intensity, which is a very serious problem in near-vacuum and vacuum environments. It is true, that using a radioactive source can make the XRF more miniature in every sense, but the lack of ability to turn it off damages its scientific characteristics and poses a hard-to-overcome engineering challenge.

In conclusion, the choice between the first and second-ranking design comes down to the fact, that since the only difference between them is the choice of source, the fact that one of them can be turned off, makes the winning combination a lot easier to handle in vacuum and more scientifically useful at the cost of being moderately less miniature. Also, it can be observed, that the lack of optics impacts the radioactive source more, while the X-ray tube remains broadly capable of performing bulk composition and element detection measurements without it.

#### 4.6.5.1 Choice of source

Following the reasoning in the above subsection, the Mini-X2 X-ray Tube Module (Au) from Amptek was chosen as X-ray source for the first MIX-DTU-mission. The spectrum of this source is shown in Fig.(4.10)

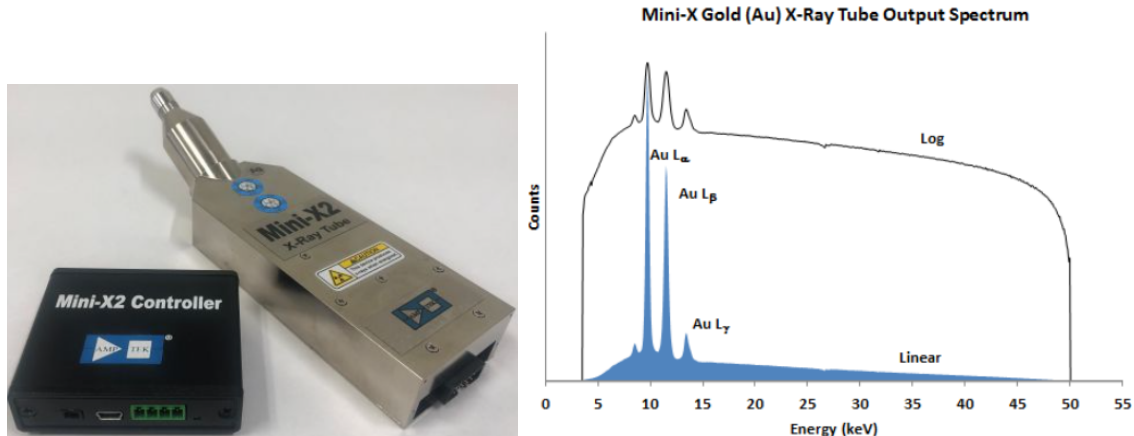


Figure 4.10: The Mini-X2 (Au) X-ray Tube Module (left) and its spectrum (right) on a linear (blue) and log (black) scale [46].

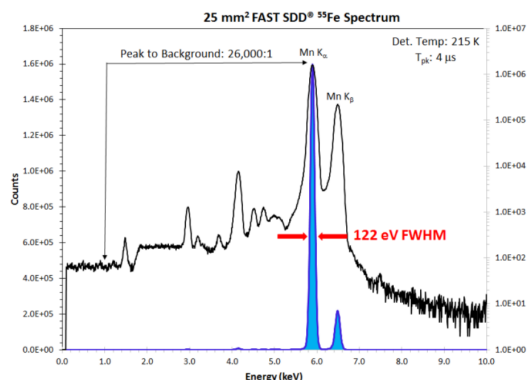
#### 4.6.5.2 Choice of detector



(a) An Amptek FAST-SDD, with hand for scale.

The portability of this technology is evident

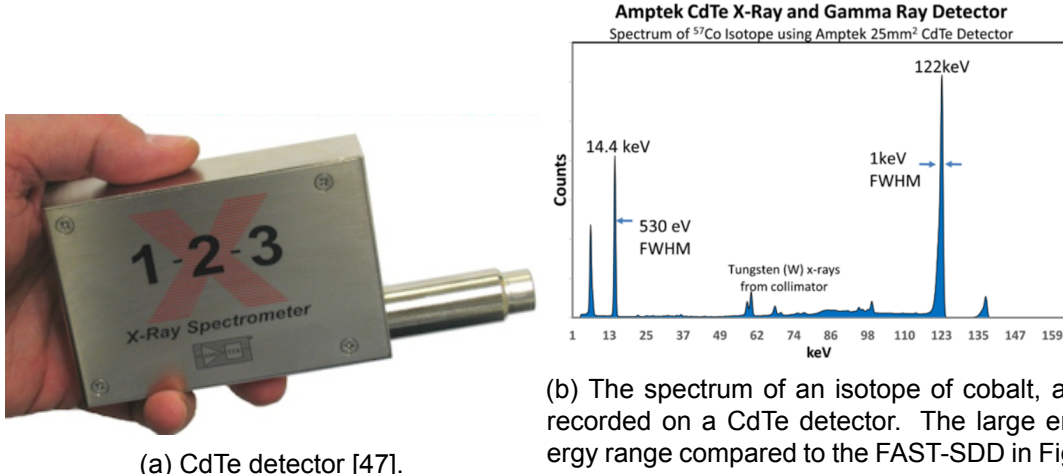
(the box contains cooling, collimation and some control circuitry) [42].



(b) The spectrum of an isotope of iron, as recorded on a FAST SDD. Clear peaks are visible between 0.1 and 7 keV, but outside this range another detector type must be employed [42].

Figure 4.11

The detector variants described in Section 4.4.2 have different benefits - SDDs have greater precision, but can only detect low-energy x-rays (see Figure 4.11 for a typical spectrum which can be detected), whereas CdTe detectors offer a larger energy range, centered on higher energies (Figure 4.12, the example here being cobalt. To detect as many elements as possible, particularly the heavier rare-earth minerals which were targeted, it was concluded that both types of detector needed to be included in the spacecraft payload. The next question for this team was where the components should be purchased from. After some internet research, two manufacturers, Amptek and Ketek, were singled out to be pursued further, as both had a large range of products, and had recently acquired space heritage (Figure 4.13). Unfortunately, neither was initially very forthcoming



(a) CdTe detector [47].

(b) The spectrum of an isotope of cobalt, as recorded on a CdTe detector. The large energy range compared to the FAST-SDD in Figure 4.11 is this technology's major strength, however, it has a full width at half maximum (FWHM) ten times larger, indicating lower precision [47].

Figure 4.12

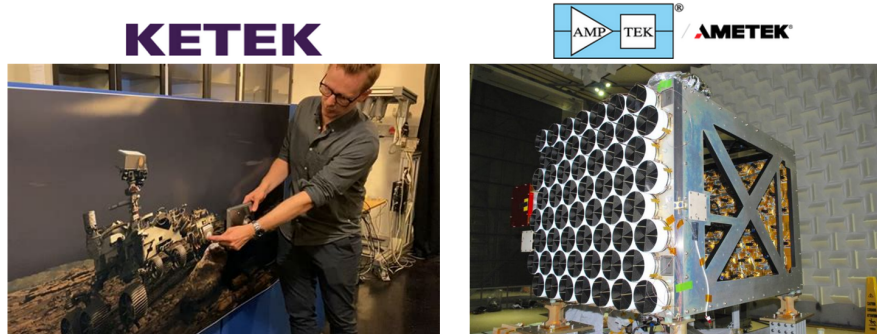


Figure 4.13: Both manufacturers considered had supplied equipment previously used in space; Ketek components were used on PIXL on the Martian surface, while Amtek ones featured on the NICER mission on the International Space Station. Picture credits: [48] and [49].

about how much their detectors were likely to cost, but after making formal quote requests the prices were determined and found to be reasonable (see Section 4.6).

After much consideration, Amtek became the chosen provider due to their greater product range, greater scope for customizability, and most importantly that they were the only one of the two currently producing a CdTe detector. Once the detectors had been decided upon, the mechanics' team was able to incorporate this into the structure, using the size of the detector casings as a maximum. This was only used as a maximum, as it is entirely possible to order all the components from within each detector casing separately, which may have been more space-efficient. This possibility was discussed and explored, with the results noted in Section 4.6.

The two detector models employed in the mission are the X-123 FAST-SDD and the X-123 CdTe. Detailed specifications for both are presented in Appendices A.2 and A.3 respectively.

#### **4.6.6 Thermal management of the XRF**

It is clear, that one of the hardest engineering challenges is posed by the heat buildup caused by the electronics inside the chassis. In general, there are four ways to deal with the excess heat in a vacuum: through the use of radiators on the chassis, using heat conduction to connect the chassis to the rest of the spacecraft, active cooling system, and finally using only the chassis for heat dissipation. It is evident that option one and three is infeasible if the goal is to miniaturize the XRF. The second solution is generally hard to achieve with the current layout, considering that the telescopic arm is not designed for this purpose, and relying on this solution constrains future applications of the XRF. This leaves the last option; however, it comes with the trade-off that the heat production itself has to be constrained so that relying only on the chassis is sufficient.

This pretty much rules out the use of a radioactive source that has similar intensity and integration time as the X-ray tube for two reasons. First, it can not be turned out, risking a runaway heat buildup, especially considering it is inside a miniature chassis, that is thermally weakly connected to the other parts of the spacecraft. Secondly, for similar intensity, it produces a lot more waste heat as a result of the geometrical arrangement. A radioisotope capsule has most of its surface covered by radiation shielding, so radiation in that direction is absorbed and ultimately converted into heat. The selected X-ray tube on the other hand has around 50% efficiency, meaning less waste heat for the same number of X-rays. There is one way around this: using a radioactive source that is a lot less intense, so heat radiation is sufficient on its own. This was done in the case of APXS [31], however, it results in a much longer integration time, which does not meet the requirements, in the case of the maximum (or close to the maximum) distance set by the requirements.

In this case, the thermal management of an XRF using a conventional X-ray tube has to be considered. It is clear, from the experience of PIXL [24], that the continuous operation time of the tube has to be restricted. The different parts are thermally isolated from each other inside the chassis by the use of Chem-Film Class 3 with an emissivity of <0.1. Both detectors and the X-ray tube is supplemented by a heat sink made from copper (The heat sinks for the detectors are actually a requirement for vacuum applications, not including them, results in the loss of warranty.) that are connected to the chassis to help with the transferring of the heat to the chassis, which radiates it into the surrounding environment, taking advantage of its much larger surface area. The interior of the chassis is gold coated to discourage heat radiation in that direction, while the exterior of it is painted white, since it has a very high emissivity in the infrared, making it good for radiating heat to the ambient environment [24].

X-ray tube operations for PIXL are constrained to 45 minutes in vacuum, during the transfer phase to Mars [24]. Given the similar protective measures taken here, and considering the much smaller power levels of the tube (4W vs 12W tube power [24]) it is reasonable to assume that an on-time of around 60 minutes can be considered safe, which is adequate to complete measurements even at a distance of 15 centimeters. However, the off-time required for cooldown is hard to estimate without extensive simulations. As a result, the duty cycle (the on/off time ratio) has to be measured during testing in a thermal vacuum chamber.

## 4.7 Verification, Validation and Future Work

The final design is evaluated via verification relative to the requirements listed in the table (4.2) and the scientific mission statement regarding the volume of the payload. The dimensions of the payload for the final design will be elaborated much more in section (5.3), from which table 5.7 can be used to verify that the volume of the final design constitutes 8.5% of the volume of PIXL, which complies with the scientific mission statement. The specs of the chosen two detectors presented in section (4.6.5.2) and the source presented in Section 4.3 also comply with the requirements, as can be seen in Table 4.5

Device	Specifications	Requirement
X-123 FAST-SSD detector	Resolution of 130 eV FWHM at 5.9 keV	The detector shall be able to detect low-energy characteristic X-ray emissions (<8keV) with a resolution of at least $150\text{eV} \pm 30\text{ev}$ FWHM
Mini-X2 X-ray Tube Module (Au)	Peak X-ray emission at 9.7, 11.5 and 13.4 keV	The source shall be able to emit X-rays with a peak at at least $8\text{ keV} \pm 0.2\text{ keV}$
X-123 CdTe detector	Resolution better than 1.5 keV FWHM at 122 keV	The detector should be able to detect high-energy characteristic X-ray emissions (>8keV) with a resolution of at least $2\text{ keV} \pm 200\text{ ev}$ FWHM

Table 4.5: Verification of chosen components by comparison of their specs to the requirements

The table clearly shows that the final design complies with the key driving requirements, and it was calculated that the integration time doesn't exceed 1 hour even in the case of a maximum distance of 15 cm. However, despite all of the requirements being fulfilled, the high-energy detector might not be able to detect a significant number of counts from secondary X-ray emissions caused by the excitation of the source compared to noise levels: Although the source does emit X-rays in the range from  $\sim 3$  to 50 keV, the peaks are centered at 9.7, 11.5, and 13.4 keV, while the spectrum flattens significantly after the 13.4 keV peak, see Fig. (4.10).

The reason for not having chosen a more powerful source is - as already described - that the level-1 mission requirement is to design a miniature XRF, which puts a constraint on how powerful the source can be, while detecting high-energy emissions is only a regular requirement. It should, however, be stressed that both the source and detectors are customizable, meaning that both their size, energy peaks, and resolution might be improved or tuned significantly in future work through more iterations in Phase-A (although the life cycle of this project is supposed to be post-Phase B). Finally, the team would need to test the design experimentally under mission-specific conditions in order to validate the final design, while experience from the first mission will most likely help to improve the design. A comparison of the XRF with other space operated XRFs is shown in Table (5.7).

## 4.8 Payload Conclusions

The payload team has agreed upon a final design that complies with the key driving requirements of the mission. The components that constitute the design are an X-123 Fast SDD and X-123 CdTe detector, a Mini X-2 source, and no optics. This will yield a spectrum up to 50 keV with peaks at maximum 13.4 keV and a spectral resolution of 130 eV FWHM @ 5.9 keV and 1.5 keV FWHM @ 122keV, which will lead MIX-DTU on the right track to detect Rare Earth Materials in future iterations of the instrument.

# 5 Mechanical Structure

To ensure the fulfilment of the mission goal and requirements from other subgroups, it is needed to design a structure to house the payload and a mechanism to lower the payload to the ground. This chapter consists of a description of the design process, a detailed explanation and the analysis of the design.

The XRF chassis that should house the payload itself is part of what is being tested, and should be able to function for other missions as well. On the other hand, the lowering mechanism is specific for this mission, and not necessarily a part of the future setup. It is therefore important that it is kept simple.

## 5.1 Early thoughts

Since most specifications were not decided upon until later in the design process, a few assumptions were made at the beginning of the design process: One, the XRF would need to be positioned with extreme precision to obtain accurate and useable data; two, the XRF would need to take multiple measurements to fulfill the mission requirements; and three, we would need to provide our own, custom lander to transport the XRF. Based on these assumptions, the earliest mechanical design included a lander with a two- or three-jointed arm and an XRF attached to the end that had extreme high precision maneuverability. This meant designing a hexapod system to accurately control the motion of the XRF.

Potential arm ideas were based off of previous rover arms such as Curiosity. However, the capabilities of these arms, including the range and weight of the payload, proved to be much greater than the necessities for this mission. Additionally, the hexapod struts were researched in great detail—materials, components such as motors, interfaces between the different subassemblies, and thermal expansion were all addressed—but later research showed that this amount of accuracy was not necessary for this system. The hexapod design was replaced with a focus on designing a chassis that would ensure functionality in the majority of environments.

When it was decided that the focus should be on demonstrating the spectrometer technology, both the custom lander and the arm were scrapped so more focus could be placed on guaranteeing the success of the XRF. The mission purpose and requirements describe a simple system with as little points of failure as possible that is capable of receiving at least one measurement from the spectrometer to prove its functionality. Based on this, a piggy-back lander was chosen instead of a custom one to simplify the trip and guarantee a space-heritage mission. Deciding upon a piggy-back lander meant having to address various requirements from an outside provider, which came to be a major focus. The arm was heavily redesigned, and after proposing many ideas including a ladder extender, a plunger with rotational movement was chosen for its simplicity and fewer number of failure points. Its ability to rotate and extend satisfies Requirement M001 in Table 2.1.

## 5.2 Astrobotic

Astrobotic provides a lander where we are assigned some space. As seen in Figure 5.1, the general structures of the mid-latitude lander and the polar lander vary on the outside [50].

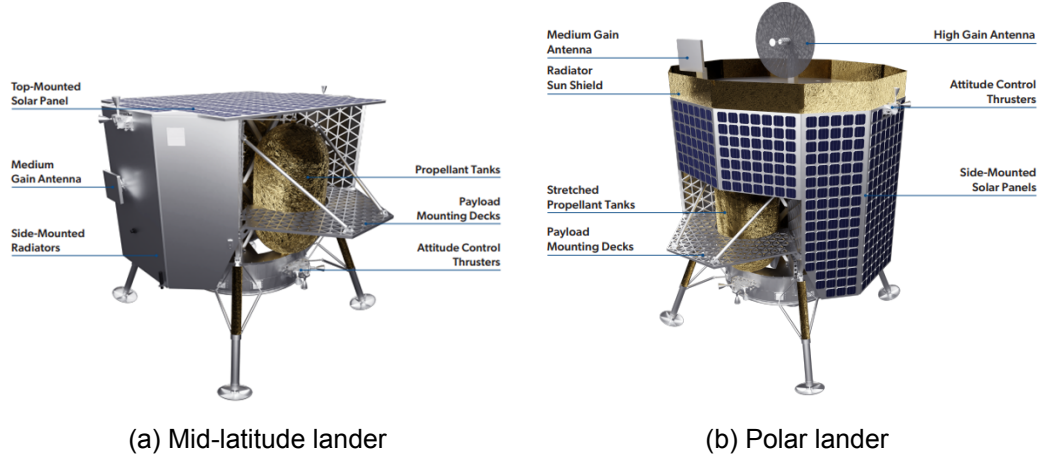


Figure 5.1: The mid-latitude and polar lander from Astrobotic Technology. From the Astrobotic Payload User Guide [50]

The solar panels are placed horizontally on the top for the mid-latitude lander and vertically on the walls for the polar lander to maximize solar exposure. However, the possibilities are the same for any payload user regardless of the lander type. A figure of the general structure of the lander is provided in figure 5.2. The Astrobotic standard lander consists of two isogrid aluminium decks that are assigned to mounting of payloads, and a smaller deck that is used for deployable payloads. The payload user guide also states that special arrangements can be made so the user can mount something on non-conventional areas; however, this would require further discussions with the Astrobotic team.

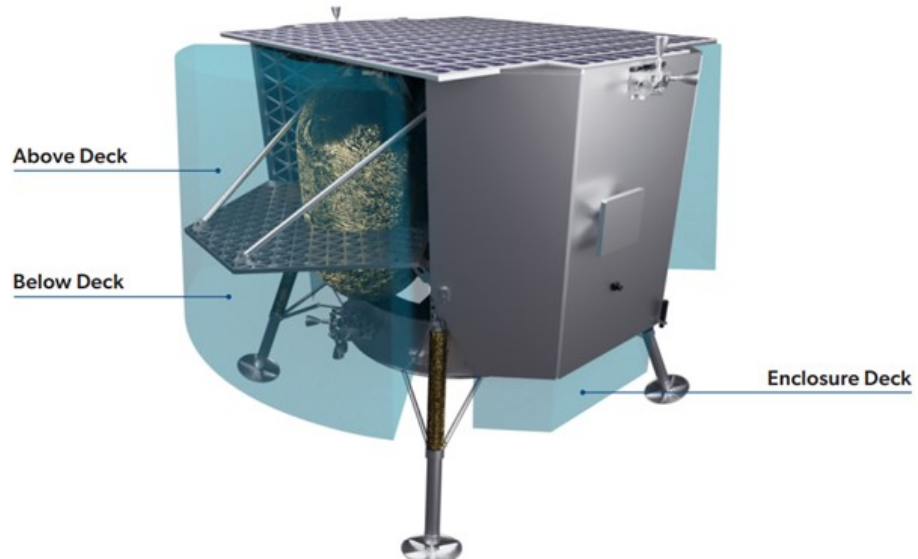


Figure 5.2: The mid-latitude Astrobotic lander. From Astrobotic Payload User Guide [50]

The blue space surrounding the mounting deck is called the envelope. In collaboration with the Astrobotic team, the payload user is assigned some space in the envelope. The envelope reaches 0.38 m below the mounting decks, and 0.57 m above the decks, and any movements outside the envelope should be scheduled in advance and in agreement with the Astrobotic team. Depending on the landing conditions, there is between 0.4 m

and 0.8 m gap to the lunar surface from the bottom of the envelope, e.g. there is between 0.8 m to 1.2 m from the mounting decks to the lunar surface.

A various number of tests should be carried out in collaboration with the Astrobotic team. Furthermore, Astrobotic will provide further information on sine vibration loads, random vibration loads, acoustic loads, and shock loads, when a specific configuration for a mission is done. Especially for the polar lander, the user guide is not that specific, but approximations are given in Table 3.2.

## 5.3 XRF chassis

### 5.3.1 Overview

The product described in this section is applicable to numerous other space projects not specific to the technology demonstration being performed. Those who wish to use this spectrometer on other missions will receive this chassis that includes all the XRF components and electronics; hence, a main goal was to make this design as versatile as possible.

This device, suitable for various applications, includes the chassis, the dust cover, the XRF components (specifically the x-ray source, the x-ray source controller, and the two detectors), and the electronics to power the XRF. Thermal and radiation protection has been accounted for in this design and the details can be found in the Launch, Orbit, and Landing section of the report as well as the thermal subsection of this section. Later sections that elaborate on the mechanism to bring the spectrometer to the Moon's surface are not included in the XRF product. A full list of components included in this specific assembly can be found in Table 5.4.

### 5.3.2 Initial Design

Upon realizing that the minute motions of the hexapods were not necessary, the final goals of the XRF chassis were to ensure functionality of the spectrometer under most environmental conditions, have a user-friendly interface that could be applied to practically all projects, and be as light, small, and efficient as possible.

The first iteration of the XRF chassis, given the parameters defined by the payload group, proved to be too similar to the current spectrometer used on NASA rovers in terms of space and weight [24]. A render of the initial model can be found in Figure 5.3 and a diagram of the chassis with the top off and dust cover open can be found in Figure 5.4.

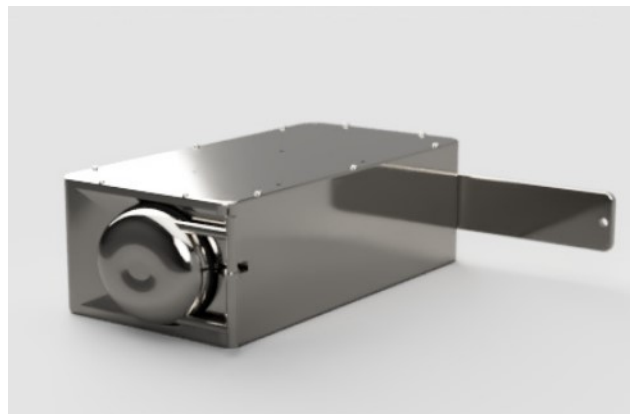


Figure 5.3: Original XRF Chassis Design

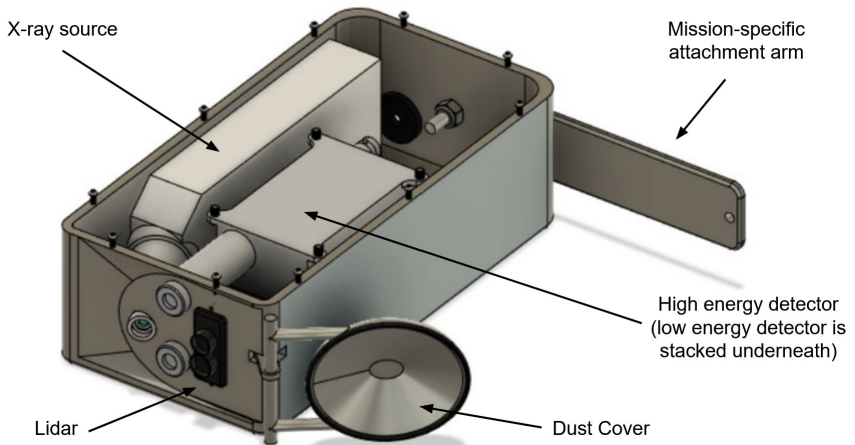


Figure 5.4: Original XRF Chassis Design with Annotations

This design was originally made from titanium with a thickness of 4.3 mm. It was equipped with a dust cover powered by a custom stepper motor to protect the components during potential dust storms (though not applicable for this specific mission, except perhaps for landing). The dust cover, as well as anyplace where a component peeks through the edge of the chassis, was to be lined with a flexible sealant to regulate the inside environment as much as possible.

An attachment arm can be seen on the back of the chassis, which functioned to hold the chassis to the lander while in launch, orbit, and landing. The bolt and nut in the back center wall is for an eye bolt. Both of these components were specific for this mission only.

Due to the material and size of the chassis, the total mass of the XRF in this design was 2.3 kilograms.

### 5.3.2.1 Mission Specific: Flight Cover

The original chassis design also came with a flight cover whose purpose was to protect the payload while in flight. The models shown in Figures 5.5 and 5.6 show a rough model of what such a flight cover would look like. These designs do not contain the top cover so that the total structure can be examined.

This flight cover was designed under the assumption that the Astrobotic lander would provide practically no protection during flight. It would attach to the lander with a launch lock that also goes through the arm of the chassis. Upon the release of the launch lock, both the cover and the chassis would be released. Since the flight cover is larger than the chassis itself, this design doubled the mass of the chassis, which would then double the cost of launching this payload on the Astrobotic lander. In later iterations the cover is removed since the XRF chassis protects its components just as well.

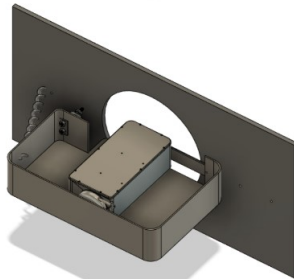


Figure 5.5: Original XRF with Flight Cover, Isometric View

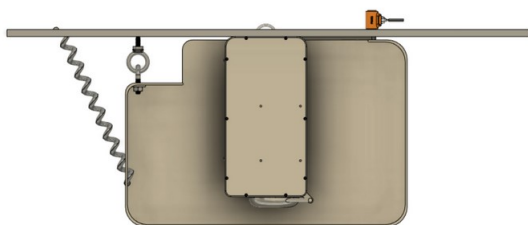


Figure 5.6: Original XRF with Flight Cover, Top View

### 5.3.3 Final Design

#### 5.3.3.1 Overall Structure

The final design of the XRF has the same general shape as the original design with a few distinct features: Firstly, this version is made of aluminum instead of titanium and the dust cover is made of carbon fiber, which significantly decreases the mass. The dust cover is still controlled by a stepper motor and will naturally be open before the XRF is deployed such that the cover does not hit the ground. Additionally, the XRF components have been customized to be more compact, which decreases the size; the specific methods of customization can be found in the XRF Component Adjustments section. The back of the chassis is purposely left untouched so it can be customized to fit a specific mission's needs.

The final chassis has a length of 18.0 centimeters (within the 38 centimeter requirement from Astrobotic), a width of 8.90 centimeters, and a height of 6.60 centimeters. The total mass is 1.50 kilograms. Table 5.4 itemizes the list of components included in this product and their masses.



Figure 5.7: Final XRF Render

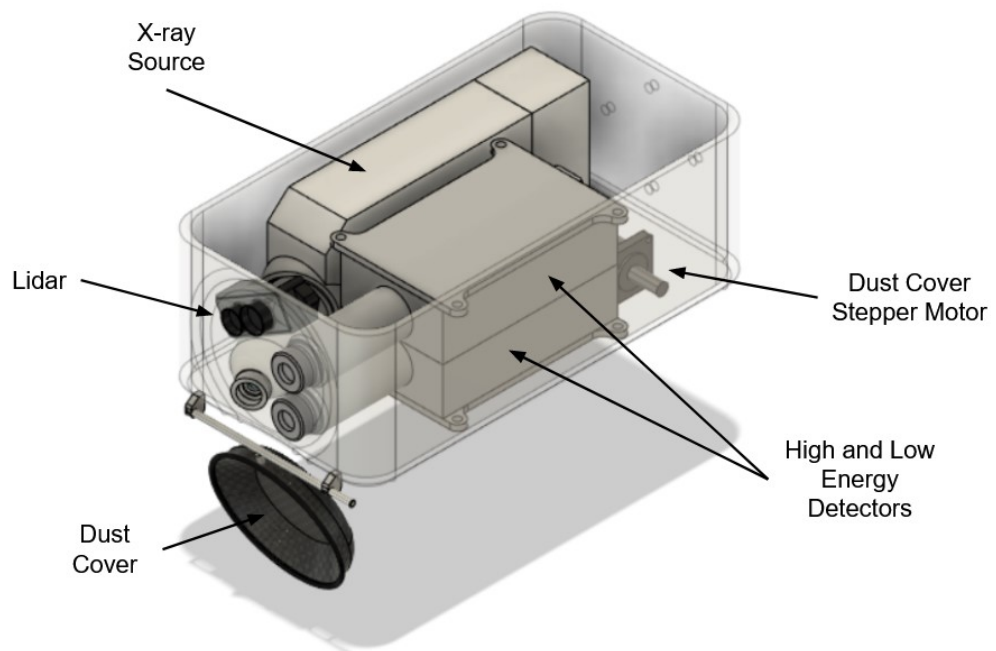


Figure 5.8: Final XRF with Labeled Components

Note that in Figure 5.8, the camera, aluminized polyester film, on-board computer, and PDU are not included, but they are listed in Table 5.4 along with their masses. The camera, whose largest dimension is 17 millimeters (the other two dimensions being 3 millimeters), will be placed at the front of the chassis near the lidar sensor. The on-board computer and PDU, whose dimensions are specified in Table 5.1, will easily fit in the back of the chassis near the stepper motor.

<b>Component Name</b>	<b>Dimensions (length [mm] x width [mm] x height [mm])</b>
On-Board Computer	50 x 20 x 10
PDU	50 x 20 x 8.2
<b>Total Available Space in Chassis</b>	<b>62 x 56 x 49</b>

Table 5.1: Dimensions of Electronics

<b>Component Name</b>	<b>Mass [kg]</b>
6061-T6 Aluminum Chassis	0.509
X-Ray Source	0.150
High Energy Detector	0.157
Low Energy Detector	0.157
On-Board Computer	0.00700
PDU	0.100
Lidar Sensor	0.0120
Camera	0.00800
Carbon Fiber Dust Cover	0.0149
Stepper Motor for Dust Cover	0.0371
Aluminized Polyester Film	0.044
Heat Sinks	0.290
<b>Total Mass</b>	<b>1.50</b>

Table 5.2: Components Included in the XRF Chassis

### 5.3.3.2 XRF Component Adjustments

The components listed in the table above and seen in the models of the chassis are off-the-shelf components used as a reference to estimate the size of the chassis. Given enough time and enough resources, the parts within these components would be removed from their respective shells and placed manually into the chassis, which would greatly decrease the amount of space it consumes. Thus, in the placement of the XRF components in the above model, certain liberties were taken in regard to the size, shape, and positioning of the x-ray source and detectors.

The manufacturer of the detectors provides an outline of the internal parts of the detectors as seen in Figure 5.9 [51] (note that both detectors are identical in size). The dimensions of the stacked DP5 and PC5 assembly were given by the provider to be 8.89 cm x 6.35 cm x 2.29 cm. Based in this information, other dimensions of the detector parts could be estimated.

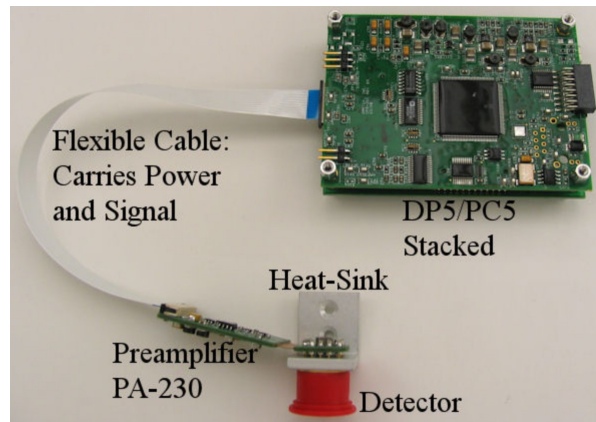


Figure 5.9: Internal Parts of the Detectors

The following figure illustrates exactly how small the x-ray source could become. Although no dimensions were given by the manufacturer, estimations were made to optimize the size of the source.

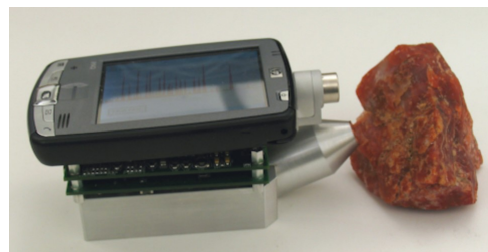


Figure 5.10: Smallest Possible Combination

Based on the size of the component in the step file given by the manufacturer and the dimensions of the parts estimated above, the changes made to the x-ray source and the detectors were decided upon as seen in the following two figures:

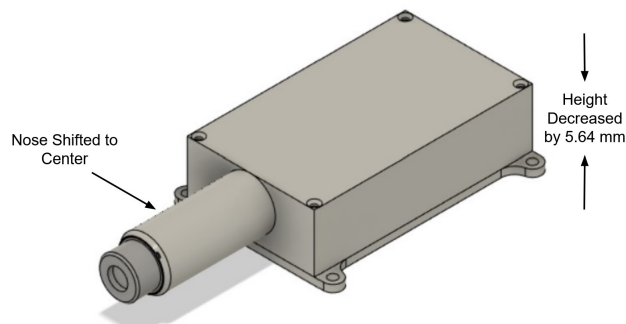


Figure 5.11: Revised Detector Dimensions

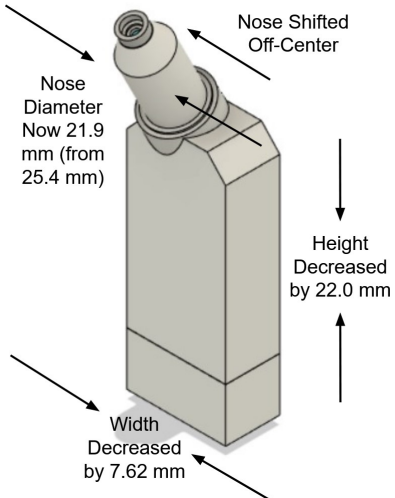


Figure 5.12: Revised X-ray Source Dimensions

#### 5.3.3.3 Dust Cover

The dust cover on the front of the chassis is made of carbon fiber and lined with sealant to ensure full protection of the XRF components in the case of a dust storm if this product were to be used in an environment with a strong atmosphere. It is powered by a custom stepper motor whose precise specifications will be determined closer to production; however, for sizing purposes, inspiration was taken from previous CDA Intercorp motors found in the Stepper Motor Engineering Reference Data brochure [52]. Based on this information, a Type 12, 4 Pole, and 3 Phase motor was chosen due to the low vibrations of a 3 phase motor and the small size of a Type 12. The dimensions, including the mass, for this motor were used in the design of the chassis. This dust cover and the chassis satisfy Requirement M007 as specified in Table 2.1.

#### 5.3.4 Thermal Control

Table 5.3 below lists various components and the corresponding temperature range under which functionality is possible. Note that the Peregrine Lander will only operate during sunlight hours, when the temperature range is between -30 and 80 Celsius.

Component	Minimum Temperature [°C]	Maxmimum Temperature [°C]
X-Ray Source	-10	50
High Energy Detector	-20	50
Low Energy Detector	-35	80
Lidar Sensor	0	60
On-Board Computer	-45	85
PDU	-40	85

Table 5.3: Temperature Requirements for Various Components

The equilibrium temperature of the chassis due to the thermal blankets and the temperature requirements throughout the payload journey can be found under the Launch, Orbit, and Landing section of this report. Heat sinks referenced in the component table will be added in addition to the aluminum chassis to provide more means of thermal radiation. Based on thermal analyses, this XRF can function for about 60 minutes before needing to cease operation due to overheating.

Symbol	Value	Units
r	10	mm
$J_s$	1371	$\text{W}/\text{m}^2$
$J_{alb}$	0.12	$\text{W}/\text{m}^2$
$J_{pla}$	1255	$\text{W}/\text{m}^2$
$A_{sur}$	$4 * \pi * r^2$	$\text{m}^2$
$A_{sol}, A_{alb}, A_{pla}$	$\pi * r^2$	$\text{m}^2$
$\sigma$	5.67e-8	$\text{W}/\text{m}^2\text{K}^4$
$\alpha$	0.95	-
$\epsilon$	0.90	-
$\dot{Q}$	10	W

Table 5.4: Heat Analysis Parameters

$$T^4 = \frac{A_{pla}J_{pla}}{A_{sur}\sigma\epsilon} + \frac{\dot{Q}}{A_{sur}\sigma\epsilon} + \frac{A_{sol}J_s + A_{alb}J_{alb}}{A_{sur}\sigma} \frac{\alpha}{\epsilon} \quad (5.1)$$

$$T^4 = \frac{A_{sol}J_s\alpha}{A_{sur}\sigma\epsilon} \quad (5.2)$$

This analysis ensures that the XRF can function in the temperatures of operation; thus, Requirement M005 from Table 2.1 is satisfied.

#### 5.3.4.1 Mission-Specific: Attachment to Telescopic Rod and Stress

The overall structure of the telescopic rod will be described in detail in later sections, but the basic motion to get the XRF to the surface of the Moon will be actuated through a telescopic motion. In order to obtain multiple measurements, the XRF will be mounted at an offset such that a circle of measurements can be acquired. A diagram of this assembly can be seen below. The mass budget of the assembly that attaches the payload can be found in Table 5.5. The launch lock listed in this table prevents the entire assembly, including the payload and the telescopic rod, from moving during transport, satisfying Requirement M003 from Table 2.1.

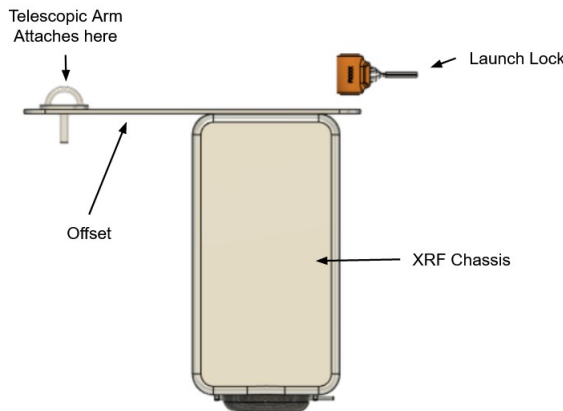


Figure 5.13: Chassis Offset Assembly

Component Name	Mass [kg]
Aluminum arm	0.0692
Eye bolt	0.0251
Launch lock	0.0394
<b>Total Mass</b>	<b>0.134</b>

Table 5.5: Attachment Assembly

The aluminum arm that provides the offset has a length of 0.122 meters, a width of 0.0508 meters, and a height of 0.00254 meters. Therefore, the cross sectional area is 0.0508 meters by 0.00254 meters with a neutral axis at the center due to its rectangular geometry. The normal stress for pure bending is defined below in Equation 5.3, where M is the moment (Eq. 5.5), y is the distance from the neutral axis to the edge of the plate (for maximum stress), and I is the moment of inertia about the neutral axis (Eq. 5.4).

$$\sigma = \frac{-My}{I} \quad (5.3)$$

$$I = \frac{1}{12}bh^3 \quad (5.4)$$

$$M = r \cdot F \quad (5.5)$$

The shear stress for pure bending can be found in Equation 5.7, where V is the shear force, Q is determined using the area above the neutral axis (Eq. 5.7), I is the inertia as defined above, and t is the width.

$$\tau = \frac{VQ}{It} \quad (5.6)$$

$$Q = \bar{y}A \quad (5.7)$$

The values of all variables, the results of utilizing the equations above, and the ultimate stresses of pure bending in Aluminum 6061-T6 are outlined in Table 5.6 [53]. The stresses determined by calculation are significantly less than the ultimate stresses, verifying a structurally sound assembly.

Parameter	Value	Units
Gravitational Acceleration (g)	1.625	m/s <sup>2</sup>
Force Applied (F and V)	2.096	N
Moment (M)	4.30	Nm
Inertia (I)	6.937e-11	m <sup>4</sup>
Distance from Neutral Axis (y)	0.00127	m
<b>Normal Bending Stress (<math>\sigma</math>)</b>	4.68	MPa
<b>Ultimate Normal Bending Stress (<math>\sigma_u</math>)</b>	290	MPa
Width (t)	0.0508	m
Centroid and Area Product (Q)	4.0968e-8	m <sup>3</sup>
<b>Shear Bending Stress (<math>\tau</math>)</b>	0.0244	MPa
<b>Ultimate Shear Bending Stress (<math>\tau_u</math>)</b>	207	MPa

Table 5.6: Stress Analysis for Chassis Offset

### 5.3.4.2 Comparison to Other XRFs

The main goal of this design, beyond the requirements set in place by the mission, was to develop a smaller and more lightweight spectrometer compared to the PIXL device currently being used on Mars. However, it is important to take into consideration other spectrometers that have been used in order to solidify the importance of our device.

A comparison of the size and weight of various spectrometers used throughout space exploration history can be found in Table 5.7. Clearly, the Mini XRF developed in this report is most efficient in terms of mass and size.

Spectrometer	Mass [kg]	Size [cm]
PIXL [24]	4.30	27 x 23 x 21.5
MARIE [54]	3.30	29.4 x 23.2 x 10.8
Mass Spectrometer for Planetary Exploration [55]	8	40 (largest dimension)
<b>Mini XRF</b>	<b>1.29</b>	<b>18 x 8.9 x 6.86</b>

Table 5.7: Comparison of Various Spectrometers

## 5.4 Telescopic Rod Design Journey

As the Astrobotic lander has fixed instrument mounting surfaces in ranges from 0.8 to 1.2 meters above the lunar surface (Figure 5.2), a mechanism for lowering the XRF is needed to position the XRF in the optimal measuring distance. In this section the different methods that have been conceived throughout the duration of the project will be discussed and how they lead to the final design.

### 5.4.1 Design Constraints and Optimizations

The design of the lowering device had to be derived by carefully considering mission-critical criteria and additional bonuses. Regarding mission-critical criteria, the lowering of the XRF to an optimal location is paramount: If this fails, the mission fails, as the XRF would not be able to demonstrate its capabilities. In addition to this, an additional criteria would be the capability of taking multiple measurements in a line or on a surface; this will be categorized as 1D and 2D measuring capabilities going forth.

#### 5.4.1.1 Robotic arm

During the initial iterations of the design, the team dabbled in the possibility of designing a three-joint robotic arm. This would in theory be able to move the XRF in a wide range of locations making it have a 2D measuring capability. This design was however plagued with a lot of downsides making it ill-suited for the application at hand. For example, the arm would need a considerable number of moving parts each of which being a potential point of failure with little redundancy. This fact alone made the arm undesirable, as the failure of one of the joints would render the mission finished. In addition to this, the design of an arm would come with a comparably huge price tag both in terms of research and development. Although this could be mitigated by implementing an already available arm, it would be at the cost of an increased mass budget.

#### 5.4.1.2 Telescopic Rod

After careful consideration, the team moved away from the design of a three-joint robotic arm in favor of a telescopic rod. This design was a product of a group lead discussion by the whole team, including every subgroup of the project, considering the overall mission requirements. In this meeting, the mission requirements were re-evaluated, resulting in a substantial decrease in XRF location precision and range of motion, as the mission was now heavily focused on risk mitigation and proof of concept of the XRF.

A design consisting of a telescopic rod would allow for more redundancy, since more shell elements in the rod could be added and a lower number of motors would be used. In addition, the motor needed for the lowering of the XRF would have a significantly lower power consumption as the action of lowering the XRF would be aided by lunar gravity. The telescopic rod by itself, however, would not allow for multiple measurements to be taken on the lunar surface, as the rod would only allow for one dimension of movement resulting in a single point of potential measurements. To mitigate this, the team considered a number of potential options to increase the range of motion. These options can be seen in Figure 5.14 below.

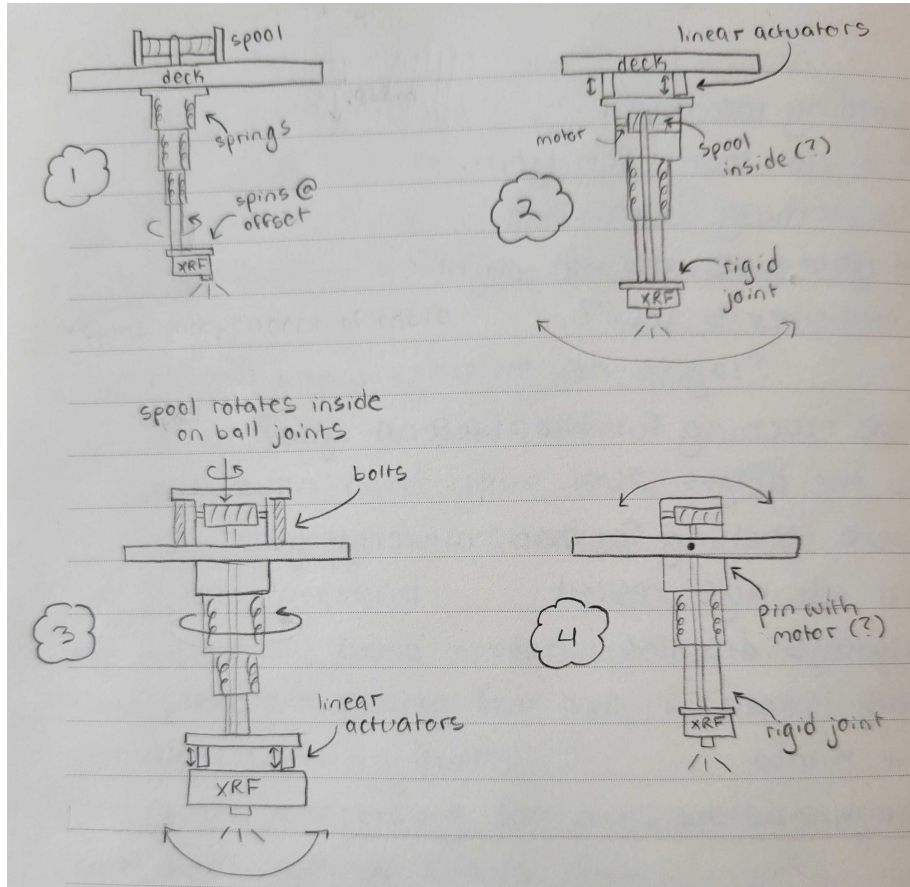


Figure 5.14: Ideas for the plunger

These four options come with their advantages and disadvantages. Looking at them side by side, one could start by investigating the range of motion each option provides. Here we are again looking at the capability of 1D or 2D measuring compared to the 0D or point measurement of the rod by itself. From the figure, it can be seen that options 1 and 4 both allow for 1D measuring, with option 1 being able to move the XRF in a circle over the surface, and option 2 allowing the XRF to swing around a pivot on the mounting surface allowing for a straight line of measurements. In comparison to this, options 2 and 3 allow for 2D measuring or a surface of measurements to be taken. These designs work by the same principle of rotating a rod whilst also pivoting around a point. The difference in these designs is the compromise between precision and range of motion. For the second option, the pivot is at the mounting surface allowing for a large range of motion in the tip at the cost of lowering the stability and accuracy. In contrast, the fourth option incorporates the pivot in the tip of the rod which decreases the range of motion drastically while also increasing

the accuracy of the device. A second and more important factor in choosing the right design is the complexity and location of moving parts. As the mission requirements do not specify a need for a large number of measurements, reducing complexity is important for mitigating risk. From this options 2 and 3 were scraped. That left options 1 and 4 for further research. In these cases, power requirements from potential motors were assessed. This led the team to choose option 1 as the power requirement and low complexity of rotation of the assembly were advantageous compared to the relatively high torque in the mounting point that needed to be overcome combined with a higher risk of jamming the rod's shell elements.

## 5.5 Telescopic and Rotating Mechanism Design

### 5.5.1 Lowering Mechanism

The chosen design of a telescopic rod lowering the XRF from the mounting deck of the Astrobotic lander to the lunar surface brings the problem of how this lowering is controlled. A controlled descent of the XRF is crucial as the distance from the mounting deck to the surface is not well defined before the launch and depends on the specific landing circumstances. In addition to this, the mounting deck might not be parallel to the lunar surface after landing due to slopes on the surface. This means that the telescopic rod connecting the lander and the XRF needs to allow the XRF to move up and down in order to facilitate a possible distance change for the rotation of the XRF described in the next section.

This motion is controlled by a threaded spool at the top of the top shell element connected to a Kevlar string. This wire is connected to the telescopic rod on both ends, the first end being the threaded spool and the second end being the last shell element. This allows for a controlled movement of lowering of the XRF. The assembly of the spool can be seen in Figure 5.15 below. A list of all components in this assembly and their weights can be found in Table 5.8.

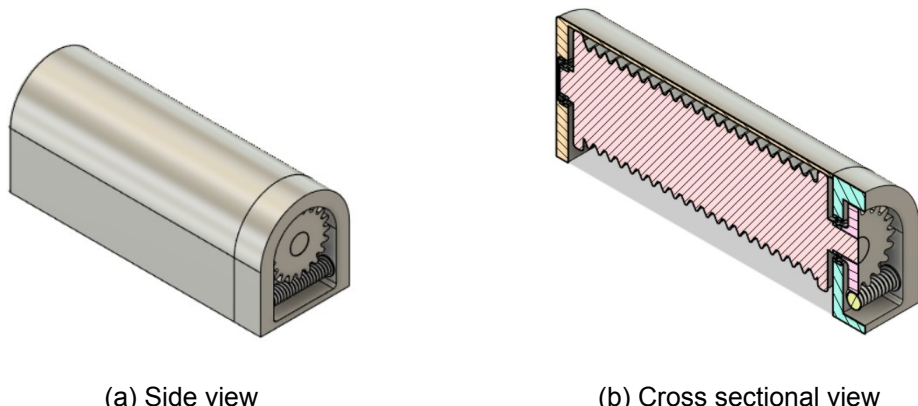


Figure 5.15: Lowering Mechanism

This spool is constrained by bearings in both ends, locking its location while still being able to rotate. The rotation of the spool is provided by a worm gear connected to a spur gear, powered by an electric motor. The use of a worm gear has two major advantages compared to other gearing alternatives. The first is the high gearing ratio in comparison

to its footprint on the mounting deck. This high gearing ratio comes from the fact that a full rotation of the worm only allows for a rotation of the spur gear by one tooth. This high gearing allows for greater positioning accuracy and the use of a low-powered motor. The other advantage of using a worm gear is its self-locking ability. This self-locking ability allows the XRF to stay fixed in a determined location while no load is applied to the motor. This allows the power requirements of the whole system, XRF, and telescopic rod to drastically decrease as the two systems can be run independently, satisfying Requirement M004 from Table 2.1.

The last crucial part of the lowering system is the integrated springs. These springs are located in each shell element to aid the lowering of the XRF. It was first discussed whether the lunar gravity would be able to reliably extend the telescopic rod and while that is possible, the risk of jams or increased friction due to dust made the introduction of springs an important factor for risk management. The shells of the telescopic rod, made of carbon fiber and reinforced with aluminum, can be seen in Figure 5.16. Note that the springs are not shown in this model.



Figure 5.16: Telescopic Rod Shells

<b>Component Name</b>	<b>Mass [kg]</b>
Top shell	0.303
Second shell	0.277
Third shell	0.252
Bottom shell	0.173
Kevlar String	0.011
<b>Total Mass</b>	<b>1.016kg</b>

Table 5.8: Components Included in the Lowering Mechanism

### 5.5.2 Rotating Mechanism

As examined in the previous section, the design of the lowering system contains a sub-system tasked with rotating the XRF in a circle over the lunar surface. This is done to increase the number of measurements the XRF is able to take during the mission. The design criteria for the rotating mechanism were to minimize the overall footprint and mass of the system in order to lower the takeoff cost of the mission and allow other instruments to fit on the mounting deck of the Astrobotic lander. For this reason, the rotating mechanism was designed to fit into the lowering mechanism's mounting plate. This can be seen in the two figures in Figure 5.17 below. All components in this assembly are tabulated in Table 5.9.

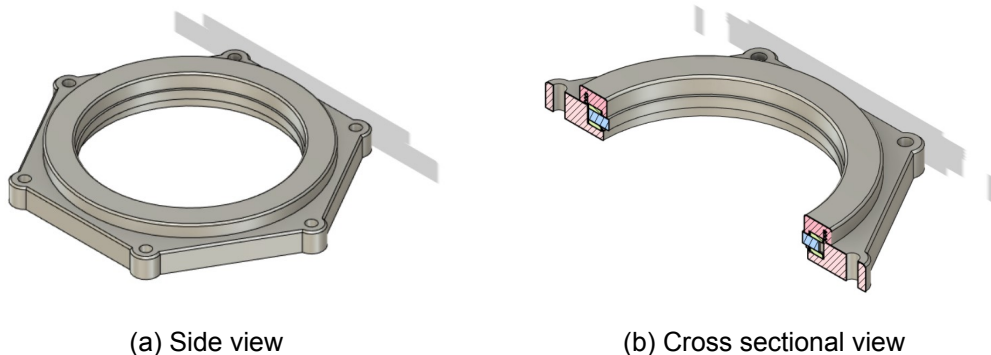


Figure 5.17: Rotating mechanism

<b>Component Name</b>	<b>Mass [kg]</b>
Lower base	0.203
Top base	0.085
Pin Bearing bottom	0.036
Pin Bearing top	0.036
Gear	0.044
<b>Total Mass</b>	<b>0.405</b>

Table 5.9: Components Included in the Rotating Mechanism

In the above figure, the structure of the rotational mechanism can be seen in the cross-sectional view. This shows how the forces and loads of the XRF and lowering mechanism are held by a pair of pin bearings on the top and bottom of a connected spur gear. The spur gear is designed to be rigidly attached to the top shell element of the telescopic rod

and thereby connecting the rotation of the spur gear and subsequent shell element. In addition to the load in the vertical direction, which comes from the lunar gravity pulling the assembly, the telescopic rod also has an additional load in the horizontal direction from the unbalanced rotation of the XRF mounted at the tip. This force is accounted for in the use of a standard ball bearing mounted in the bottom of the telescopic rod's mounting plate as shown in Figure 5.17 b. The rotation of the system is, as previously described, driven by a spur gear connected to the telescopic rod. This rotation is facilitated by a gear connection between the load-bearing spear gear and an externally mounted screw gear. The reason for designing the system around a screw gear is its ability to deliver a precise rotation and its ability to be self-locking, ergo the rotation will be in a locked position while the XRF is conducting the measurements. The hexagonal shape of this design allows it to be mounted to the isogrid deck of the Peregrine Lander, satisfying Requirement M002 from Table 2.1.

### 5.5.3 Mechanical analysis

The following section describes the analysis of the Telescopic and Rotating Mechanism mentioned in Section 5.5. The material used for the shells is a Carbon Fiber Reinforced Polymer (CFRP).

#### 5.5.3.1 Springs

In order to assist the extending of the telescopic rod by gravitational acceleration, the design uses springs inside the extending elements. By controlling the parameters of the springs used in the telescopic rod, it is possible to prioritise what element will extend first. Due to different diameters of the elements the friction and the spring properties change from element to element.

The resulting force from the springs is estimated to be  $F_{Springs} = 50N$

#### 5.5.3.2 Static load

To ensure that the lowering mechanism can withstand the static load the Kevlar string sees a longitudinal force provided in Eq. 5.9 with the  $m_{Payload} = 1.50kg$  (see Tab. 5.4),  $m_{Rod} = 1.016kg$  (see Tab. 5.8) and  $F_{Springs} = 50N$  (see Section 5.5.3.1).

$$\begin{aligned} F_{longitudinal} &= F_{Payload} + F_{Rod} + F_{Springs} = \\ &= (m_{Payload} + m_{Rod}) \cdot g_{moon} + F_{Springs} = \\ &= (1.50kg + 1.016kg) \cdot 1.625 \frac{m}{s^2} + 50N = 54N \end{aligned} \quad (5.8)$$

The used Kevlar 49 String [56] provides a ultimate tensile strength of  $\sigma_{Ultimate} = 3000MPa$ . The choosen diameter of String is  $d = 0.5mm$

$$\sigma_{String} = \frac{F_{longitudinal}}{\pi \cdot \frac{d^2}{2}} = \frac{54N}{\pi \cdot \frac{1mm^2}{2}} = 276MPa \quad (5.9)$$

This ensures that the String is capable of withstanding the static load of the lowering mechanism.

#### 5.5.3.3 Friction

To reduce the friction between the shells, the outside of them is coated with PTFE. This also helps to reduce wear on the sliding surfaces and helps to reduce the settlement of dust, due to a high surface finish.

Assembly Name	Mass [kg]
Spool for Lowering	0.187
Rotation Mechanism	0.442
Telescopic Rod Shells	1.01
Communications SpaceWire	0.274
Arm to Attach Mini-XRF	0.134
Mini-XRF	1.50
<b>Total Mass</b>	<b>3.53</b>

Table 5.10: Total Mass Budget

#### 5.5.3.4 Vibrations and Shock

According to Requirement M006 in 2.1 the system has to withstand the loads from launch to landing (see Section 5.2). The lowering mechanism is fixed in place with the launch lock as described in Section 5.3.2.1. It ensures that the lowering mechanism can withstand the loads in its collapsed configuration. To validate this, it requires a thorough analysis of the dynamics and real test hardware. It is therefore not within the scope of this report.

#### 5.5.4 Thermal Analysis

As mentioned in Table 3.2, the mechanical structure should be able to handle temperatures between -30°C and 80°C, while it is on the lunar surface.

The thermal expansion ratio of the used CFRP is very low and it is therefore not relevant to ensure the fulfilment of the requirements.

As mentioned in the Userguide [50] a thermal isolation must be designed between the system and the lander. It is taken care of by layering a PTFE ring between the lander and the Rotating Mechanism seen in Fig. 5.17. This satisfies Requirement M005 as specified in Table 2.1.

### 5.6 Complete and Final Design

Based on all considerations and solutions that are described in previous sections, one summary of the final design is made. This would need further testing and considerations when continuing the project; however, it fulfills the requirements so far.

#### 5.6.1 Final Design

The total, complete design can be seen in Figure 5.18, and the total mass budget can be found in Table 5.10.

#### 5.6.2 Future work

We have several items that Astrobotic most likely can fulfill based on the information from their Payload User's Guide. In case any of the following items cannot be fulfilled by Astrobotic, further design considerations must be made:

- That we can use the required area on the mounting deck for our system.
- That we can get a location on the mounting deck that has a clear sight to the surface.
- That we are assigned the space under and above our area on the mounting deck.
- That there is a larger hole in the isogrid mounting deck that can be used for the telescopic rod.

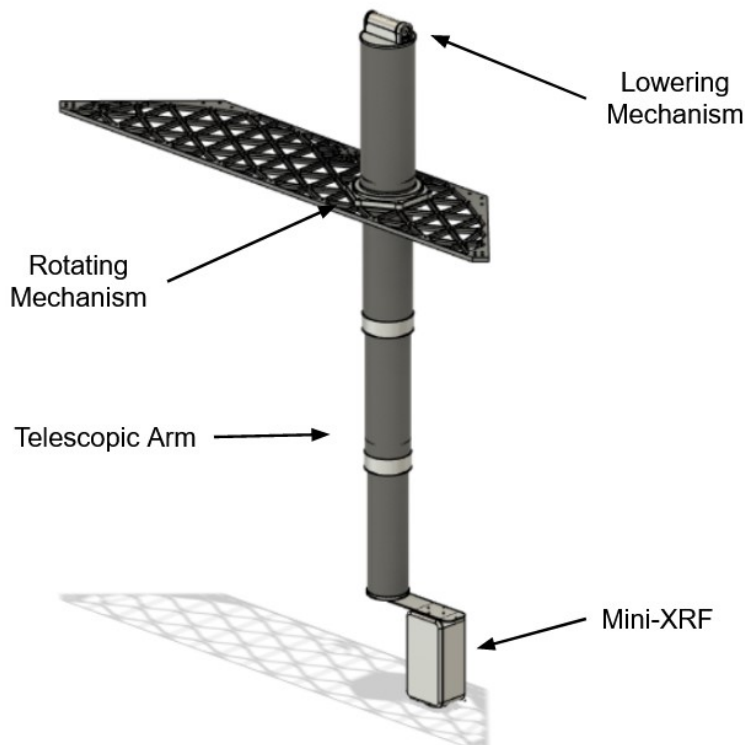


Figure 5.18: Complete Assembly

- That we can schedule the telescopic rod to extend downwards (out of the envelope) to the surface after the lander has landed, and it can stay there for the rest of the mission.
- That the mechanical part can pass all the the tests that Astrobotic might require.

In addition to these discussions, given more time and resources, more investigation would be spent on the vibration response of the system, the placement of the XRF components in the chassis, and the specification of certain components such as motors. Furthermore, a number of tests could be made to reevaluate the performance of the final design of the telescopic rod.

# 6 Electrical Power System

In this chapter the electrical power system of the mission will be presented. Initially, the various power sources are discussed in Section 6.1, comparing the various pros and cons based on the mission requirements, followed by a power budget in Section 6.2. Power management is presented in the subsequent Section 6.3, and the on-board computer is detailed in Section 6.4.

## 6.1 Power source

To power the different instruments on the payload, a certain amount of electrical power is required. To meet these requirements and to distribute power to the different subsystems, power needs first and foremost to be generated. The Peregrine lunar lander from Astrobotic Technologies provides a certain amount of power based on the weight of the payload and gives the opportunity to buy more power if required. However the questions arise, is the power provided sufficient and can it power the different subsystems or would it be more beneficial to generate our own power? This subsection will present the different power sources considered, weight the benefits and downsides and also look at the option of using the power provided by the Peregrine lunar Lander, to see if it is enough to power all the subsystems that require electrical power.

The ideas and proposed solution were made based on the requirements of providing enough power to the various subsystems, and at the same time to limit the payloads total weight and thereby total cost. The mission lifetime also plays a factor when choosing a power source and as seen in the Figure 6.1 below, different power sources are presented based on the electrical output and mission duration.

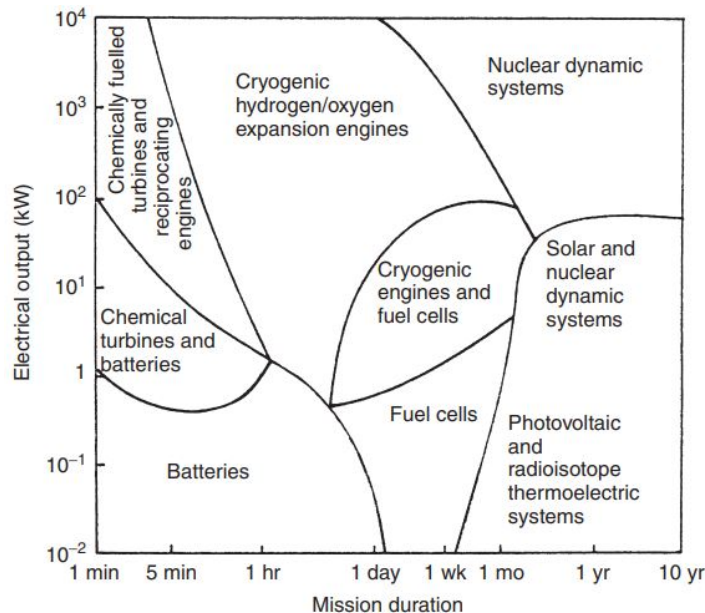


Figure 6.1: Graph showing the relationship between the electrical output (kW) and mission duration for different power sources. From [57].

From the different power sources shown in the Figure 6.1 above, the proposed solution includes using our own solar cells system or using a rechargeable battery with the power

from the lander to charge up the battery for use. Alternative energy sources that could be considered, could include using fuel cells or radioisotope thermoelectric systems, but these will not be considered for this mission. Fuel cells cannot be recharged and are primarily used for small spacecraft propulsion systems rather than power sub-systems and radioisotope thermoelectric systems are more suited for missions where the Sun is too far away, which for this mission, it isn't.

### 6.1.1 Solar array

The proposed solution with using solar cells as a power source would exclude using a battery, as this would increase the total weight of the payload by a lot. So instead, power would be drawn directly from the solar cell to the subsystems. Using solar cells would make the payload more complex (increased risk of failure), but would be sufficient to provide for the power requirements needed, as well as being light in weight. The downside of using solar cells typically includes no power generation during eclipse periods, degradation due to radiation exposure, high surface area, mass and cost.

The state of art of solar cells used for space applications are multi junction cells. They have a high efficiency-to-cost ratio, compared to single-junction cells that are much cheaper in cost, but also much lower in efficiency as well, usually around 20 % and will therefore not be considered for this mission.

There exists many types of solar cells and the most optimal one for the mission should be chosen based on the requirements for power to the different subsystems and the total weight, as this is desired to be as low as possible. Since not a whole lot of power is required to be provided for the payload, it is sufficient to look at using a few solar cells, which can be connected in series, instead of looking at manufacturers that produce solar panels for space applications.

In Figure 6.2, different manufacturers that offer solar cells for space applications can be seen. By weighing the efficiency, weight and power output of the different solar cells, the solar cell TJ 3G28C from AZUR space proved to be the most efficient for this specific type of mission. The TJ 3G28C is a state of the art triple junction GaAs solar cell with a 28 % efficiency.

The specifications can be seen in Table 6.1 from the datasheet [58].

General Parameters	Details	Units
Base Material	GalnP/GaAs/Ge on Ge substrate	-
AR-Coating	TiO <sub>x</sub> / Al <sub>2</sub> O <sub>3</sub>	-
Dimensions	40 x 80 ± 0.1	mm
Cell Area	30.18	cm <sup>2</sup>
Average Weight	≤ 860	g/m <sup>2</sup>
Average Power (28 % eff.)	1367	W/m <sup>2</sup>

Table 6.1: Specifications of the TJ 3G28C from AZUR space.

Table 3-1: Solar Cells Product Table									
Company	Cell Name	BOL Efficiency	Voc (V)	Vmp (V)	Jsc (mA/cm <sup>2</sup> )	Jmp (mA/cm <sup>2</sup> )	Pmp (W/m <sup>2</sup> )	Ref	
AZUR Space	Silicon S 32	16.8	0.628	0.528	45.8	43.4	229.2	(3)	
	3G30-Adv	29.5	2.7	2.411	17.2	16.71	403	(3)	
	4G32-Adv	31.5	3.426	2.999	15.2	14.37	431	(3)	
	TJ 3G28C	28	2.667	2.37	16.77	16.14	1367	(3)	
SolAero	ZTJ	29.5	2.726	2.41	17.4	16.5	397.7	(10)	
	ZTJ+	29.4	2.69	2.39	17.1	16.65	397.9	(10)	
	ZTJ Omega	30.2	2.73	2.43	17.4	16.8	408.2	(10)	
	Z4J	30.0	3.95	3.54	12	11.5	407.1	(10)	
	IMMα	32.0	4.78	4.28	10.7	10.12	433.1	(10)	
	ZTJM	29.5	2.72	2.38	17.1	16.5	392	(10)	
SpectroLab	XTJ	29.5	2.633	2.348	17.76	17.02	399.6	(6)	
	XTJ-Prime	30.7	2.715	2.39	18.1	17.4	415.9	(6)	
	XTE-SF	32.2	2.75	2.435	18.6	17.8	433.4	(5)	
	XTE-HF	32.1	2.782	2.49	18	17.4	427.9	(5)	
	XTE-LILT	31.6	2.755	2.459	18.1	17.4	427.9	(5)	
	UTJ	28.4	2.66	2.35	17.14	16.38	384.93	(7)	
	TASC	27	2.52	2.19	32	28	270	(8)	
	ITJ	26.8	2.565	2.27	16.9	16	1353	(9)	
	Emcore	BTJ	28.5	2.7	2.37	17.1	16.3	386	(4)
	Emcore	ZTJ	29.5	2.726	2.41	17.4	16.5	397	(4)

Figure 6.2: Overview over different manufactures that produce small spacecraft solar cells for space applications with the product specifications listed [59].

From Table 6.1, the weight, size and number of solar cells needed can be calculated for the payload as seen in Table 6.2.

It can be seen from Table 6.2, that the solar cells will not influence the weight of the payload too much while also providing for the necessary power. Using solar cells could prove to be a good solution for generating power by being light in weight and small in size, however the solar cells have some downsides, such as, it would be needed to be lifted above the lander in order to generate power from sunlight at all times, otherwise the solar cells could be mounted on the payload, which would only make for measurements being taken once

Power (W)	Size ( <i>cm</i> <sup>2</sup> )	Weight (g)	Number of cells
10	60	6.29	2
15	90	9.4	3
20	120	12.58	4
25	150	15.72	5

Table 6.2: From Table 6.1, the size, weight and number of solar cells required is shown for different expected power amounts needed.

General Parameters	Details	Units
Cell Chemistry	Lithium-Ion	-
Mass	980	g
Capacity	11.6 Ah, (125.28 Wh)	-
Voltage range	7.5 to 12.6	V
Operating temperature	0 to 40 (Charge)	°C
Dimensions	98 x 86 x 59.8	mm
Space Heritage	Yes	-

Table 6.3: Table for the specifications of the ABSL 3s4p Li-ion rechargeable battery from EnerSys [60].

every time the Sun is at the right orientation. Lifting the solar cells above ground, would make for an even more complex system and would require an additional system that could lift the solar cells above the lander. Also, the solar cells will not work without sunlight and will lose efficiency over time due to radiation, but due to the low lifetime of the mission, this would not be a huge problem.

### 6.1.2 Rechargeable battery

Another proposed solution would be using a rechargeable battery to power the electrical subsystems, with the use of the power provided by the Peregrine lunar lander to charge up the battery. Batteries used for space applications are very popular for low lifetime missions and the technology has improved a lot, where smaller batteries can store more energy for longer times. The most popular form for batteries used for space applications are lithium-ion batteries and rechargeable lithium-ion batteries that use liquid electrolytes. However, these have an inherent risk of overcharging, lose capacity over time and require cooling/heating, which would require more of the power to be distributed to. However, batteries are still advancing and there are a lot of good products to be found on the market.

The battery has been chosen based on being rechargeable for this mission, low in weight, providing at least 12 V for the XRF and providing minimum 10-20 watts.

The chosen battery proposed, is the Li-ion Rechargeable Battery ABSL 3s4p from EnerSys [60], which is a satellite battery with mass of 980 grams and the specifications listed in Table 6.3.



Figure 6.3: An image of the ABSL 3s4p Li-ion rechargeable battery from EnerSys [60].

From Table 6.3 and Fig. 6.3, the chosen battery and the specifications of the battery for the mission is presented. The battery meets all the requirements, but are heavy in weight. This would ultimately mean an increase in cost for the mission and is the biggest concern to using a rechargeable battery. Also note from Table 6.3, that the operating temperature falls between 0 to 40 degrees Celsius and on the Moon the temperature can easily fall between -/+ 120 degrees Celsius, which means that the battery needs a heating/cooling system to operate. Basically, most of the generated power will go towards keeping the battery in the operating range in order for the subsystem to be able to draw from the batteries power efficiently, which could mean that it would take even longer for the battery to be charged in a rate, where the power could be drawn from.

### 6.1.3 External power provided - Peregrine lunar Lander

The final proposal to a power source for the payload, is to use the power provided by the lunar lander itself. The Peregrine lunar Lander provides a certain amount of electrical power to the payload depending on the weight, which is specified in their user guide. This power is limited, but can be increased if the customer desires more power. It would be optimal for the mission to be designed based on the amount of power available from the lunar Lander as to decrease the overall size, complexity and cost for the finial mission. However, components and subsystems might not meet the set requirements and would require more work to get them to work with the available power from the lander such as getting the right input voltage/current.

From the user guide of the Peregrine lunar Lander the following is offered as a power service to the payload [5]:

- OFF: No power is provided to payloads.
- Nominal: 1.0 W per kilogram of payload.
- Peak: 2.5 W per kilogram of payload as scheduled by Astrobotic
- Release: 30 W peak payload power for approximately 60 seconds.

The amount of power provided by the Peregrine lunar Lander is based on the payloads total weight. However, it is stated in the user guide that additional power services are

available for purchase.

Since the weight of the payload is only a few kilograms, the provided power by the weight alone, even at peak efficiency, will not be sufficient. However, using the power available from the lander and in addition to also buying more power might be sufficient and is an option. By going with this proposal, the downsides and limitations of using a battery and solar cells will disappear and is by far the best solution to acquire the right power level for the payload of the mission.

## 6.2 Power budget

We are in an interesting position regarding available power, as our main power source, the Astrobotic lander, provides our mission with power depending on the size (mass) of our mission. They promise a constant supply of 1 W pr. kg of weight at all times, and 2.5 W per kg of weight at peak hours. Additionally, power can be purchased from the lander via previous agreement with Astrobotic Technology. Information about how much power this entails, how long periods one can expect and the cost of additional power. This makes it hard to rely upon, but as will be made clear from the following, it very well might be our only option to meet our power requirements.

The mass of the mission turns out to be the big limiting factor, as while most teams were trying to limit the mass of their subsystems to limit cost. This put strain on the power budget. With the current mass estimate, we have 3.33 W of power and 8.25 W peak.

### 6.2.1 Power requirements

The total list of instruments requiring power is shown below in Table 6.4. The power usage of the X-Ray source depends on both the distance from the ground and the integration time. Figure 6.4 shows the relationship for two different distances from the ground. For the best results, we would like the integration time to be as short as possible in order to maximize the number of tests we can make. It is therefore in our best interest to allocate as much power to the X-Ray source as possible.

Instrument	Power requirement	Operational voltage
Lander power	1-2.5W/kg	28VDC
Mechanical plunger	10 W	12VDC
Imaging distance sensor	0.117 W	3.3VDC
Routing switch	0.7 W peak	3.3VDC
High energy XRF detector	2 W	5VDC
Low energy XRF detector	2 W	5VDC
X-Ray Source	1-9 W	12VDC
On-board computer	0.5-1 W	3.3VDC
Camera	0.12 W	3.3VDC
Power distribution unit	0.16W	N/A

Table 6.4: Power requirements of the system.

In order to minimize the peak power consumption, we want to schedule the power usage to only use an instrument when needed. Some components, like the PDU and OBC, will need to be active at all times, but only need power when actively used. We have thus made three different states we will be operating in: Moving the mechanical structure, operating the XRF and low power mode. A breakdown of these are shown in Table 6.5.

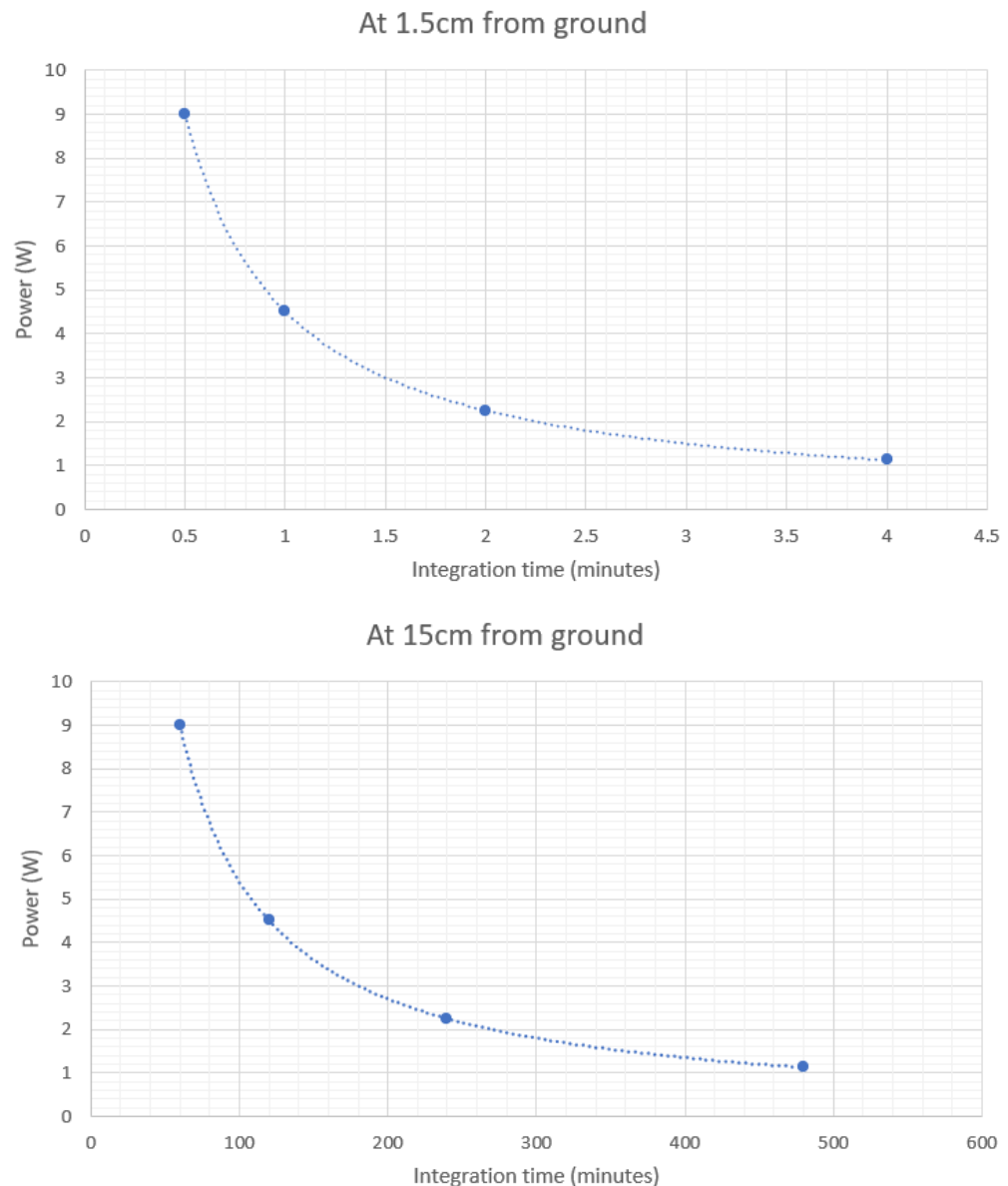


Figure 6.4: Power usage of the X-Rays source at a 1.5 cm distance and 15 cm distance for different integration times.

<b>Instrument</b>	<b>Power requirements</b>
<i>Moving the mechanical structure</i>	
OBC	1 W
PDU	0.16 W
Mechanical plunger	10 W
Routing switch	0.7 W
Imaging distance sensor	0.117 W
Camera	0.12 W
Total	~12.1 W
<i>XRF</i>	
OBC	1 W
PDU	0.16
Routing switch	0.7 W
High energy XRF detector	2 W
Low energy XRF detector	2 W
X-Ray source	6 W
Camera	0.16 W
Total	~12 W
<i>Low power</i>	
OBC	1 W
PDU	0.16
Routing switch	0.7 W
Camera	0.16 W
Total	~2 W

Table 6.5: Power budget for all major components.

Here, moving the mechanical structure requires the most power, and as such sets the limit for our operation. The power for the X-Ray source has been allocated to allow the total XRF power usage to be equal to the power we use to move the mechanical structure. This means that it is still not possible to operate the X-Ray source at peak intensity.

From optimizing the power usage, we still need to provide around 12 W of power for extended periods of time. It is not possible to provide this amount of power with the power we receive from the lander, even at peak power. At a state of low power, we are able to supply enough power, but we would have to purchase additional power from Astrobotic in order to meet the power requirements for actually operating the system.

## 6.3 Power Management

In this miniature XRF project, different subsystems have been proposed such that the overall system meets its mission objectives. These subsystems contain the instrument itself, the XRF, which consists of two X-ray detectors that differentiate in spectral detection area, and a X-ray emitting source. As good measurements were important, a mechanical plunge subsystem were proposed to lower the XRF-unit to the local surface area.

Both of these subsystems require controlled and regulated power in order to reach optimal functionality which is done by the Power Control and Distribution Unit, PCDU. This unit provides monitoring and protection for the bus current normally achieved by current limiting or fusing, where the latter usually require a redundant path to be switched into operation, usually remotely. Furthermore, power management system is required to meet operational load voltages, power converters solves this as it supply the loads with individual voltage/currents, normally DC-DC converters are utilized.

In this section the different options that have been considered for this project will be introduced. These options are again depended on the different power sources, which are:

- *Direct power from solar cells without battery storage*
- *Direct power from lander with battery storage*
- *Direct power from lander without battery storage*

Furthermore, the subsystem requirements will be taken into account where additional safety mechanisms are introduced. An example of an space-grade modular power management unit that roughly fits our system design requirements will be presented, as this reveals a realistic expectation in terms of size, power and functionality of such a system.

### 6.3.1 Management options

The power management options are related to the power option of choice. Due to the general design uncertainties in early phases of the project, various options of design were investigated as illustrated in the diagram below.

#### **Array regulator:**

*Regulates the voltage in/out from the solar panel array by the use of shunt regulator module, as the input to the solar array and the system loads vary in time. This is further monitored and controlled by an mode control unit, MCU, which ensures stable voltage generation.*

#### **Battery Management Unit, BMU:**

*Monitors battery cell voltage, temperature and pressure. Additionally, controls the discharge and charging of battery.*

#### **On Board Computer, OBC**

#### **Power Control and Distribution Unit, PCDU**

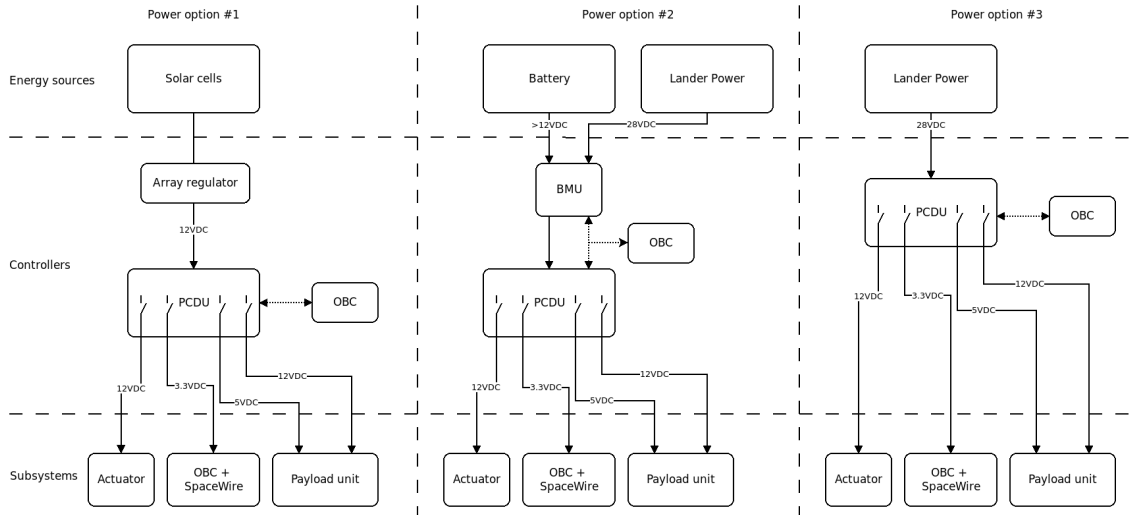


Figure 6.5: Illustration of the the power management with different power options.

As illustrated and described in the diagram, different power sources, typically the ones with increased complexities, features hazards which are required to be dealt with. Without the functions which are briefly addressed, instabilities, hazards and failure will potentially occur.

### 6.3.2 The p31-u

The power management unit p31-u by GomSpace handles about the same amount power required in this project, hence it is a suitable and realistic reference for what to expect of a power management unit. The modular p31-u is mainly made for solar cells as main power source and battery as secondary source, with inbuilt redundancies. This covers about all the power options considered and more.



Figure 6.6: Illustration of the p31-u with a modular small battery storage package added.

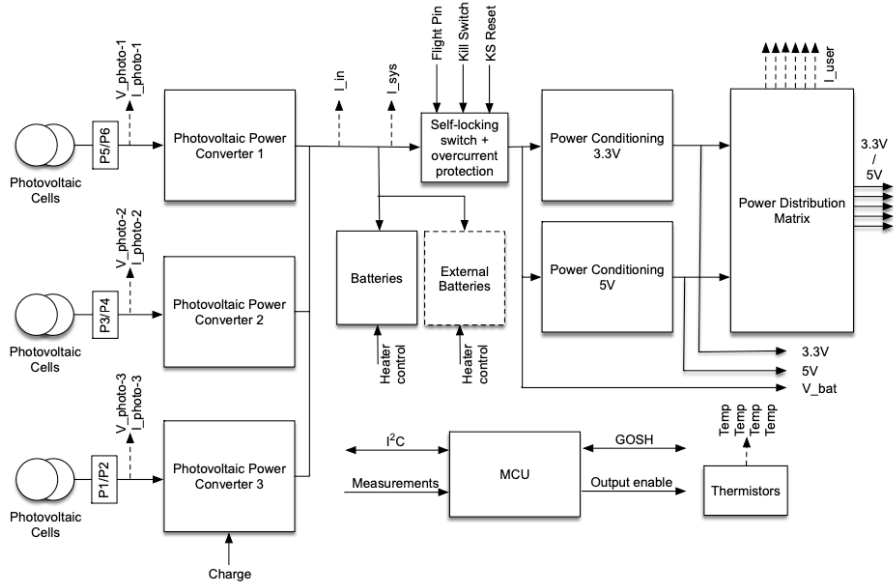


Figure 6.7: Illustrative diagram of the p31-u with three solar power inputs for redundancy, battery storage options, two power conditioning units and distribution of power to the individual loads.

As with all other systems, the p31-u is not an ideal system and suffers from power losses. These are typically represented as efficiencies in different parts in the system. By looking at the power-conditioning converter data sheet, known as DC-DC converters, it shows that the losses are related to the increase of current.

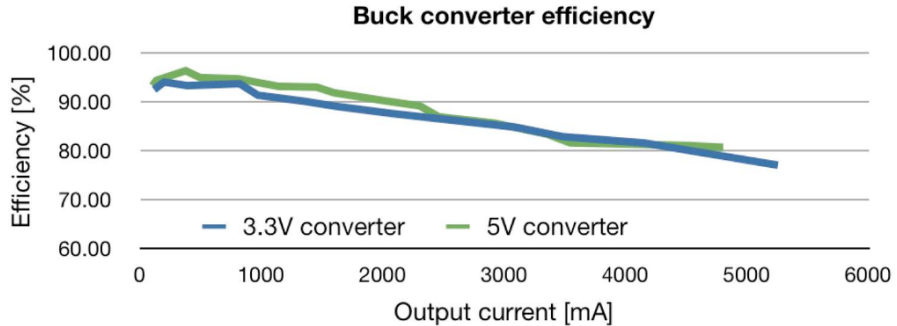


Figure 6.8: Comparing the values to the X-ray two detectors operating at 4W in our design, this reveals that it is realistic to expect a efficiency of 95% yielding a 0.2W loss within the converter.

## 6.4 The On Board Computer

The On Board Computer (OBC) is the main processing unit controlling the entire system. The OBC runs the main software, and is such a vital piece of hardware for the mission. There exist many commercial options with extensive flight heritage. The choice of computer depends a lot on the requirements we set for ourselves. A total of six parameters are important for choosing the optimal OBC for the mission:

1. Processing: The OBC must be able to handle the processing requirements of all systems, often with several processes working in parallel.

2. Memory: We need enough storage and RAM for storing both the various programs, but more importantly the data we collect before it can be transmitted to the ground base on Earth.
3. Interfacing options: The OBC needs to be able to interface with all subsystems.
4. Software reliability: The software the OBC uses should be able to be relatively clear to use and robust for our needs.
5. Size and weight: We need to be able to fit the OBC and preferably not use too much of our weight budget.
6. Power consumption: The OBC will be running at all times, and therefore the power consumption will be constantly present in the power budget.

The following is the considerations that have gone into the choice of OBC for our mission:

#### **6.4.0.1 Processing capacity**

By far the most processing will be done by the XRF subsystem itself. Several processes will need to run in parallel. The device itself does not need to run that many computations on site, so a single processing unit is deemed to be enough, though though was given to having a processing unit just for the XRF and another for regulating all other subsystems.

#### **6.4.0.2 Memory**

With the data rate available to us through Astrobotic we would not need to store a huge amount of data, which will be explained in Section 7.1.

#### **6.4.0.3 Interfacing options**

We have quite a few interfacing requirements, with both mechanical systems and several systems for the XRF. Most can be done via USB connection

#### **6.4.0.4 Software**

Most OBC's use variations of LINUX as operating systems and are therefore pretty doable to work with. This should not be a limiting factor.

#### **6.4.0.5 Weight and size**

A good rule of thumb is that the weight and size of the OBC is proportional to the processing power and memory capacity. The optimal choice will then be a trade-off between this.

#### **6.4.0.6 Power requirements**

As we are working with very limited power, optimally we would like the OBC to use as little power as possible. This turned out to be one of the leading restrictions when choosing the OBC unit.

### **6.4.1 The CP400.85 Payload Processor Module**

The chosen commercial option is the CP400.85 Payload Processor Module<sup>1</sup>. While this is on the very low end of the performance scale, we have determined it to be powerful enough to manage the mission.

---

<sup>1</sup><https://satsearch.co/products/aac-clyde-cp400-85-payload-processor-module>



Figure 6.9: CP400.85 Payload Processor Module

With the above restrictions, it was clear that we would need to limit ourselves with the OBC as much as possible. The downlink data rate has been determined to be large enough that we can make do with no more than 512 MB storage. Even so, if later in the process it turns out that we are in need of additional storage, it is very easy to add additional storage without adding much more than an SD card. For this small processing board, one could be concerned that the OBC would not have enough processing power to run everything at a reasonable rate, however since not all of the payload processing will be handled by the OBC, this is deemed to be enough. The main advantages of using this unit is the low power requirements of 500 mW to 1000 mW peak, as well as the very small size and weight. With this unit, if it turns out to be unfeasable to continue with this module, it would not be extraordinarily hard to scale up to a larger unit, however especially the already strained power budget would be run thinner.

## 6.5 Conclusion

We are able to receive 3.234 W min and 8.085 W peak power from the Astrobotic lander. We are able to operate in low power mode within the minimum received power, but even with peak power we cannot run the XRF or move the mechanical structure, which both are estimated to consume just around 12 W. While we have discussed providing our own power source either with solar panels or an included battery, the added weight and complexity will most likely far outweigh the benefits of providing power ourselves. The only option left to us is purchasing the additional power from the Astrobotic lander. As we do not at the time of writing have information about the cost, availability and amount of power up for sale, it is extensively difficult to lay out the actual limitations of this solution. As the current ceiling for peak power consumption is just over 12 W, if we purchase additional power we might be able to increase this number. This would most importantly allow us to decrease the integration time of the XRF as well as operate it further from the ground. The ideal power to reach is 16 W, as this would allow us to decrease the integration time as much as possible.

### **6.5.1 Future work**

If we were to continue work on this project (as if) we would have to get actual information from Astrobotic. Without the detailed information about how purchasing additional power works, we have only been able to estimate the constraints we put on the rest of the mission. Then we would also be able to determine whether it is more beneficial to implement our own power supply, which would greatly change much of the internal design.

We would also have liked to have more time to work on the on-board computer, as the current choice of computer is likely to change. We would need to work out the actual process flow of the entire system.

Furthermore, looking into the efficiencies losses throughout the system and its components will reveal a more realistic power budget, which will cause a slight increase in our need for power from Astrorobotics. The converter efficiencies of 3.3V and 5V where introduced as this was a part of the p31-u. An additional insight of other converters, such as 28VDC to 12VDC, is also required, as this coupled in series with the converters to 3.3V and 5V yields more losses. Other losses should also be investigated further.

# 7 Communications and ground segment

In this section, the communication subsystem will be explained. The details of the requirements set by different stakeholders will be explained, and the margins for the requirements and how they were resolved will be presented.

The data sample sizes produced by the Miniature XRF will be estimated to ensure we have a good data flow and are able to transmit them to the ground station within a reasonable time. To ensure the internal communication of the entire system is handled, a block diagram will be presented with details as to how the internal communication works and how the data is sent to the ground station. It will also be detailed on how it will be connected to the Astrobotic lander, to ensure data flow between our payload and the lander. Finally, the transmission from the lander to the ground segment will be explained with details on different subjects, which has been a focus during different parts of the project.

## 7.1 Requirements and limitations

As a part of this mission is to test an XRF on the Moon, it is critical that data can get to and from the instrument during the mission. Because of this there are some requirements that the communications part of the mission has to adhere to. The full list of requirements can be seen in Figure 2.1.

The first requirement for the communication is to be able to send a collected data sample to Earth within 24 hours. This transmission time is both dependant on the amount of data (addressed in Section 7.2.2) that has to be sent and the transmission speed at which it is possible to sent this data (Section 7.3.2).

If the data can not be sent immediately after it is obtained, the system must be able to store at least 20 data samples. This will enable the XRF to continue operating in case of a communication breakdown, and ensure the data is not lost. The aspect of storing data versus sending it right away will be addressed in Section 7.2.2.1.

In Table 7.1 is a list of different requirements that has to be fulfilled during the mission, and what is the limit for that specific requirement. It is also listed where the requirement is set and who sets the limiting factor for it. For transmitting data to Earth, it is required that the data arrives within 24 hours, which means the transmission speed should be at a minimum of 0.304 kbps. With the payload discussed in this report, Astrobotic is able to deliver 35.3 kbps of throughput, giving a margin of 116 times the needed speed. The storage requirement is limited by the on board storage of the system and has a margin of 7.78. And the transmission speed of the internal wiring is limited by Astrobotic's use of SpaceWire. The internal transmission speed should be at least as fast as speed of transmission to Earth, which gives a margin of 33 thousand. This margin is particularly high as wired transmission is much faster than wireless, especially when the wireless transmission is inter planetary.

Requirement	Value	Set By	Deliverable Value	Set by	Margin
Transmission speed: Lander to ground (Continues)	0.304 kbps	Mission req	35.3 kbps	Astroboitic delivered link speed	116 x
Storage capability in case of communication blackout	20-3.29 MB	Mission req	512 MB	EPS onboard storage	7.78 x
Link speed in payload	(0.304 kbps)	Payload	10 Mbps	Our internal link	(33k x)
Link speed: Payload to lander	(0.304 kbps)	Payload	10 Mbps	Astroboitic internal link	(33k x)

Table 7.1: A list of requirements and limitations in the communications part of the mission. Included is also who sets the requirement sand where the limiting factor is. These values are used to calculate how big of a margin the requirements have.

None of the margins presented in Table 7.1 presents any need for concern. With the lowest margin of 7.78, there is plenty of room for unforeseen events, and the communications part of the mission will be able to handle such events.

## 7.2 Internal payload communication

In this section the data sample size and rate will be explained and calculated to ensure there is enough bandwidth in the Astroboitic piggyback mission and it will be assessed if it is required to buy more bandwidth from Astroboitic. A block diagram will be presented with details on how the internal communication works.

### 7.2.1 Block diagram

To visualize how the different components are connected and how the flow of the data rate, a block diagram has been made. This is shown in Figure 7.1, where all of the different components are controlled by a SpaceWire Routing Switch. The SpaceWire router connects together many components and provides a means of routing packets from one node to one of many other possible components.

The switch enables packets arriving at one interface to be transferred to and sent from another link interface. This routing switch then ensures that the different components are connected properly and ensures the data transfer between different components of the system.

The system has to be able to communicate internally, where a controller has to be connected to the different components through BUS connections. To control the plunger, the micro-controller, then has to be connected with the different servo motors, which the switch ensures are possible to do. The launch lock also has to be connected to the system, to ensure the release mechanism can be activated. The payload source needs to be activated, to start the log of the data, which is done with the BUS connection in the On-Board Computer and a direct connection to the XRF components.

An imaging sensor and a proximity sensor is also connected to the system, which needs to be able to send information back to our ground station, to ensure that the payload does not get too close to a rock and therefore may be in risk of destroying the payload.

There is going to be communication to and from the ground station, which is visualized by the *Datalink through lander* block. Everything that is logged inside of the system should be sent to our ground station and, in different ways, managed or analyzed. The different data from the payload should be analyzed, but the data from the proximity sensor and

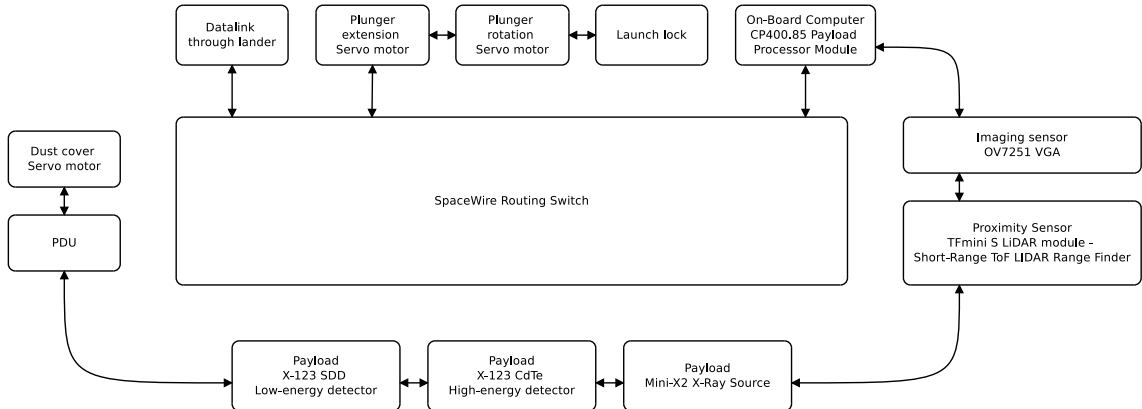


Figure 7.1: A block diagram which shows how the different components are controlled in the entire system. All connections are done through SpaceWires, which is controlled by a SpaceWire Routing Switch.

imaging sensor should be managed in order to control plunger or to tell if the payload should be activated or not. The servo motors are then controlled based on how the current system are rotated at that point of time, which then depends on information gathered by the imaging sensor and proximity sensor.

The connection to the lander is also through the *Datalink through lander* block which is a SEC connection, which is explained in Section 7.2.3.

### 7.2.2 Data sample size and rate

The data generated by the payload consists of both of XRF data and pictures from the context camera. Data size for the XRF is calculated based on the number of channels the two detectors measure at, the number of bits required for storage of one channels value and the desired integration time for one data sample. One channel for the detector requires 20 bits to store, and the two detectors measure in 237 different channels [51]. A full sample is integrated from 30 seconds to 1 hour, depending on the distance from instrument to the measured surface. In interest of being sure to be able to transfer all data, the worst case scenario has to be taken into account. The biggest sample the XRF is going to produce is then:

$$\begin{aligned}
 DS_{XRF} &= t_i \cdot N_{bits} \cdot N_{channels} = 3600 \text{ s} \cdot 20 \frac{\text{b}}{\text{ch} \cdot \text{s}} \cdot 237 \text{ ch} \\
 &= 17064000 \text{ b} \Rightarrow DS_{XRF} = 2.13 \text{ MB}
 \end{aligned}$$

where  $DS_{XRF}$  is the data size of the XRF data,  $t_i$  is the integration time,  $N_{bits}$  is the number of bits and  $N_{channels}$  is the number of channels. The context camera also produce data, the size of which can be calculated from the cameras resolution, refresh rate and the number of bits required to store the value of one pixel. A resolution of  $640 \times 480$  pixels is set for the camera and 10 bits of storage are required per pixel in the image [27]. The camera is also capable to produce 100 images per seconds however, with a one way delay of 4 seconds from the payload control center to the lander, it will not be possible to control the payload in real time [5]. Because of that, the focus will be to send individual images for positioning of the payload and when XRF data is collected, up to three reference images will also be collected to give some context to the data. The size of one image is calculated to be:

$$\begin{aligned}
DS_{1-image} &= Res \cdot N_{bits} = (640 \cdot 480) \text{ px} \cdot 10 \frac{\text{b}}{\text{px}} \\
&= 3072000 \text{ b} \Rightarrow DS_{1-image} = 0.384 \text{ MB}
\end{aligned}$$

where  $DS_{1-image}$  is the data size for one image and  $Res$  is the resolution.

All in all, one whole measurement, with reference images will be at a size of:

$$DS = DS_{XRF} + 3 \cdot DS_{1-image} = 2.13 \text{ MB} + 3 \cdot 0.384 \text{ MB} = 3.29 \text{ MB}$$

where  $DS$  is the data size. This is the absolute maximum size of the data files, and thus will be the worst case scenario for what is needed to be sent to Earth, between components in the payload or from the payload to the lander.

#### 7.2.2.1 Transmitting data

It is the goal to transmit the data continuously as it is collected, which will take 11 minutes and 32 seconds. This data sample will take 1 hour of integration time, so it will not be a problem to transmit everything as it is collected by the payload. However, in case there is something interruption the transmission from the lander to the ground segment, there has been set a storage buffer in the On-Board Computer.

In case of non-optimal transmission situations in the lander, it is wished to be able to store at least 20 data samples in the payload. The On-Board Computer comes with storage of 512MB, which then means that it is possible to store up to  $512\text{MB}/3.29\text{MB} = 155.62$  times. This is of course for the total mission time, and assuming there would be 20 samples every day, it should be possible to store data for  $155.62/20 = 7.78$  days, if there is a total communication and transmission blackout. This is the worst case scenario and it is not expected to take a picture each time there will be made a sample from the miniature XRF. It is also not expected that there will be a transmission blackout, however it is always great to be sure there is enough storage in case there will happen a blackout.

#### 7.2.3 Communication standards

Astrobotic gives the choice between choosing RS-422 or SpaceWire standards to integrate the payload to their system.

First, the RS-422 has a data rate limitation based on the length. It has the most optimal data signalling rate at a rate of 10 Mbps when the length of the cable has a max length of 10 meters. When the cable is at a length of 12000 m, the data signalling rate is at its lowest, which is somewhere between 10 kbps to 100 kbps [61]. This can be seen in Fig. 7.2.

The RS-422 interface operates in full-duplex mode, which allows it to send and receive information at the same time, since there are different wires used for receiving and transmitting the data [61].

In the RS-422 network, there can only be one transmitting device and up to 10 receiving devices [61]. The RS-422 line is 4 wires for data transmission, where 2 twisted wires are for transmission and 2 twisted wires are for receiving, and finally there is one common ground wire [61].

In general, SpaceWire has been proposed for use on many space missions for the last many years [63]. It is a low-power and high-speed communications technology that was

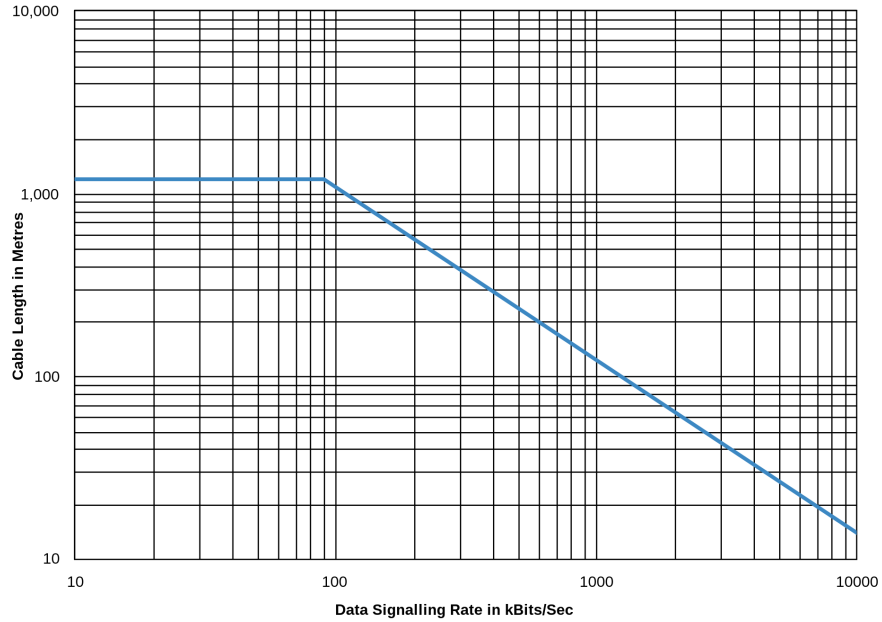


Figure 7.2: An illustration of the data rate depending on the length for the RS-422 cable[62].

designed to be simple to implement in digital logic and is rapidly replacing widely prolific legacy communication technologies such as RS-422 and MIL-STD-1553B [63].

SpaceWire is supported by several radiation tolerant ASICs designed for ESA, NASA and JAXA. The current radiation tolerant devices are capable of up to 200 Mbps data signalling rate, with a data rate of up to 160 Mbps per link or 152 Mbps bi-directional per link. This level of performance meets the demands of many missions, including this one [64].

One of the main advantages of the SpaceWire is the low complexity and the fact it can be implemented easily in both ASICs and FPGAs. The interface of the SpaceWire can be implemented in around 5000 to 8000 logic gates. This makes it possible to include one or more SpaceWire interfaces together with application logic or a micro-computer [64]. A network is constructed from point to point links and routing switches. When more than one link connects a pair of routing switches, group adaptive routing can be used to share the bandwidth of the links or to provide for fault tolerance, with rapid recovery from a link failure. SpaceWire provides support for the distribution of time information to all nodes on a SpaceWire network. This can be done with a resolution of a few microseconds [64].

The use of the SpaceWire standard ensures that equipment is compatible at both the component and subsystem levels. Processing units, mass-memory units and down-link telemetry systems using SpaceWire interfaces developed for one mission can be readily used on another mission [64]. This reduces the cost of development, improves reliability and increases the science.

So in general, as SpaceWire is the more affordable and the newest technology, which typically means that it is more reliable and effective, then it would be the best choice to go with the SpaceWire. The data rate of the different interfaces does not make a big difference, however going for the fastest data rate, it would be the obvious choice to go with the SpaceWire.

Because of these reasons, it has been chosen to continue the work with the internal

communication with the SpaceWire interface.

#### 7.2.4 Payload to lander

Astrobotic provides data services through a Standard Electrical Connector (SEC) and the connectors are typically available in regular and small size, each with a standard pin configuration. Since it has been chosen to use the SpaceWire configuration, the regular size SEC must be used. This and RS-422 supports time at the tone, which is a time synchronization service that enables payloads to synchronize the internal clock with the lander and by extension UTC time. As the SpaceWire is chosen, the pin configuration is as shown in Fig. 7.3.

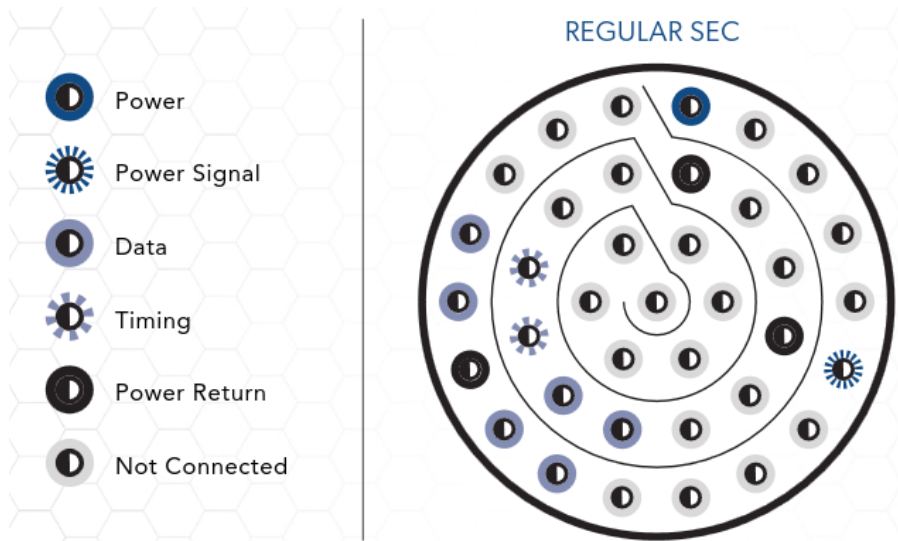


Figure 7.3: The standard pin configuration for the regular size SEC, which is used in configurations using SpaceWire [5].

The SEC is a Glenair SuperNine connector of the MIL-DTL-38999 Series III screw type connector [5]. If everything is as planned, then the connection to the lander is dealt with by Astrobotic and the integration of the payload to the lander will be done by Astrobotic [5].

The payload computer installed in the lander manages the individual payloads as well as their contractual services. The payload monitors payload power consumption and communication directly with the payloads. Commands from the payload ground software are sent directly to the payload via the payload computer and payload telemetry is packaged for downlink to Earth. The payload features Error Detection And Correction and robust software with proven networking standards [5].

For doing the SpaceWire setup both cables and a router is required. The cables can be costume made at specific lengths [65]. A long cable of 1.5 m is needed for components like the x-ray detectors in the payload. A shorter run of 0.4 m can be used for the plunger motors. And then 8 cables of 0.1 m and one at 0.2 m is needed for running between components. The total weight and cost of these cables is 1856 USD at 640 USD/m and 94 g at 32.5 g/m. It was not possible to find a specific SpaceWire Router that was suitable to go to space and also had information on price and weight. Therefore to be able to have some of this information, another router was wound priced at 4100 USD with a mass of 180 g [66].

### 7.3 Lander to ground station

In the following section, the communication between the lander (Astrobotic) and the ground station will be described. This will include a short description of the used bandwidths for space exploration, the antenna specifications of the Astrobotic landers and the preliminary plan for a ground segment configuration. As a reference for the communication pipeline, see Figure 7.4 below [5].

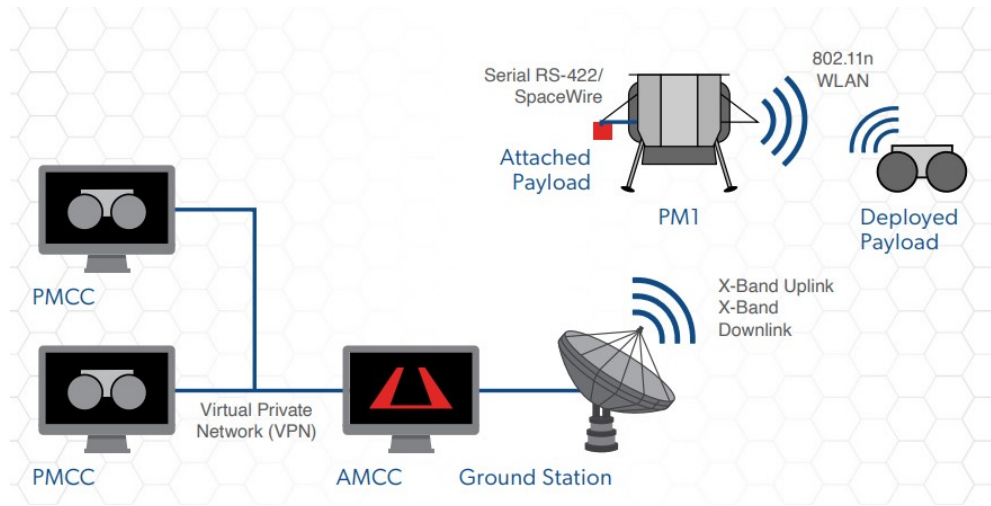


Figure 7.4: Overview of the Communication pipeline for the Astrobotic landers missions. [5].

As the mini XRF system, is a payload directly mounted on the Astrobotic lander, the 802.11n WLAN wifi connection between the lander and a "deployed payload" such as a rover, is not in the area of interest for this mission. The other subsystems of the communication system will be described, in according to grouping. Such that the full ground station and VPN is explained together, and the lander to Earth is explained together.

The information about transmission latency, is given from Astrobotic, to be approximately 4s, during the stationary period of the lander, this value is to be expected to be larger, during the flight and landing maneuvering. This is however not relevant for this proposed mission [5].

#### 7.3.1 Allocated Bandwidth for Earth to Lander communication

This section will include in a description of the lander to Earth communication, focusing on the used bandwidths. As described in the Astrobotic user manual [5], the communication between the lander and the ground station, is performed in the X-band frequency range. This range is in the United States defined between 7.9 GHz - 12.2 GHz [67]. Not all frequency bands in the range is open for public use, as it can be seen in Figure 7.5. As per described by Astrobotic, the X-band frequency range is used for both downlink and uplink.

As it can be observed in Figure 7.5, only a few sub ranges of the X-band frequency range is open for the type of mission that is being proposed. This means that the Lander to Ground station communication, would possible only happen around the frequency of 8.45-8.5GHz for the downlink and at around 10.6-10.7GHz for the uplink to the lander.

#### 7.3.2 Data transfer rate

The speed at which the collected data can be sent to Earth is impacted by a few factors. Mainly, the size of the XRF data and reference photos will negatively impact the data

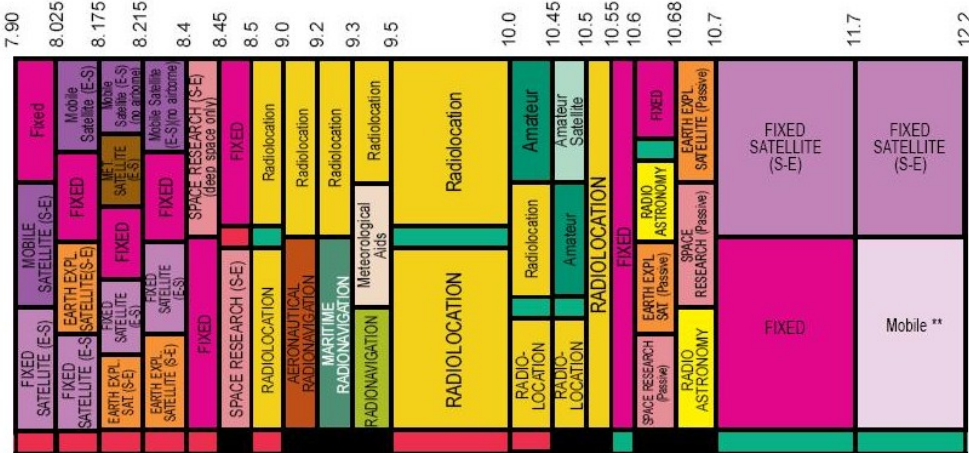


Figure 7.5: The X-band allocated frequencies in the United States, range between 7.9GHz to 12.2GHz [67]. The full allocation spreadsheet can be found in Appendix A

transfer time with larger file sizes, but also the data rate provided by Astrobotic will have an effect on this. Astrobotic states that 10 kbps is available for every 1 kg of payload on board their lander [5]. The payload weighs 3.53 kg and thus 35.3 kbps of bandwidth is available for use to download files and upload commands to the payload.

The acquired data is required to be delivered to the payload control center at the latest, 24 hours after the acquisition. This is to ensure that it can be analysed and the payload can be controlled according to the findings in the analysis. At the worst case scenario for the data file size, calculated in Section 7.2.2, the data rate necessary for complying with this requirement is:

$$DR_{req} = \frac{DS}{TT_{req}} = \frac{3.29 \text{ MB}}{24h \cdot 60 \frac{\text{min}}{\text{h}} \cdot 60 \frac{\text{s}}{\text{min}}} = 38.0 \text{ Bps} \Rightarrow DR_{req} = 0.304 \text{ kbps}$$

where  $DR_{req}$  is the required data rate and  $TT_{req}$  is the maximum allowed transfer time. This data rate is lower than what is advertised from Astrobotic, meaning the requirement of data transfer within 24 hours is possible to fulfill. In fact, this data transfer can occur even faster. The time to transfer one dataset from the lander to Earth is:

$$TT_{min} = \frac{DS}{DR_{max}} = \frac{3.29 \text{ MB}}{35.3 \text{ kbps} \cdot \frac{1}{30} \frac{\text{B}}{\text{s}}} = 744 \text{ s} \Rightarrow TT_{min} = 12 \text{ min } 24 \text{ s}$$

where  $TT_{min}$  is the the fastest possible transfer time and  $DR_{max}$  is the maximum data rate. This will make it possible to analyse the data faster and thus leave more time for determining where to point the payload next. The maximum data rate leaves a margin of 116 times the transfer speed.

### 7.3.3 Lander antenna details

The Astrobotic piggyback options include both Griffin and Peregrine. The Peregrine has an upgraded communications system to ensure a good communication to the ground station while being in the polar areas [5].

The Peregrine lander utilizes multiple low gain antennas for optimal coverage during cruise and lunar orbit operations and then switches to an actuated medium- or high-gain antenna following touchdown on the lunar surface for increased bandwidth. The Peregrine

relays payload telecommands and telemetry in near real-time. However, it is expected to have a one-way latency in connection between the ground station and the payload on the Moon with a nominal 4 second delay, although there might be increases in this latency during some mission events. The medium- and high-gain antennas are places as seen in Fig. 7.6.

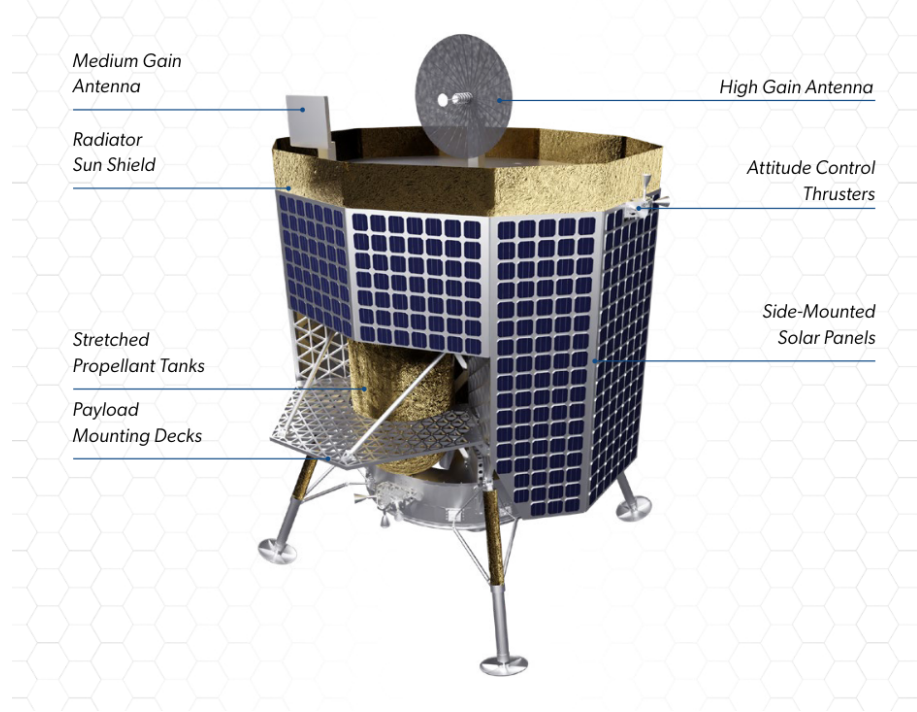


Figure 7.6: An image of the Peregrine lander showing the placement of the medium- and high gain antennas [5].

Payload telemetry and telecommands are transmitted from the lander to the Astrobotic Mission Control Center and then to our own ground station without modification of payload data [5]. Unfortunately, more specific details are not given by Astrobotic.

During the next decade, it is expected to have a network of relay satellites, for all the future lunar missions happening [68]. It is planned that the network will be available by both space agencies and commercial entities. It is a collaboration between the Italian aerospace company Argotec and NASA's Jet propulsion Laboratory, where the relay satellite constellation is called Andromeda.

Earth to Moon communications will revolutionize based on the Andromeda project. The plan is to provide coverage to most of the Moon at any given time. It calls for 24 satellites to move in four highly elliptical orbits [69]. The orbits can be seen in Fig. 7.7. The network is not designed to deliver a fast rate of data, however it is meant to deliver a steady flow of data consistently on most of the surface of the Moon.

It would not be completely out of the question that this is a typical network of satellites, which could be used in a mission not unlike the Astrobotic piggyback mission. This would however limit the data transfer rate from the lander to the ground station, and would definitely limit controls over the plunger arm.

It is hoped for that the system, if using a relay satellite, would utilize the same system, as it has been done earlier, like in the lunar Reconnaissance Orbiter. This would give a data transfer rate, which does not have a slow connection, but the speed is optimal for

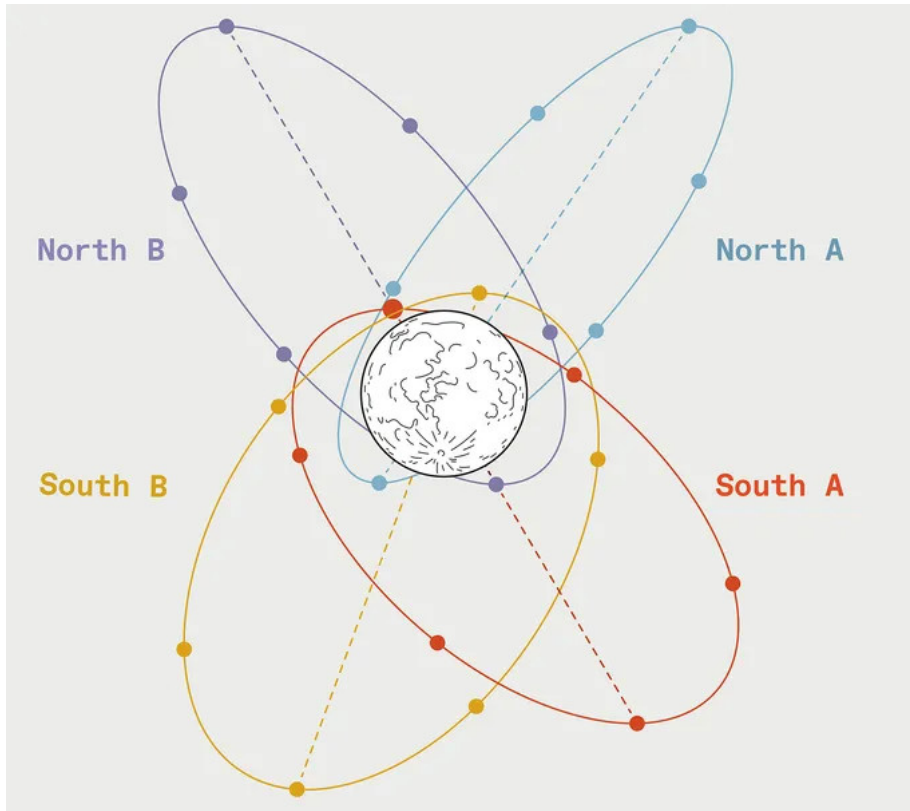


Figure 7.7: An illustration of the Moon surrounded by four differently coloured rings, resembling the 24 satellites of the future relay system Andromeda [68].

controlling mechanical systems on the lander.

The Lunar Reconnaissance Orbiter was designed with a 13 inch (33.02 cm) long tube called a Traveling Wave Tube Amplifier, which makes it possible for scientists to receive massive amounts of data from the orbiter [70].

With the new amplifier, it has been possible to transmit 461 GB of data per day, with a transmission rate of 100 MBps. The device uses electrodes in a vacuum tube to amplify microwave signals to high power. It's ideal for sending large amounts of data over a long distance because it provides more power and efficiency than the alternative transistor amplifier.

The Chang'e 3 lander mission utilizes a direct communication between the lander and the Earth [71]. It utilizes a miniature X-band deep space transponder, which was also used in the Chang'e 2 mission. The lander had stereo, navigation cameras and communication antenna mounted on a mast, which stood 1.5m tall.

The Chang'e 2 mission defines the data transfer rate to be up to 12 Mbps through the miniature X-band deep space transponder. It also has less signal attenuation [72]. The main difference between the communication subsystems between Chang'e 2 and 3, is only that the Chang'e 2 is in an orbit around the Moon, thus higher altitude, and the Chang'e 3 is a lander on the Moon. It must be specified that the communication antenna, which are attached to the mast, can be folded down into a warmed electronics box to shield them from the damaging effects of the Moon's nightfall, when temperatures plunge dramatically below -180°C [71].

### 7.3.4 Lander transmission vs relay satellite

Due to the geographical location of the preliminary mission objective, a problem with the direct line of sight with Earth is encountered. The design of the communication link between the Astrobotic lander, and the ground station, is based on a direct line of sight between the two. Meaning that a relay satellite is not used. This means that during the time when Earth is below the Moon horizon, no downlink or uplink to and from the lander is possible. This is illustrated in Figure 7.8 below. As shown in Figure 7.8 and explained

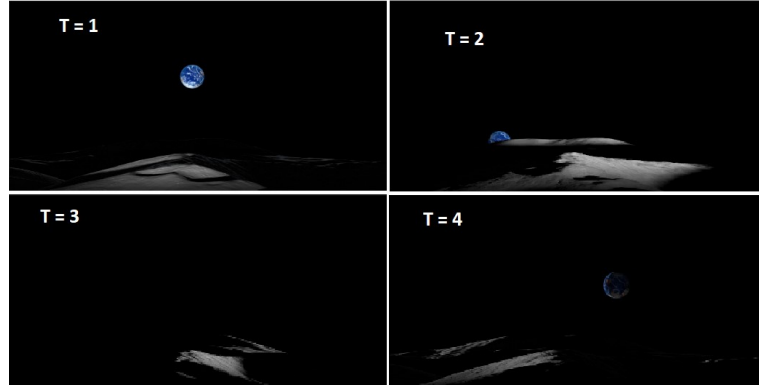


Figure 7.8: Illustration of the line of sight problems, regarding direct transmission between a lander on the south pole of the Moon and Earth. The illustration is snapshots of an animation made by [73]. the full animation covers approximately three lunar days, meaning that from T=1 to T=4 is approximately 1 lunar day. (29.5 Earth days)

in [73], the Earth is below the lunar horizon for a time period of approx. 14 Earth days in a row, meaning that the direct transmission between the lander and ground station is not possible. The Astrobotic lander, is capable of providing the mini XRF payload with power for up to 14 days, meaning that the problem with line of sight with Earth, can be avoided, by the planning and timing of the mission. This is also to be preferred, to keep cost and complexity down for the mission, as the mission should act as a product-test mission.

If another mission needed to be in a location, where a direct line of sight is not possible, then an relay satellite would be necessary. On the Moon, an example of this could be the Queqiao relay satellite also called Chang'e 4 Relay satellite. This is a Chinese communication satellite, which is placed in a halo orbit around the L2 Earth - Moon Lagrange point, approx. 64,000 kilometers beyond the far lunar dark side [74, 75, 76]. This solution would significantly increase the down- and up-link time frame, for a mission. But would also add the extra element of a two stage mission, which again would increase the cost and complexity of the system.

### 7.3.5 Antenna standards

**ECSS-E-ST-20C** is the Electrical and electronic ECSS standard, which contains the antenna details. Since the antennas are not specified by Astrobotic, it cannot be verified that everything holds to the standards, however it is assumed that Astrobotic have tested everything in accordance to the ECSS standard or similar. Since we do not have access to different PDRs or similar from Astrobotic, then it can only be assumed that they live up to the different standards given in this ECSS.

## 7.4 Ground Segment

In a ground segment, it must be considered that there are different users, different needs and different kinds of networks.

A ground segment is a network of Earth stations and user terminals that provides applications and services to end users. The most important part of the ground segment, and is needed to include is a central point of management and control and a means to connect distant users to sources of content or other networks [77].

The control center, which is the central point of management, which process, analyze and distribute spacecraft telemetry and issue commands and manages data uploads to and from the spacecraft. The control centers may also be responsible for configuration management and data archival.

### 7.4.1 Astrobotic ground segment

The Astrobotic ground segment, also called Astrobotic Mission Control Center (AMCC) [5], is the data hub for all the different missions, which uses their lander as a piggyback mission. They ensure standardized, transparent and safe networking to payload customers [5]. The payloads for the missions will be controlled directly from the AMCC inside the headquarters of Astrobotic, which are located in the heart of Pittsburgh's North Side [78].

Astrobotic does not have their own parabolic dishes to receive the data transmitted from the lander. The Peregrine mission used dishes in Australia, Spain and in California to receive the data [79]. They are contracting the DSN global network to ensure the data is received properly [79].

It is possible to setup the Payload Mission Control Center (PMCC) inside of their AMCC, otherwise it is possible to set up a VPN and work remotely [5]. However, if it is chosen to work remotely via a VPN, it is required to provide an on-site representative at the AMCC during mission operations for rapid response to off-nominal situations [5]. Astrobotic states that they deliver payload telecommands and telemetry without modifications, so it is not needed to consider different mediums and channels traversed by data packets.

Further details are not provided, however it is assumed that cost of ground support is included in the price of attaching the payload to the lander.

### 7.4.2 Our ground segment

The most practical way of operating the PMCC is to have it based where the team is. In this case, the control center should be based in Denmark and the center will use a VPN to access Astrobotic's AMCC.

Some personnel is needed in the PMCC as the mission expects to deliver data at least one time every day for the missions duration. This data has to be analysed and depending on the results, the instrument needs to be moved or rotated to capture data from another area. Thus, at least one person capable of doing the data processing and analysis should be present. One person for controlling the movement of the payload. Ideally this could be done by the same person however, having two people to make the decisions might be wise. And lastly we of course have to have the, at least, one person stationed in the AMCC in Pittsburgh as Astrobotic requires.

The PMCC also need some storage capacity for the data collected during the mission. Luckily this data is not very demanding in terms for storage space. One dataset with context photos is around 3 MB. During this mission not more than 100 datasets are going to be created. This data will be able to be stored on relatively inexpensive hardware. One

copy fits on a almost all sizes of harddrive, and for redundancy, the data should be stored in at least one on-site backup and one off-site backup.

As the dataset generated by the XRF and the on board camera are fairly small and not very complex, it should be able to be handled on very simple hardware. There is therefore no need for advanced computers in the PMCC, a normal workstation or desktop would be able to handle the data processing work fine.

## 7.5 Conclusion

The communication internally in the system has been analysed and there has been a clear definition of how the team should move forward when ensuring that the entire system should be able to communicate internally. The data rates of the system allows the payload to work as efficient as possible without having to limit the science due to transfer rates, neither internally nor within transmission times to the ground station. There has been presented different possible ways of transmitting data from the lander and to the ground station, as Astrobotic does not deliver many details regarding the data transmission hereof. Because of this, it has been necessary to look at different possibilities, for how the transmission should be handled the best in this lunar mission. Astrobotic also allows our team to send commands up to the payload, for the team to control the plunger and activate the payload.

This concludes that the communications lives up to the set requirements for the system.

For future work, there needs to be defined a specific VPN setup, to be setup within the Astrobotic AMCC for our team to work remotely.

## 8 Conclusion

In summary, this report has presented a comprehensive overview of the Miniature XRF Tech Demo, which is currently in its pre-phase A. The mission could be launch in the early 2030s with the goal of operating a mini XRF for around two weeks on the lunar south pole. The report has presented the concept studies of the communication, power, mechanical structure, and Mini XRF design, along with a detailed explanation of the project's objectives and requirements.

In the ConOps chapter requirements have been defined and a clear picture of the project as a whole has been set. The hierarchy of requirements was presented in the RTM, and in addition, the operational phases and risks were discussed.

In the Launch, Orbit and Landing chapter a preliminary assessment of the environmental overview has been conducted, and the requirements for imaging sensors have been discussed.

In the Payload chapter, the final design of the miniature and improved XRF has been presented. The design complies with the key driving requirements of the mission, as set forth earlier.

The chapter about Mechanical structure has concluded on the final design of the mechanics and movable structure, and the overall instrument design including a simple mechanical arms.

In the Electrical power systems chapter, the use of a battery for power storage and other power sources were discussed. Furthermore, the purchase of additional power from Astrobotic was deemed a good solution.

The different possibilities for transmitting data to and from the lander and ground station were discussed in the Communications and Ground segment chapter.

Overall, the completion of the pre-phase A brings the Miniature XRF Tech Demo closer to its ambitious mission of advancing our understanding of the lunar environment and other celestial bodies while advancing current technology.

## 9 Action items from PDR

The following is a list of action items outlined during the preliminary design review (PDR) by a panel comprising David Flannery (DF), Christina Toldbo (CT), Katcha Koch Winther (KKW), and David Arge Klevang Pedersen (DAKP).

Number	Action Item	Assigned by	Assigned to	Resolved by	Addressed in
AI1	Make timeline dates more realistic.	All	ConOps	Researching the durations on similar space missions	Section 2.5
AI2	Compare Astrobotic to other piggyback missions.	DF	ConOps	Presenting the selection process behind	Section 2.1.2
AI3	Explain reasoning behind the level 1 requirement.	All	ConOps	Presenting the brainstorming and selection process behind	Section 2.1
AI4	Explain future use of the mission output, assuming success.	DF	ConOps	Careful considerations from all subteams as well as comparison to real-life examples	Section 2.6
AI5	Provide a more detailed cost budget.	All	ConOps	Predicting and analyzing future expenses, however, providing a detailed cost budget at this point is challenging. Nonetheless, we can identify some of the main expenses involved	Section 2.5
AI6	Include a Plan B in case something happens to Astrobotic.	DF	ConOps	Creating a plan B based on our second choice of piggyback mission along with a detailed calculation of anomalous scenarios	Section 2.1.2

AI7	Clarify future payload destinations and coordinate with other groups based on specific celestial body environments.	DF	ConOps	A discussion with the other subteams and within the subteam	Section 2.6
AI8	Clarify minimum and maximum distance to soil.	DAKP	ConOps	A discussion with the other subteams	Section 2.1
AI9	Define the size and reason for using XRF miniature and clarify why it is required.	DAKP	ConOps	A discussion and evaluation within sub- teams.	Section 2.1
AI10	Specify which mechanical structure to use, such as Nanoracus or other CLPS.	CT	ConOps	Evaluating the possibilities at hand.	Section 2.1
AI11	Clarify why the operational mission time is 14 days and why it is at the south pole.	CT	ConOps	Explaining the main groups reasonings.	Section 2.2.4
AI12	Improve the design by specifically stating the scientific question and all other requirements that arise from it.	DF	ConOps	A discussion with the other subteams	Section 2.1
AI13	Layout and identify all components in the design.	DAKP	ConOps	Block diagram of overall instrument.	Section 2.3
AI14	Clearly state which specifications belong to the spacecraft delivery system and which belong to the design.	DAKP	ConOps	Proposing that all subteams clarify this within the scope of their subteam.	Section 2.1
AI15	Highlight the key driving requirements.	DAKP	ConOps	A discussion within the subteam and with DAKP and DF.	Section 2.1 Req. P001,P003
AI16	Relate the design to the current state of the art, such as APX, PIXL, and other missions, in terms of weight, volume, power, etc.	DAKP	ConOps	A discussion and evaluation with the Payload subteam.	Section 4.2

AI17	Evaluate use of camera and specify the type of camera if necessary.	DAK	LOL	A discussion in class in which the inclusion of a camera was deemed a good idea. A chapter is included describing the chosen camera.	Section 3.6.3
AI18	Research and report on the uncertainty of the LiDAR.	DAK	LOL	Information added to the section on setup for LiDAR.	Section 3.6.2
AI19	Consider and determine how the instrument will be placed.	DAK	LOL	Specifics regarding the placement is discussed in section 5, where the general/expected environment is covered.	Section 3.2
AI20	Clarify temperature ranges for different phases of the mission and specify if they are operating or storing temperatures.	DAK	LOL	A discussion of the scope of environmental factors.	Section 3.2
AI21	Refine and narrow down requirements for the mission.	DF	LOL	A discussion in the subteam that further considerations regarding EMC need to be covered in depth.	Section 3.1.2
AI22	Improve analysis by comparing with previous missions.	DF	Payload	Research and comparison to previous missions.	Table 4.1 and 5.7
AI23	Include the periodic table with outlines of detectable elements.	DF	Payload	Inserting figure.	Figure 4.6
AI24	Evaluate the effect of integration time on intensity and distance.	DF	Payload	Further research on the topic.	Section 4.2
AI25	Analyze performance envelope in presence and absence of atmosphere.	DF	Payload	Further research on the topic.	Section 4.7
AI26	Identify driving requirements such as location, modularity, and science objectives.	CT	Payload	Further evaluation on the topic.	Table 4.2
AI27	Discuss the significance of integration time for a stationary lander.	KKW	Payload	A discussion within the subteam.	Section 4.2
AI28	Address the temperature and environmental requirements.	DF	Mech	Thermal analysis.	Sections 5.3.4, 5.5.4

AI29	Attempt to reduce weight as much as possible.	DAKP	Mech	Flight cover is removed; material is changed; XRF components are adjusted.	Sections 5.3.2.1, 5.3.3.1, 5.3.3.2
AI30	Clarify which parts belong to the payload and which parts are specific to this mission.	DAKP	Mech	Tables are added throughout the report for clarification.	Sections 5.3.3.1, 5.5.1, 5.5.2, 5.6
AI31	Mitigate stress-related concerns.	DAKP	Mech	Stress analysis.	Sections 5.3.4.1, 5.5.3
AI32	Assess structural durability in relation to dust, temperature, shock, and vacuum conditions.	KKW	Mech	Mechanical analysis.	Section 5.5.3.4
AI33	Consider battery thermal operating conditions.	DF	EPS	The system will require more power for cooling/heating, if the battery is placed outside the lander.	Section 5.5.3.4
AI34	Discuss the placement of battery compared to the lander.	All	EPS	The rechargeable battery will most likely be outside, since the possibility of having the battery inside is unknown.	Section 6.1
AI35	Evaluate tradeoffs associated with using energy storage.	DAKP	EPS	A discussion within the subteam.	Section 6.1
AI36	Investigate the feasibility of purchasing additional power.	CT	EPS	Astrobotic provide a service of buying additional power, however, the amount of power that can be bought is unknown.	Section 6.1
AI37	Assess the consequences of utilizing the battery.	CT	EPS	A discussion within the subteam.	Section 6.1.2
AI38	Assess the pros and cons of the mission providing its own battery.	KKW	EPS	Battery increases the amount of power that can be drawn at once.	Section 6.1.2
AI39	Provide the temperature range for the lithium battery.	KKW	EPS	0 to 40 Degree C (Discharge/Charge).	Section 6.1

AI40	Identify other power sources that may be required in addition to Astrobotic.	All	EPS	A discussion within the subteam.	Section 6.1
AI41	Reevaluate the size of the battery.	All	EPS	Investigation of other methods of power.	Section 6.1
AI42	Ensure that the power budget accounts for the heat generated by the battery.	All	EPS	The power budget is reevaluated.	Section 6.2
AI43	Provide margin in data communication.	DAKP	Comms	Making list of requirement and deliverable performance with margins.	Section 7.1
AI44	Differentiate between possible envelope and design needs for budget and margin.	DAKP	Comms	Making list of requirements and limits and who they are set by.	Section 7.1
AI45	Provide more detailed requirements.	DAKP	Comms	Trying to make the requirements more detailed and give explanation to them.	Section 7.1 and Figure 2.1
AI46	Evaluate the requirements with little margin.	DAKP	Comms	Margins are calculated and addressed.	Section 7.1
AI47	Consider the size of the data package and whether the current data sample is too large.	DAKP	Comms	Final data size is calculated.	Section 7.2.2
AI48	Include the cost of ground support in the budget and clarify what is included in the price of the payload from Astrobotic.	DF	Comms	By reading through user guide from Astrobotic and looking through details for customer support in [5]. This Action item could unfortunately not be addressed as there are no such details from Astrobotic.	Section 7.4.1
AI49	Assess if the necessary ground support is available to receive data every 5 minutes.	CT	Comms	By reading through user guide from Astrobotic and looking through details for customer support in [5]. This Action item could unfortunately not be addressed as there are no such details from Astrobotic.	Section 7.4.1
AI50	Determine the basis for data size and speed (1.25 MB or 2 MB) and how many measurements are required.	KKW	Comms	Clearly stating the size of the data, the transmission speed and how it is calculated.	Sections 7.2.2 and 7.3.2

# Bibliography

- [1] A.C. Allwood, L.A. Wade, and M.C. et al. Foote. *Correction to: PIXL: Planetary Instrument for X-Ray Lithochemistry*. DOI: <https://doi.org/10.1007/s11214-021-00801-2>. 2021.
- [2] A.W. Beck, P.N. Peplowski, and Z.W. Yokley. “A miniaturized XRF instrument for in situ planetary exploration: The Active X-Ray Spectrometer (AXRS)”. In: *Planetary and Space Science* 190 (2020), p. 104990. ISSN: 0032-0633. DOI: <https://doi.org/10.1016/j.pss.2020.104990>. URL: <https://www.sciencedirect.com/science/article/pii/S003206331830309X>.
- [3] Demet Yilmaz, Mevsen Pirimoglu Dal, and Tuba Akkus. “Effect of mechanical noise upon X-ray fluorescence analysis”. In: *Instrumentation Science & Technology* 47.6 (2019), pp. 666–677. DOI: 10.1080/10739149.2019.1664828. URL: <https://doi.org/10.1080/10739149.2019.1664828>.
- [4] *NASA Systems Engineering Handbook*. eng. NASA, 2007. ISBN: 0160797470, 1628705116, 9780160797477, 9781628705119.
- [5] Astrobotic. “ASTROBOTIC LUNAR LANDERS Payload User’s Guide”. In: August (2021), pp. 1–67.
- [6] Abigail C. Allwood et al. “PIXL: Planetary Instrument for X-Ray Lithochemistry”. In: *Space Science Reviews* 216.8 (Nov. 2020), p. 134. ISSN: 1572-9672. DOI: 10.1007/s11214-020-00767-7.
- [7] P. Gläser et al. “Illumination conditions at the lunar south pole using high resolution Digital Terrain Models from LOLA”. In: *Icarus* 243 (Nov. 2014), pp. 78–90. DOI: 10.1016/j.icarus.2014.08.013.
- [8] Peter Fortescue, Graham G. Swinerd, and John Stark. “Spacecraft Systems Engineering, Fourth Edition”. In: *Spacecraft Systems Engineering, Fourth Edition* (Aug. 2011), pp. 1–691. DOI: 10.1002/9781119971009. URL: <https://onlinelibrary-wiley-com.proxy.findit.cvt.dk/doi/book/10.1002/9781119971009>.
- [9] “Supersedes GSFC-STD-7000 GENERAL ENVIRONMENTAL VERIFICATION STANDARD (GEVS) For GSFC Flight Programs and Projects”. In: (). URL: <http://standards.gsfc.nasa.gov>.
- [10] “DEPARTMENT OF DEFENSE INTERFACE STANDARD REQUIREMENTS FOR THE CONTROL OF ELECTROMAGNETIC INTERFERENCE CHARACTERISTICS OF SUBSYSTEMS AND EQUIPMENT”. In: (2015). URL: <https://assist.dla.mil>.
- [11] NASA. *Peregrine Mission 1 (TO2-AB)*. URL: <https://nssdc.gsfc.nasa.gov/nmc/spacecraft/display.action?id=PEREGRN-1>.
- [12] Astrobotics. *Astrobotic Selects SpaceX Falcon Heavy Rocket for Griffin-VIPER Moon Mission | Astrobotic Technology*. URL: <https://www.astrobotic.com/astrobotic-selects-spacex-falcon-heavy-rocket-for-griffin-viper-moon-mission/>.
- [13] NASA. “National Aeronautics and Space Administration”. In: () .
- [14] Erik Stalcup. *Lunar Thermal Environment*. URL: [https://www.nasa.gov/sites/default/files/atoms/files/ericstalcup\\_lunar\\_thermal\\_environment\\_v2.pdf](https://www.nasa.gov/sites/default/files/atoms/files/ericstalcup_lunar_thermal_environment_v2.pdf).
- [15] S Hobbs. *Spacecraft Systems Engineering*. Vol. Fourth Edition. 2. 1997. ISBN: 9780470750124.
- [16] E Moeini et al. “Thermal performance evaluation of a fabricated multilayer insulation blanket and validity of Cunningham-Tien correlation for this MLI”. In: (2002).
- [17] Lina Tran. *How NASA Prepares Spacecraft for the Harsh Radiation of Space*. URL: <https://www.nasa.gov/feature/how-nasa-prepares-spacecraft-for-the-harsh-radiation-of-space>.

- [18] Carl Christian Liebe et al. "Autonomous Sensor System for Determining Instrument Position Relative to Unknown Surfaces Utilized on Mars Rover". In: *IEEE SENSORS JOURNAL* (2022).
- [19] Shawn. *Types of Distance Sensors and How to Select One?* <https://www.seeedstudio.com/blog/2019/12/23/distance-sensors-types-and-selection-guide/>. 2020.
- [20] *24GHz Microwave Radar Sensor Wiki*. [https://wiki.dfrobot.com/24GHz\\_Microwave\\_Radar\\_Sensor\\_SKU:%20SEN0306](https://wiki.dfrobot.com/24GHz_Microwave_Radar_Sensor_SKU:%20SEN0306).
- [21] *Grove - 80cm Infrared Proximity Sensor - GP2Y0A21YK*. <https://www.seeedstudio.com/Grove-80cm-Infrared-Proximity-Sensor.html>.
- [22] *Microwave Sensor - 24GHz Doppler Radar Motion Sensor - MW2401TR11*. <https://www.seeedstudio.com/Microwave-Sensor-24GHz-Doppler-Radar-Motion-Sensor-MW2401TR11-p-4690.html>.
- [23] *TFmini S LiDAR module - Short-Range ToF LiDAR Range Finder*. <https://www.seeedstudio.com/TFmini-S-LiDAR-module-Short-Range-ToF-LIDAR-Range-Finder-p-4425.html>.
- [24] Abigail C. Allwood et al. "PIXL: Planetary Instrument for X-Ray Lithochemistry". In: *Springer* (2020).
- [25] Rohit Bhartia et al. "Perseverance's Scanning Habitable Environments with Raman and Luminescence for Organics and Chemicals (SHERLOC) Investigation". In: *Springer* (2020).
- [26] J. Bob Balaram et al. "Mars Helicopter Technology Demonstrator". In: *Atmospheric Flight Mechanics Conference* (2018).
- [27] *1/7.5 B&W CMOS VGA (640 x 480) Image Sensor with OmniPixel 3 GS Technology*. <https://www.ovt.com/products/ov7251/>.
- [28] *3mm FL f/2.5, Blue Series M12 Lens*. <https://www.edmundoptics.eu/p/3mm-fl-f25-blue-series-m12-mu-videotrade-imaging-lens/31866/>.
- [29] Amptek. *X-Ray Fluorescence (XRF): Understanding Characteristic X-Rays*. URL: [https://web.archive.org/web/20131228123922/http://www.amptek.com/pdf/characteristic\\_xrays.pdf](https://web.archive.org/web/20131228123922/http://www.amptek.com/pdf/characteristic_xrays.pdf).
- [30] Center for X-ray Optics and Advanced Light Source, Lawrence Berkeley National Laboratory. *X-Ray Fluorescence (XRF): Understanding Characteristic X-Rays*. URL: [https://xdb.lbl.gov/Section1/Table\\_1-2.pdf](https://xdb.lbl.gov/Section1/Table_1-2.pdf).
- [31] *Alpha Proton X-ray Spectrometer (APXS)*. <https://nssdc.gsfc.nasa.gov/nmc/experiment/display.action?id=2004-006C-03>.
- [32] X-ray Consultant for the Electronics Industry Dr. David Bernard. *History of X-rays – 125 years in the making (pt 2)*. <https://www.exillum.com/history-of-x-rays-x-ray-tubes/>.
- [33] *Mars Curiosity Rover*. <https://nssdc.gsfc.nasa.gov/nmc/experiment/display.action?id=2004-006C-03>.
- [34] H. Boehnhardt et al. JP. Bibring H. Rosenbauer. "THE ROSETTA LANDER ("PHILAE") INVESTIGATIONS". In: *Space Sci Rev* 128 (2007). DOI: \textbf{https://doi.org/10.1007/s11214-006-9138-2}.
- [35] *Miniature X-Ray Generator with Pyroelectric Crystal*. <https://www.amptek.com/-/media/ametekamptek/documents/resources/products/specs/retired/cool-x-pyroelectric-x-ray-generator-specifications.pdf?la=en&revision=0e2b8dfb-58e1-42e4-a8f9-48a9c44c2824>.
- [36] Amptek. *COOL-X X-Ray Generator*. <https://www.amptek.com/internal-products/obsolete-products/cool-x-pyroelectric-x-ray-generator>.

- [37] Niels de Jonge Mauricio Terrones Humberto Terrones and Jean–Marc Bonard. “Carbon nanotube electrosources and applications”. In: *The Royal Society* (2004). DOI: \textbf{\{https://doi.org/10.1098/rsta.2004.1438\}}.
- [38] Niels de Jonge. “Chapter 3 Carbon Nanotube Electron Sources for Electron Microscopes”. In: *Advances in IMAGING AND ELECTRON PHYSICS*. Ed. by Peter W. Hawkes. Vol. 156. Advances in Imaging and Electron Physics. Elsevier, 2009, pp. 203–233. DOI: [https://doi.org/10.1016/S1076-5670\(08\)01403-1](https://doi.org/10.1016/S1076-5670(08)01403-1). URL: <https://www.sciencedirect.com/science/article/pii/S1076567008014031>.
- [39] Ahmad Shukri Mustapa Kamal Chong Chon Sing Ibrahim Salih Elyaseery and Abdul Aziz Tajuddin. *Gamma ray spectrum of Am 241 in a backscattering geometry using a high purity germanium detector*. *Proceedings of INC ’97*. 1997.
- [40] Roberto Cesareo et al. “Portable and Handheld Systems for Energy-Dispersive X-ray Fluorescence Analysis”. In: Mar. 2009. ISBN: 9780470027318. DOI: 10.1002/9780470027318.a6803.pub2.
- [41] Gwendy Hall Angelina Buchar Graeme Bonham-Carter, CANADIAN MINING INDUSTRY RESEARCH ORGANIZATION (CAMIRO) EXPLORATION DIVISION. *Quality Control Assessment of Portable XRF Analysers: Development of Standard Operating Procedures, Performance on Variable Media and Recommended Uses*. URL: <https://www.appliedgeochemists.org/images/stories/XRF/pXRF%5C%20Report%5C%20Phase%5C%20I%5C%20Report%5C%20rev%5C%20Oct%5C%202013.pdf>.
- [42] Amptek. *Fast SDD Ultra High Performance Silicon Drift Detector*. URL: <https://www.amptek.com/products/x-ray-detectors/fastsdd-x-ray-detectors-for-xrf-eds/fastsdd-silicon-drift-detector>.
- [43] G. Margaritondo. “Photoelectron Spectromicroscopy”. In: *Encyclopedia of Condensed Matter Physics*. Ed. by Franco Bassani, Gerald L. Liedl, and Peter Wyder. Oxford: Elsevier, 2005, pp. 272–279. ISBN: 978-0-12-369401-0. DOI: <https://doi.org/10.1016/B0-12-369401-9/00587-8>. URL: <https://www.sciencedirect.com/science/article/pii/B0123694019005878>.
- [44] X-ray-Optics.de. *Fresnel Zone Plates*. URL: <http://www.x-ray-optics.de/index.php/en/types-of-optics/diffracting-optics/fresnel-zone-plates>.
- [45] X-ray-Optics.de. *Capillary Optics*. URL: <http://www.x-ray-optics.de/index.php/en/types-of-optics/reflecting-optics/capillary-optics>.
- [46] Amptek. *Mini-X2 X-Ray Tube*. URL: <https://www.amptek.com/products/mini-x2-x-ray-tube>.
- [47] Amptek. *X-123CdTe Complete X-Ray & Gamma Spectrometer with CdTe Detector*. URL: <https://www.amptek.com/internal-products/x-123-cdte-complete-x-ray-gamma-ray-spectrometer-with-cdte-detector>.
- [48] Videnskab DK. *Mars 2020 begynder nu: Dansk udstyr skal jagte liv på vores naboplanet*. URL: <https://videnskab.dk/rummet/mars-2020-begynder-nu-dansk-udstyr-skal-jagte-liv-paa-vores-naboplanet/>.
- [49] HiTechs. *NASA’s NICER Begins Neutron Star Exploration Mission*. URL: <https://hitechs.org/nasas-nicer-begins-neutron-star-exploration-mission-48902017/>.
- [50] Astrobotic. *PEREGRINE LUNAR LANDER*. <https://www.astrobotic.com/wp-content/uploads/2021/01/Peregrine-Payload-Users-Guide.pdf>. [Accessed 03-May-2023]. 2020.
- [51] AMETEK. *OEM Solutions for XRF Systems*. <https://www.amptek.com/products/x-ray-detectors/oem-xrf-solutions/oem-solutions-for-xrf-systems>. [Accessed 03-May-2023]. 2023.

- [52] CDA Intercorp. *STEPPER MOTOR ENGINEERING REFERENCE DATA*. [https://1drv.ms/b/s!AsPX4XacuEMkvWGUrVBpk\\_74dSMK?e=yMRN9x](https://1drv.ms/b/s!AsPX4XacuEMkvWGUrVBpk_74dSMK?e=yMRN9x). [Accessed 03-May-2023]. 2000.
- [53] Ferguson Perforating. *6061 Aluminum Alloy*. <https://www.fergusonperf.com/the-perforating-process/material-information/specialized-aluminum/6061-aluminium-alloy/>. [Accessed 03-May-2023]. 2023.
- [54] NASA. *MARIE*. <https://mars.nasa.gov/odyssey/mission/instruments/marie/>. [Accessed 03-May-2023].
- [55] Wikipedia. *Mass Spectrometer for Planetary Exploration*. [https://en.wikipedia.org/wiki/Mass\\_Spectrometer\\_for\\_Planetary\\_Exploration](https://en.wikipedia.org/wiki/Mass_Spectrometer_for_Planetary_Exploration). [Accessed 03-May-2023].
- [56] Matweb. *DuPont™ Kevlar® 49 Aramid Fiber*. URL: <https://www.matweb.com/search/datasheet.aspx?MatGUID=77b5205f0dcc43bb8cbe6fee7d36cbb5&ckck=1>.
- [57] S.W. Angrist. *Direct Energy Conversion*. 4th. Allyn and Bacon, 1982. ISBN: 9780205077588. URL: <https://books.google.dk/books?id=SO1SAAAAMAAJ>.
- [58] AZUR SPACE. *TJ Solar Cell 3G28C*. <https://satsearch.co/products/azur-space-tj-solar-cell-3g28c>. [Accessed 03-May-2023]. -.
- [59] NASA. *3.0 Power*. <https://www.nasa.gov/smallsat-institute/sst-soa/power>. [Accessed 03-May-2023]. -.
- [60] EnerSys. *Product Data Sheet Li-ion Rechargeable Battery ABSL 3s4p 10.8V 11.6Ah*. [https://www.enersys.com/493bb4/globalassets/documents/product-documentation/absl/amer/am-absl-3s4p-fl-aa\\_0320.pdf](https://www.enersys.com/493bb4/globalassets/documents/product-documentation/absl/amer/am-absl-3s4p-fl-aa_0320.pdf). [Accessed 03-May-2023]. -.
- [61] IPC2U. *The Main Differences Between RS-232, RS-422 and RS-485*. <https://ipc2u.com/articles/knowledge-base/the-main-differences-between-rs-232-rs-422-and-rs-485/>. Accessed: May 3, 2023. 2019.
- [62] EE JRW. *RS-422 CableLength-DataRate*. [https://commons.wikimedia.org/wiki/File:RS-422\\_CableLength-DataRate.svg](https://commons.wikimedia.org/wiki/File:RS-422_CableLength-DataRate.svg). Accessed: May 3, 2023. 2016.
- [63] Rüdiger Klar, Thierry Delmotte, and Bruno Delord. “Experience with Multi-Gbit/s SpaceWire Networks”. In: *Proceedings of the 5th International SpaceWire Conference*. Accessed: May 3, 2023. 2008, pp. 31–36. URL: <http://2008.spacewire-conference.org/downloads/Papers/Networks%5C%20%5C%26%5C%20Protocols%5C%203/Klar.pdf>.
- [64] Star-Dundee Ltd. *An Overview of the SpaceWire Standard*. <https://www.star-dundee.com/spacewire/getting-started/an-overview-of-the-spacewire-standard/>. Accessed: May 3, 2023. Accessed: 2023.
- [65] *SpaceWire Cable Inter connect SpaceWire devices, extend cables, standard and straight through, plating options, compliant with ECSS-E-ST-50-12 Type A and Type AL — dyneng.com*. <https://www.dyneng.com/SpaceWireCable.html>. [Accessed 03-May-2023].
- [66] *SpaceWire - PCIe SpaceWire bus interface with 4 SpaceWire ports - PCIe-SpaceWire is compliant with ECSS-E-ST-50-12C time code RMAP DMA Dynamic Engineering PCIe-SpaceWire — dyneng.com*. <https://www.dyneng.com/PCIe-SpaceWire.html>. [Accessed 03-May-2023].
- [67] -. *X Band Frequency Band Usage*. <https://sites.google.com/site/interfacebus/Home/radar-gear/x-band-frequency-band-usage>. [Accessed 02-May-2023]. -.
- [68] Alessandro Balossino & Faramaz Davarian. *The Plan to Give the Moon Decent Wireless Coverage — spectrum.ieee.org*. <https://spectrum.ieee.org/lunar-communications>. [Accessed 02-May-2023].
- [69] Glenn Zorpette. *The Do-or-Die Moments That Set the Fate of the Internet — spectrum.ieee.org*. <https://spectrum.ieee.org/computer-networking>. [Accessed 02-May-2023].

- [70] Jan Wittry. *The Ultimate Long Distance Communication — nasa.gov*. [https://www.nasa.gov/mission\\_pages/LRO/news/LRO\\_twta.html](https://www.nasa.gov/mission_pages/LRO/news/LRO_twta.html). [Accessed 02-May-2023].
- [71] Herbert J. Kramer. *Chang'e-3 Moon-landing Mission — eoportal.org*. <https://www.eoportal.org/satellite-missions/chang-e-3>. [Accessed 02-May-2023]. 2013.
- [72] Herbert J. Kramer. *Chang'e-2 (Lunar-2 Mission of China) / CE-2 — eoportal.org*. <https://www.eoportal.org/satellite-missions/chang-e-2>. [Accessed 02-May-2023]. 2012.
- [73] Ernie Wright. *Earth and Sun from the Moon's South Pole*. [https://svs.gsfc.nasa.gov/4944#section\\_credits](https://svs.gsfc.nasa.gov/4944#section_credits). [Accessed 02-May-2023]. 2021.
- [74] Mike Wall. *China Launching Relay Satellite Toward Moon's Far Side Sunday*. <https://web.archive.org/web/20180518183823/https://www.space.com/40626-china-launching-moon-mission-sunday-change-4.html>. [Accessed 02-May-2023]. 2018.
- [75] Dr. David R. Williams. -. <https://nssdc.gsfc.nasa.gov/nmc/spacecraft/display.action?id=QUEQIAO>. [Accessed 02-May-2023]. 2018.
- [76] Lihua Zhang. *Development and Prospect of Chinese Lunar Relay Communication Satellite*. <https://spj.science.org/doi/10.34133/2021/3471608>. [Accessed 02-May-2023]. 2021.
- [77] JSET International. *Ground Segment — web.archive.org*. <https://web.archive.org/web/20150920224012/https://www.jsati.com/why-satellite-how-GroundSegment.asp>. [Accessed 03-May-2023]. 2015.
- [78] *Affordable Space Technology & Missions | Astrobotic Technology — astrobotic.com*. <https://www.astrobotic.com/company/>. [Accessed 02-May-2023].
- [79] Doug Messier. *NASA's Deep Space Network Ground Testing with Astrobotic's Peregrine Lunar Lander a Success — parabolicarc.com*. <https://parabolicarc.com/2022/08/16/nasas-deep-space-network-ground-testing-with-astrobotics-peregrine-lunar-lander-a-success/>. [Accessed 02-May-2023]. 2022.
- [80] Amptek. *FAST SDD® Ultra High Performance Silicon Drift Detector*. URL: <https://www.amptek.com/products/x-ray-detectors/fastsdd-x-ray-detectors-for-xrf-eds/fastsdd-silicon-drift-detector>.
- [81] Amptek. *CdTe X-Ray & Gamma Ray Detector*. URL: <https://www.amptek.com/products/x-ray-detectors/cdte-x-ray-and-gamma-ray-detectors/cdte-x-ray-and-gamma-ray-detector>.



## A.2 X-123 FAST SDD Specifications

All figures (Figure A.1 and Figure A.2) in this section are reproduced from the manuals associated with the FAST-SDD. Full copies are available to download from Amptek's website [80].

### 5.4. Amptek 25 mm<sup>2</sup> FAST SDD® Specifications

General	
Detector Type	Silicon Drift Detector (SDD)
Detector Size	25 mm <sup>2</sup>
Collimated Area	17 mm <sup>2</sup>
Thickness	500 µm
Collimator Type	Internal Multilayer
Preamplifier Type	CMOS reset type
Energy resolution @ 5.9 keV ( <sup>55</sup> Fe)	
122 to 129 eV FWHM (guaranteed) at T <sub>pk</sub> =4.0 µs	
126 eV (typical) at 1.0 µs	
134 eV (typical) at 0.2 µs	
Energy resolution @ C K <sub>a</sub> : 45 eV (typical)	
Other Performance	
Peak to background	≥ 20,000:1 (typical)
Signal risetime	< 35 ns
Maximum input count rate	> 1 Mcps
Throughput count rate stability	Determined by signal processor & its settings
Cooler type	Two stage thermoelectric
Temp monitor	Diode
Power	
HV Bias	-100 V to -180V @ 25 µA
Max cooling power	3.5 V / 0.45A
Total power	< 2 W (full cooling)
Other	
Operating range	-35°C to +80°C Performance degrades at elevated detector temperatures.
Storage & shipping	-40°C to +85°C, 10% to 90% RH noncondensing
RoHS	Compliant
Lifetime	Typical 5 to 10 years, depending on use
Warranty Period	1 year

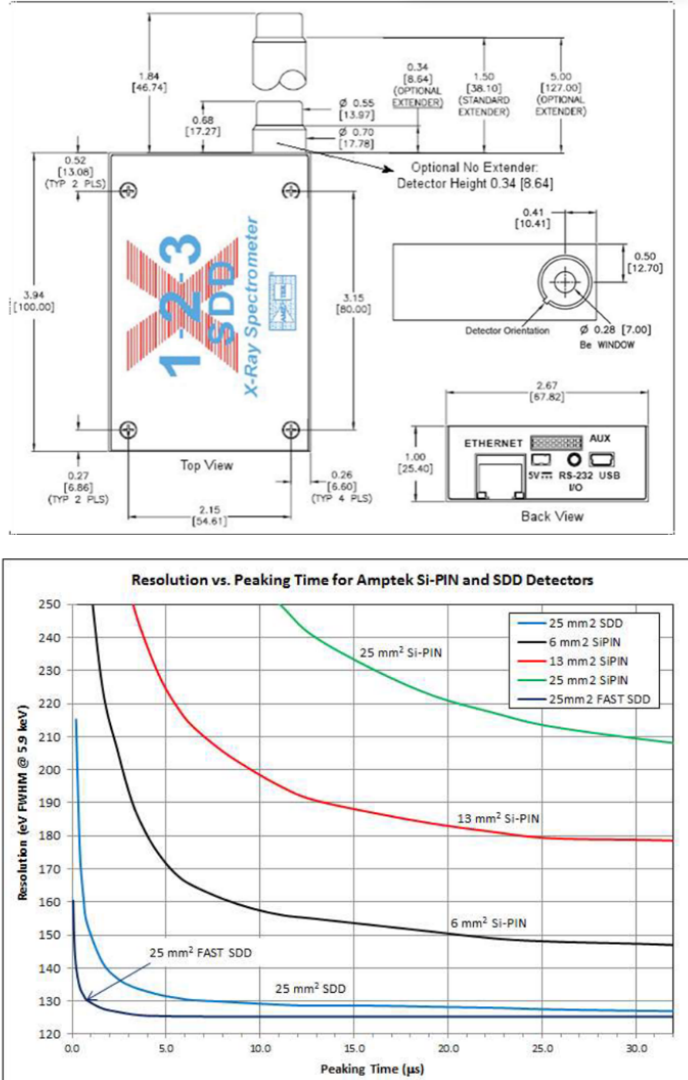


Figure A.1: Specifications of the FAST-SDD by Amptek. Diagrams show the dimensions of the external casing, and the resolution vs peaking time for various technologies.

## A.3 X-123 FAST SDD CdTe Specifications

As with the FAST-SDD, the figures (Figure A.3 and Figure A.4) in this section are reproduced from Amptek's manuals, available from their website [81].

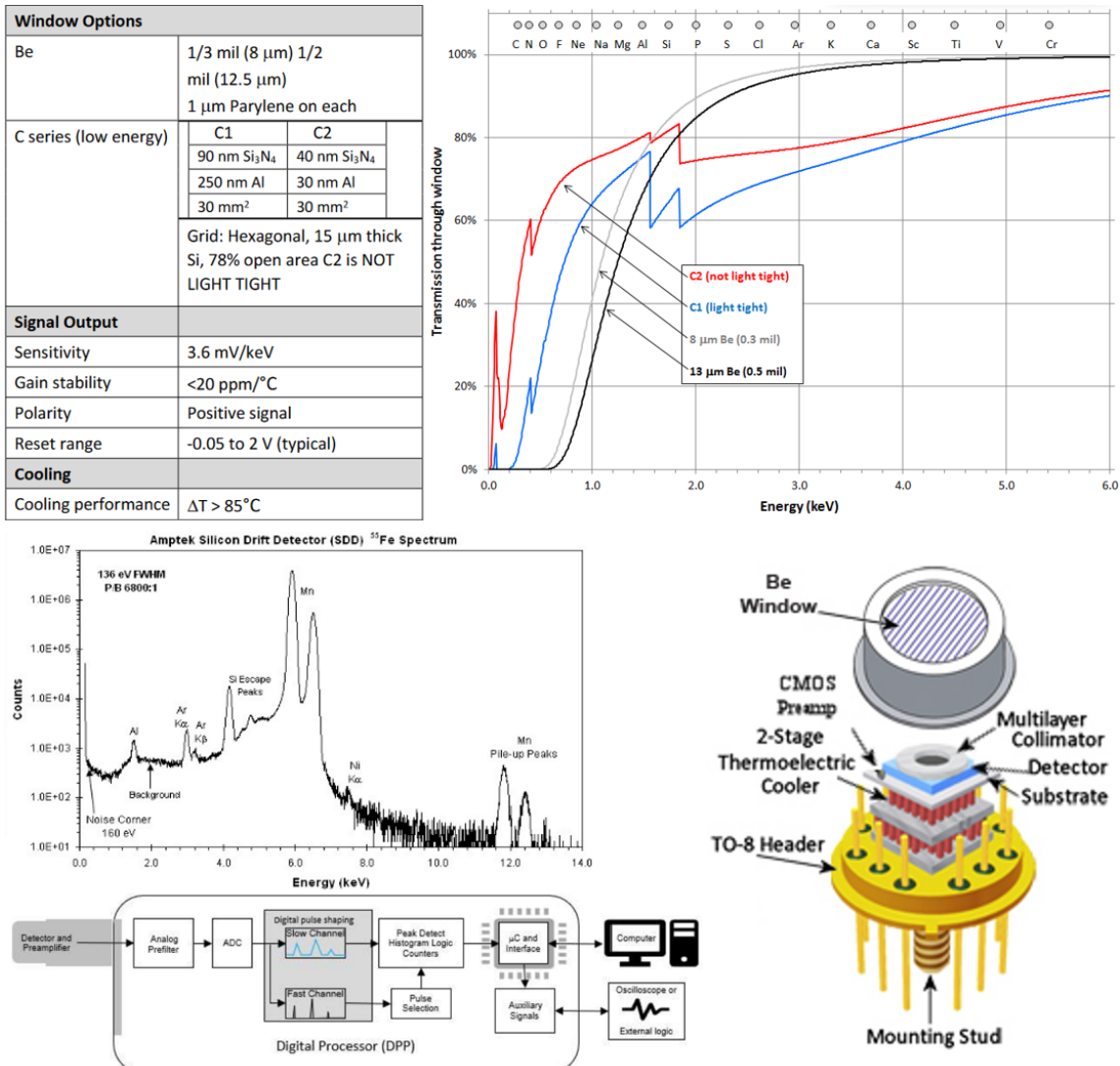


Figure A.2: More specifications of the FAST-SDD. Clockwise from top: graph showing the transmission of levels of different window options, internal structure of detector element, layout of data processing elements, spectrum when detecting iron and more general technical information.

SYSTEM PERFORMANCE		POWER	
Energy Resolution @ 122 keV, 57Co	25 mm: <1.5 keV FWHM for Tpk of 2.4us	Nominal Input	+5 VDC at 500 mA (2.5 W) (typical). Current depends strongly on detector $\Delta T$ . Ranges from 300 to 800 mA at 5 VDC. AC adapter provided.
Energy Range	5-150 keV. May be used at higher energy with lower efficiency, contact Amptek.	Input Range	4 V to 6 V (300 to 200 mA, 500 mA max))
Maximum Recommended Count Rate	CC CdTe detectors (reset preamplifier) - 50kCPS RC CdTe detectors (tail pulse preamplifier) - over 200kCPS but with varying resolution.	High Voltage Supply	Internal multiplier, set to 500 V, adjustable to 800 V
DETECTOR AND PREAMPLIFIER		Cooler Supply	Closed loop controller with $\Delta T_{max} = 85^\circ C$
Detector Type	CdTe	GENERAL and ENVIRONMENTAL	
Detector Area	25 mm <sup>2</sup>	Operating Temperature	-20 °C to +50 °C
Detector Thickness	1 mm	Warranty Period	1 year
Window Options	4 mil Be (100 $\mu m$ ) or 25um Graphite	Typical Device Lifetime	5 to 10 years, depending on use
Thermoelectric Cooler	2-stage	Storage and Shipping	Typical: -20 °C to +50 °C, 10 to 90% humidity non-condensing Long-term storage: 10+ years in dry environment
Preamplifier Type	Amptek custom design, Reset-type	Compliance	RoHS Compliant
PULSE PROCESSOR		TUV Rheinland	TUV Certification Certificate #: CU 72101153 01 Tested to: UL 61010-1: 2009 R10.08 CAN/CSA-C22.2 61010-1-04+GI1
Gain	Combination of coarse and fine gain yields overall gain continuously adjustable from 0.84 to 127.5		
Coarse Gain	Software selectable settings from 1.12 to 102 in 16 log steps. 1.12, 2.49, 3.78, 5.26, 6.56, 8.39, 10.10, 11.31, 14.56, 17.77, 22.42, 30.83, 38.18, 47.47, 66.26, 102.0		
Fine Gain	Software selectable, 0.75 to 1.25, 10 bit resolution Full Scale 1000 mV input pulse @ x1 gain		
COMMUNICATIONS			
USB	2.0 full-speed (12 Mbps)		
Serial	Standard RS232 at 115.2 k or 57.6 Kbaud		
Ethernet	10 base-T		

Figure A.3: Specifications of the X-123 CdTe detector by Amptek.

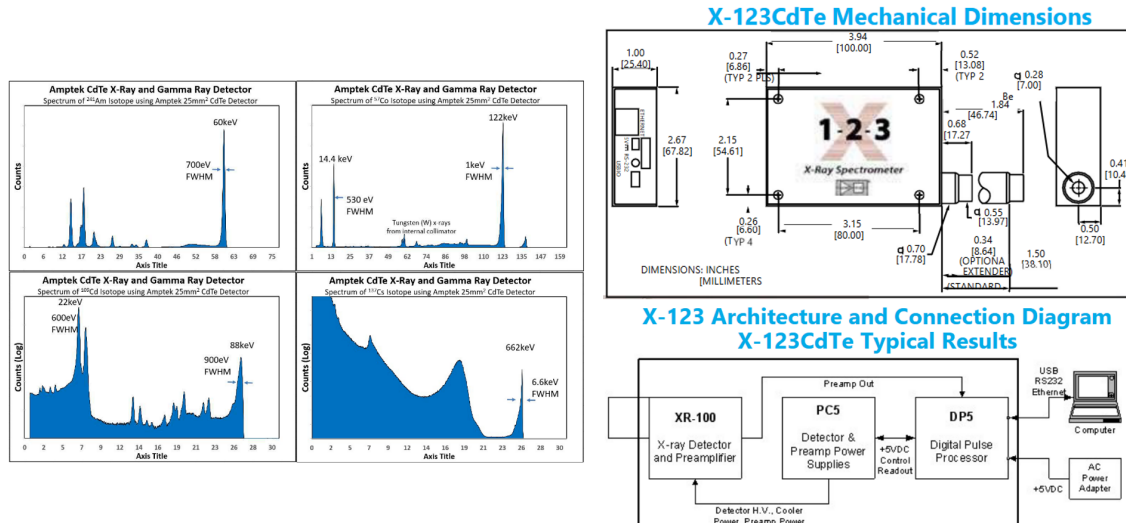


Figure A.4: Spectra for various sources (left) and mechanical structure and architecture (right) of the X-123 CdTe detector. This features the aforementioned heinous crime against science, which is the unit 'Axis Title' on the x-axis of all four graphs.



Technical  
University of  
Denmark

Elektrovej, Building 328  
2800 Kgs. Lyngby  
Tlf. 4525 9500

[www.space.dtu.dk](http://www.space.dtu.dk)